

Report No. SRIC 70-14

KINETIC STUDIES ON THE PYROLYSIS, DESULFURIZATION, & GASIFICATION OF COALS WITH EMPHASIS ON THE NON-ISOTHERMAL KINETIC METHOD

**Marvin L. Vestal, Alan G. Day, III, J.S. Snyderman,
Gordon J. Fergusson, F.W. Lampe, R.H. Essenhight,
and Wm. H. Johnston**

With contributions from

**Charles E. Waring, A.L. Wahrhaftig, J.H. Futrell,
and Pamela P. Farkas**

Final Report December 1969

Phase II Contract No . PH 86-68-65



**Scientific Research
Instruments Corporation**

Specializing in Air and Water Pollution Control Systems

6707 Whitestone Rd. Baltimore, Md. 21207 Cable: SRICORP Tel. (301) 944-4020

Report No. SRIC 70-14

KINETIC STUDIES ON THE PYROLYSIS, DESULFUR-
IZATION, & GASIFICATION OF COALS WITH EMPHA-
SIS ON THE NON-ISOTHERMAL KINETIC METHOD

Marvin L. Vestal, Alan G. Day, III, J.S. Snyderman,
Gordon J. Fergusson, F.W. Lampe, R.H. Essenhight,
and Wm. H. Johnston

With contributions from

Charles E. Waring, A.L. Wahrhaftig, J.H. Futrell,
and Pamela P. Farkas

Final Report December 1969

Phase II Contract No . PH 86-68-65

with the

NATIONAL AIR POLLUTION CONTROL ADMINISTRATION

Paul W. Spalte, Director, Bureau of Engineering and Physical Sciences
E.D. Margolin, Chief, New Process Development Unit
Leon Stankus, Contract Project Officer

Scientific Research Instruments Corporation
Baltimore, Maryland

TABLE OF CONTENTS

| | <u>Page</u> |
|---|-------------|
| INTRODUCTION | 1 |
| THE EXPERIMENTAL APPARATUS | 3 |
| THE INTERPRETATION OF NON-ISOTHERMAL KINETIC EXPERIMENTS | 4 |
| Example of CH ₃ SH from Coal | 11 |
| H ₂ S EVOLUTION IN REACTIONS CHARACTERISTIC OF COAL DESULFURIZATION | 14 |
| Iron Pyrite | 15 |
| Organic Sulfur | 17 |
| KINETICS OF H ₂ S EVOLUTION FROM TEN COALS | 25 |
| Identification and ASTM Analyses of Ten Coals | 28 |
| DEPENDENCE OF DESULFURIZATION KINETICS ON HYDROGEN PRESSURE | 48 |
| FORMS OF SULFUR IN CHAR AS FUNCTIONS OF CARBONIZING TEMPERATURE | 52 |
| THE KINETICS OF H ₂ S REACTIONS WITH COAL CHAR | 56 |
| KINETICS OF H ₂ S REACTION WITH CARBON | 60 |
| KINETICS OF H ₂ S CAPTURE BY Fe AND BY CaO | 71 |
| KINETICS OF CALCINATION OF DOLOMITES AND LIMESTONES | 76 |
| KINETICS OF DECOMPOSITION OF IRON SULFATES | 80 |
| PYROLYSIS AND GASIFICATION OF COAL MIXED WITH CALCIUM OXIDE | 84 |

TABLE OF CONTENTS

| | <u>Page</u> |
|--|-------------|
| KINETICS OF REVERSIBLE DESULFURIZATION REACTIONS | 87 |
| SUMMARY | 92 |
| Chemical Kinetics | 93 |
| Applications of Kinetic Data | 96 |
| Diffusion and Mass Transport | 99 |
| Future Work | 100 |
| REFERENCES | 101 |

LIST OF FIGURES

| Figure | | Page |
|--------|--|------|
| 1 | Typical outgassing kinetics curve vs. temperature. | 8 |
| 2 | Graph for determining the activation energy for first order reaction from the experimental parameters, defined in Figure 1. | 10 |
| 3 | Evolution of CH_3SH in a non-isothermal pyrolysis in hydrogen. | 13 |
| 4 | H_2S evolution in a non-isothermal experiment at one atmosphere of hydrogen on Illinois 5% sulfur coal, SRI No. 4 | 18 |
| 5 | H_2S evolution in a non-isothermal experiment at one atmosphere of hydrogen on pyrite. | 19 |
| 6 | Kinetic analysis of the non-isothermal measurement on pyrite. | 20 |
| 7 | Graph for obtaining the kinetic parameters from non-isothermal experimental data. | 21 |
| 8 | H_2S evolution in non-isothermal experiment at one atmosphere of hydrogen on sulfurated carbon prepared from charcoal. | 23 |
| 9 | Non-isothermal H_2S evolution in H_2 from coals SRI Numbers 1 through 5. | 30 |
| 10 | Non-isothermal H_2S evolutions in H_2 from coals SRI Numbers 6 through 10. | 31 |
| 11 | Kinetic analysis and resolution into individual processes of the H_2S evolution in a non-isothermal experiment at one atmosphere of hydrogen on Illinois 5% sulfur coal, SRI No.4. | 32 |
| 12 | Kinetic analysis and resolution into individual processes of the H_2S evolution in a non-isothermal experiment at one atmosphere of hydrogen on Illinois 5% sulfur coal, SRI No.1. | 38 |

LIST OF FIGURES

| Figure | | Page |
|--------|---|------|
| 13 | Kinetic analysis and resolution into individual processes of the H_2S evolution in a non-isothermal experiment at one atmosphere of hydrogen on Illinois 1% sulfur coal, SRI No. 2. | 39 |
| 14 | Kinetic analysis and resolution into individual processes of the H_2S evolution in a non-isothermal experiment at one atmosphere of hydrogen on Illinois 2.5% sulfur coal, SRI No. 3. | 40 |
| 15 | Kinetic analysis and resolution into individual processes of the H_2S evolution in a non-isothermal experiment at one atmosphere of hydrogen on Illinois 4.5% sulfur coal, SRI No. 5. | 41 |
| 16 | Kinetic analysis and resolution into individual processes of the H_2S evolution in a non-isothermal experiment at one atmosphere of hydrogen on Ohio 3% sulfur coal, SRI No. 6. | 42 |
| 17 | Kinetic analysis and resolution into individual processes of the H_2S evolution in a non-isothermal experiment at one atmosphere of hydrogen on Maryland 3% sulfur coal, SRI No. 7. | 43 |
| 18 | Kinetic analysis and resolution into individual processes of the H_2S evolution in a non-isothermal experiment at one atmosphere of hydrogen on Ohio 3.5% sulfur coal, SRI No. 8. | 44 |
| 19 | Kinetic analysis and resolution into individual processes of the H_2S evolution in a non-isothermal experiment at one atmosphere of hydrogen on Pennsylvania 1% sulfur coal, SRI No. 9. | 45 |
| 20 | Kinetic analysis and resolution into individual processes of the H_2S evolution in a non-isothermal experiment at one atmosphere of hydrogen on Kentucky 4% sulfur coal, SRI No. 10. | 46 |
| 21 | 1 st order dependence on H_2 pressure: comparison of non-isothermal rate constants (straight lines) with isothermal data at 475° C and pressures of 1, 4, 9 and 10 atms. of H_2 . | 51 |

LIST OF FIGURES

| Figure | | Page |
|--------|---|------|
| 22 | Variations in the amount and forms of sulfur in coke produced from the nominally 5% sulfur Illinois coal carbonized in hydrogen as functions of carbonizing temperature for a H_2 flow rate of 1000 ml /min. | 54 |
| 23 | Variations in the amount and forms of sulfur in char and gas produced from the normally 5% sulfur Illinois coal carbonized in hydrogen as a function of carbonizing temperature for a H_2 flow rate of 100 ml /min. | 55 |
| 24 | Relative H_2S concentrations in the effluent gases from six non-isothermal measurements on the kinetics of the reactions of H_2S with coke. | 58 |
| 25 | H_2S absorption in non-isothermal experiments on char, charcoal and iron. | 61 |
| 26 | Non-isothermal absorption of hydrogen sulfide on (a) 1 gram activated charcoal (b) 1 gram graphite and (c) a blank in which the quartz wool plug normally used to hold the sample in place was used but with no sample. These experiments used 0.1% H_2S in He at a flow of 220 ml/min. | 63 |
| 27 | Non-isothermal measurement of the desulfurization of high sulfur char from 5% sulfur Illinois coal, SRI No. 1 resolved into contributions from FeS and organic sulfur III from sulfured charcoal. | 68 |
| 28 | Desorption in He of H_2S adsorbed on (a) charcoal (b) char from SRI coal No. 1, (c) graphite. | 69 |
| 29 | Non-isothermal measurements of the desulfurization of sulfured charcoal. | 70 |
| 30 | Arrhenius type plot of the H_2S absorption by iron in a non-isothermal kinetic experiment. | 72 |
| 31 | H_2S absorption in non-isothermal kinetic experiments on calcium oxide. | 74 |
| 32 | Arrhenius type plot of the H_2S absorption by calcined No. 1930 dolomite in a non-isothermal kinetic experiment. | 75 |

LIST OF FIGURES

| Figure | | Page |
|--------|--|------|
| 33 | Runs N-46 and N-47 are calcination runs on calcium carbonate in helium with residence times of 0.47 seconds and 0.024 seconds, respectively. | 77 |
| 34 | Carbon dioxide evolution from the non -isothermal calcination in helium of precipitated calcium carbonate (1), Limestone sample 1683B (2), Dolomite sample 1930 (3), and Dolomite sample 1380 (4). | 78 |
| 35 | Sulfur gas evolution from pyrolysis in 4 litres/minute of (a) 1 gram and (b) 0.036 grams of ferric sulfate. | 81 |
| 36 | Sulfur gas evolution from pyrolysis in 4 litres/minute of (a) 1 gram and (b) 0.028 grams of ferrous sulfate. | 82 |
| 37 | Sulfur gas evolution from pyrolysis of ferrous sulfate in (a) 4 litres/minute of Helium and (b) 4 litres/minute of Hydrogen. | 83 |
| 38 | Rate constants for coal desulfurization reactions and for important back reactions as functions of temperature. | 95 |

LIST OF TABLES

| <u>TABLE NO.</u> | <u>DESCRIPTION</u> | <u>PAGE</u> |
|------------------|---|-------------|
| I | Detailed Analysis of Non-Isothermal Experiment on Pyrite | 22 |
| II | Summary of Analyses of Ten Coals - Coal Sample Identification | 33 |
| III | Summary of Analyses of Ten Coals - Forms of Sulfur (Percent of Coal) | 34 |
| IV | Summary of Analyses of Ten Coals - Mineral Analyses (Percent of Coal) | 35 |
| V | Summary of Analyses of Ten Coals Proximate Analysis (Percent of Coal) | 36 |
| VI | Summary of Analyses of Ten Coals - Sulfur in Ash and Coke | 37 |
| VII | Resolution of the H ₂ S Evolution Curves into Individual Reactions | 47 |
| VIII | Summary of Data on Reactions of H ₂ S with Coke | 59 |
| IX | Sulfur Comparison Data for Isothermal Reactions of Nominally 5% Sulfur Coal Mixed with Calcium Oxide, in Helium and in Hydrogen | 86 |
| X | Summary of Kinetic Data | 94 |

INTRODUCTION

This is the final report on work accomplished during Phase II of contract PH 86-68-65 on sulfur control by means of coal gasification. Our studies⁽¹⁾ have emphasized the theoretical and experimental application and extension of the new method of non-isothermal kinetic measurements developed originally by Juntgen and co-workers⁽²⁻⁹⁾. Previous work has shown that desulfurization reactions on coal during pyrolysis and gasification are inefficient under equilibrium conditions; therefore, knowledge of the kinetics of the parallel and opposing reactions are important to the efficient development of a useful process.

During Phase I of this work the non-isothermal kinetic method evolved as a most powerful and useful technique. The theory of the non-isothermal technique for study of the kinetics of complex heterogeneous reactions was extended to include reactive flush gases and back reactions of the products. An experimental laboratory was constructed for performing these non-isothermal experiments and twenty-three non-isothermal experiments were completed during Phase I. In addition, nineteen isothermal experiments were conducted.

During Phase II minor modifications and improvements were made to the experimental apparatus and a total of one hundred and forty two non-isothermal experiments and forty eight isothermal experiments were accomplished. These experiments included measurements on the desulfurization kinetics for ten bituminous

coals from a variety of sources throughout the East and Midwest. A systematic procedure was developed for interpreting the H_2S evolution data obtained in the non-isothermal kinetic measurements on the reactions of hydrogen with coal. Measurements were conducted on the dependence of the H_2S evolution from coal on the hydrogen pressure.

An extensive series of measurements were conducted on the kinetics of H_2S reactions with coal char and with the principal reactive constituents of char including carbon, iron, and calcium oxide. The results indicate that calcium oxides obtained from calcination of various dolomites and limestones fulfill some of the requirements of a suitable H_2S absorbent for use in conjunction with gasification and desulfurization. The kinetics of calcination for several dolomites and limestones were investigated. Non-isothermal kinetic measurements were also conducted on the decomposition of iron sulfates.

During the course of this work attention has been paid to developing the techniques for applying the kinetic data by the non-isothermal method to the development of processes for the practical desulfurization of coal during gasification or combustion. Experiments were conducted on the pyrolysis of coal mixed with calcium oxide and on the gasification of coal with steam and oxygen both in the presence and absence of calcium oxide.

THE EXPERIMENTAL APPARATUS

The apparatus used in this research was described in Report No. SRIC 68-13; however, some modifications and improvements to the apparatus were made.

Improvements in the experimental apparatus accomplished during Phase II include the installation of a thermocouple directly into the reactant bed inside the reactor to allow more precise measurement of temperature during the non-isothermal kinetic measurements. A series of experiments were conducted to estimate the error resulting from temperature measurement with the thermocouple located at the outside surface of the reactor. These measurements showed that the bed temperature was in the range from 10 to 20°C below the temperature at the outside surface of the reactor over the entire range from 100°C to 1100°C. In the non-isothermal experiments using the mass spectrometer, this error is partially compensated for by the time delay between gas evolution at the sample and detection by the mass spectrometer. The overall results of the temperature measurements indicate that in the Phase I non-isothermal experiments the maximum errors in the indicated temperatures were in the range from 0 to +20°C from the true bed temperatures.

An electrical flow meter has been installed into the gas handling system replacing the rotometer flow meter to improve the accuracy and reliability of the measurements of the flow of the sweep gas. Also, some modifications to the mass spectrometer have been made to improve the stability, absolute accuracy and flexibility of the mass spectrometer for these measurements. These modifications include a new ion source, an improved electron emission regulator, and a new power supply for the mass spectrometer magnet which allows the scan speed to be varied over a wide range.

THE INTERPRETATION OF NON-ISOTHERMAL KINETIC EXPERIMENTS

We may write a general irreversible heterogenous reaction representing one of the desulfurization reactions of coal as follows:



The rate of the reaction is given by the rate equation,

$$-\frac{d(A)}{dt} = k(B) (A) \quad (2)$$

Where $-\frac{d(A)}{dt}$ is the rate of loss of specie A, (A) is the concentration of the solid reactant, (B) is the concentration of the gaseous reactant usually expressed as partial pressure, and k is the rate constant as given by the Arrhenius equation,

$$k = k_0 e^{-E/RT} \quad (3)$$

In this equation k is the rate constant of Equations (1) and (2), k_0 is the temperature-independent Arrhenius constant, E is the activation energy of the reaction, and R and T are the universal gas constant and the absolute temperature, respectively.

In the rate expression, Equation (2), (A) is actually the instantaneous concentration of specie A in the solid phase. Since continuous measurement of this solid phase concentration is generally difficult, it is helpful to express (A) in terms of the volume of evolved gas D. In this way the solid concentration of A at time t, which is written as (A)

is proportional to the total amount present at zero time minus the amount evolved up to the time, t . This may be written in terms of the volume of evolved gas, D , as follows:

$$(A) = b (V_0 - V) \quad (4)$$

where V_0 is the total volume of gas evolved as Reaction 2 goes to completion, V is the volume of gas evolved up to time t , and b is the proportionality factor.

With this beginning, we may derive the kinetic expression for the non-isothermal desulfurization kinetics leading to an expression for the rate of gas evolution as a function of instantaneous temperature when the sample is heated at a constant rate of M degrees per minute. The details of this derivation are given in the report SRIC 68-13 on Phase I. In terms of all of the parameters which have been defined above, this basic equation for non-isothermal kinetics of reaction (1), neglecting any back reaction, is given by,

$$\frac{dV}{dT} = \frac{V_0 k_0}{M} \exp \left\{ -\left\{ \frac{E}{RT} + \frac{k_0 RT^2}{ME} \right\} \right\} \quad (5)$$

Before discussing changes in this expression which result from desulfurization by pyrolysis with the absence of a reactive gas, or discussing the extensions to include back reactions, let us review the actual experiment and see how this equation may be used to obtain the kinetic parameters of the rate constant from the experimental data. A sample of solid, in this case coal, is heated at a constant rate of

heating, M , from a temperature from which no reaction occurs to an elevated temperature at which reaction is completed. During this period a constant gas flow is maintained of reactant gas, specie B; and continuous analyses of the effluent gas stream are made to identify the product gas, specie D, and measure its rate of evolution as a function of instantaneous temperature. In our experiments, we initially analyzed by a series of techniques including gas-liquid chromatography, plasma spectrometry, and mass spectrometry. The most useful technique for these measurements was the continuous recording mass spectrometer. For most of the kinetic measurements the product gas measured was H_2S (specie D in Equation (1)). Although we measured and identified a number of other sulfur containing gases including methyl mercaptan and carbon disulfide during pyrolysis or gasification of coal in an inert atmosphere, in hydrogen, and in steam, most of the sulfur evolved (typically 98% or more) is as H_2S .

With the mass spectrometer we obtain essentially instantaneous measurements of the concentration of the product gas D in the effluent stream. This instantaneous concentration is uniquely related to the rate of gas evolution $\frac{dV}{dt}$ or $\frac{dV}{dT}$ by the expression,

$$\frac{dV}{dT} = \frac{1}{M} \frac{dV}{dt} = \frac{PQ}{MG} \quad (5a)$$

where P is the concentration of the product gas D as determined by the mass spectrometer, Q is the flow rate, M is the heating rate, and G is the initial weight of the solid sample, A . Since for a given experiment Q , M , and G are constant, either the concentration P or the rate $\frac{dV}{dT}$ may be used in the kinetic interpretations.

A typical curve for Equation (5) showing the change in the instantaneous concentration of gas product, dV/dT , as a function of temperature (or time) is shown in Figure 1. The definition of V_0 defined in Equation (4) is shown as the shaded integral. This curve in Figure 1 is a graphical representation of Equation (5) for a given activation energy, E , and rate constant, k_0 . It is interesting to note that in Equation (5) there are two terms in the exponential. One of these terms controls the rise of the curve in Figure 1 and the other term produces the fall of this curve.

We next define T_0 and $(dV/dT)_{T_0}$ which are shown in Figure 1. T_0 is the temperature at the maximum in this curve. $(dV/dT)_{T_0}$ is the value of dV/dT at this maximum.

Mathematically, the next step is to evaluate the activation energy E and the frequency factor k_0 from the experimental measurement of a curve such as shown in Figure 1. In order to accomplish this, Equation (5) is differentiated with respect to temperature and set equal to zero, thus defining the conditions for the maximum of the curve in Figure 1. When this is done the resulting equation can be rearranged to give us expressions for E and k_0 .

$$E = \frac{eRT_0^2}{V_0} (dV/dT)_{T_0} e^{2RT_0/E} \quad (6)$$

$$k_0 = \frac{EM}{RT_0} e^{E/RT_0} \quad (7)$$

Note that the expression for activation energy in Equation (6) is a transcendental equation which cannot be solved explicitly for E . We can, however, solve this equation graphically and, of course, one could also

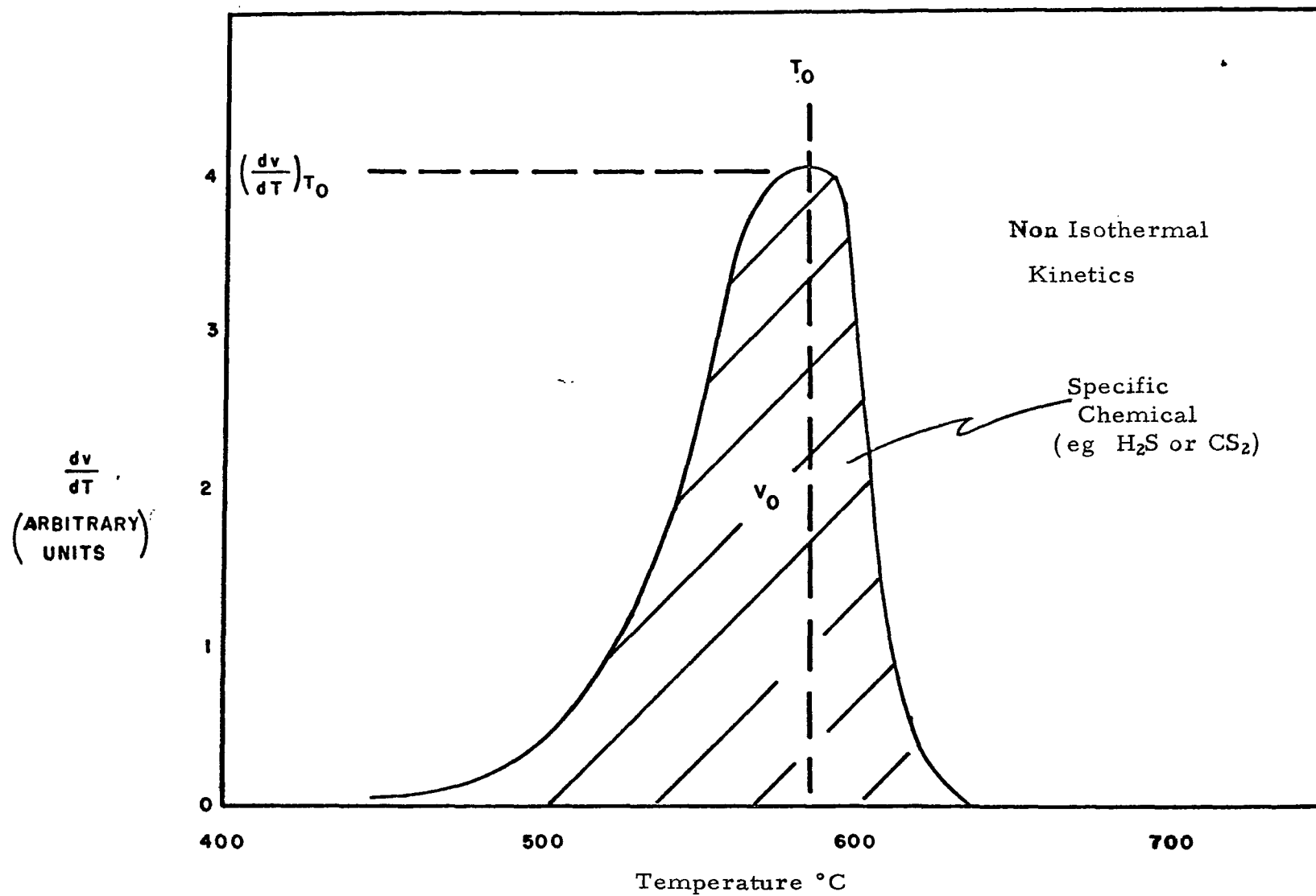


Figure 1. Typical outgassing kinetics curve vs. temperature. T_0 is temperature at peak, $(dv/dT)_{T_0}$ is peak height, V_0 is area.

solve it by successive approximation. To do this we define two dimensionless parameters, alpha and beta

$$\alpha = \frac{E}{RT_o} \quad (8)$$

$$\beta = \frac{T_o}{V_o} \left(\frac{dV}{dT} \right)_{T_o} \quad (9)$$

When these dimensionless parameters, defined by Equations (8) and (9), are substituted in our transcendental Equation (6), we obtain the following relationship

$$\alpha = \beta e^{(1-2/\alpha)} \quad (10)$$

which by taking logarithms may be written as,

$$\ln \alpha + \frac{2}{\alpha} = 1 + \ln \beta \quad (11)$$

Experimentally we may immediately compute beta from the experimental measurement of the curve in Figure 1 from a non-isothermal run.

The experimental quantities of this curve are:

$$\left. \begin{array}{l} V_o \text{ area} \\ (dV/dT)_{T_o} \text{ peak height} \\ T_o \text{ peak location} \\ M \text{ heating rate} \end{array} \right\} \quad (12)$$

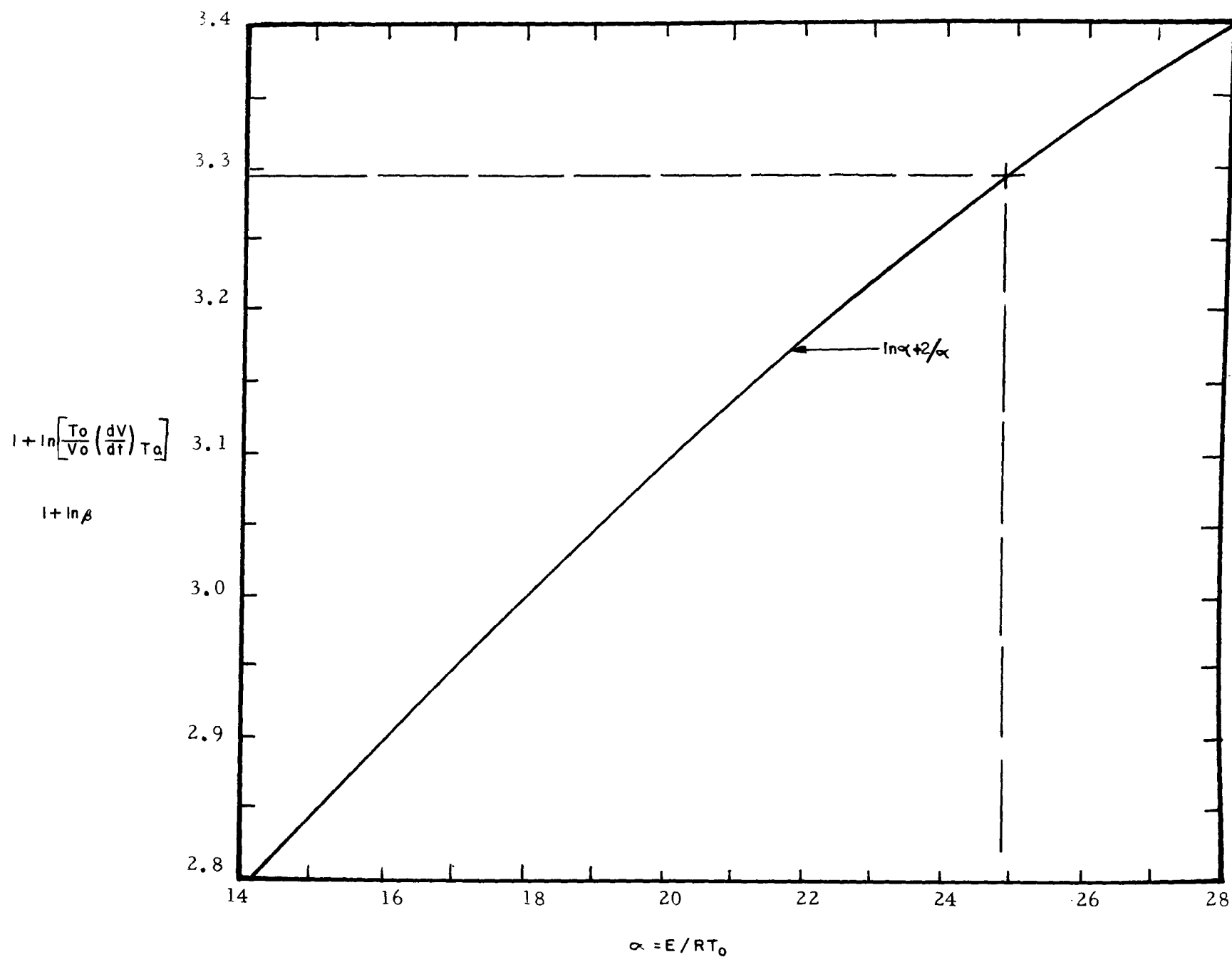


Figure 2. Graph for determining the activation energy for first order reactions from the experimental parameters, defined in Figure 1.

We have now the relationship,

$$\ln \alpha + \frac{2}{\alpha} = \text{experimentally determined number} \quad (13)$$

This equation can be solved graphically by plotting this function of α . This graph is shown in Figure 2.. We read from the abscissa the value of α corresponding to the experimentally determined $1 + \ln \beta$.

Knowing α we compute the activation energy, E, and the k_0 from the following forms of Equations (7) and (8),

$$E = RT_0 \alpha \quad (14)$$

and

$$k_0 = \frac{M}{T_0} \alpha e^{-\alpha} \quad (15)$$

Example of CH₃SH from Coal

Let us apply the non-isothermal kinetic method to the desulfurization of methyl mercaptan from a 5% Illinois coal in hydrogen. The heating rate, M, is set at 5°C per minute. The analyses for the rate of evolution of CH₃SH, the dV/dT, are by mass spectrometer, using the mass 47 peak which is the most intense peak in the mercaptan spectrum. Since the parameters α and β are dimensionless, we must simply use consistent units.

The experimental curve is shown in Figure 3. The corresponding values of the kinetic parameters are:

$$\begin{aligned} E &= 36 \text{ kilocalories per mole} \\ k_0 &= 8.0 \times 10^9 \text{ min}^{-1} \end{aligned} \quad (16)$$

The dotted lines on Figure 2 show $1 + \ln \beta$ and the corresponding α for this non-isothermal measurement of the desulfurization of methyl mercaptan from coal. If the resulting kinetic parameters shown in expression (16) are inserted in our basic Equation (5) we obtain the dotted curve shown in Figure 3. This agreement is quite good and provides evidence that the assumption of a single reaction like reaction (1) is valid for this case. We may now proceed to measurements on the more abundant reactions to produce hydrogen sulfide during the pyrolysis and gasification of coals.

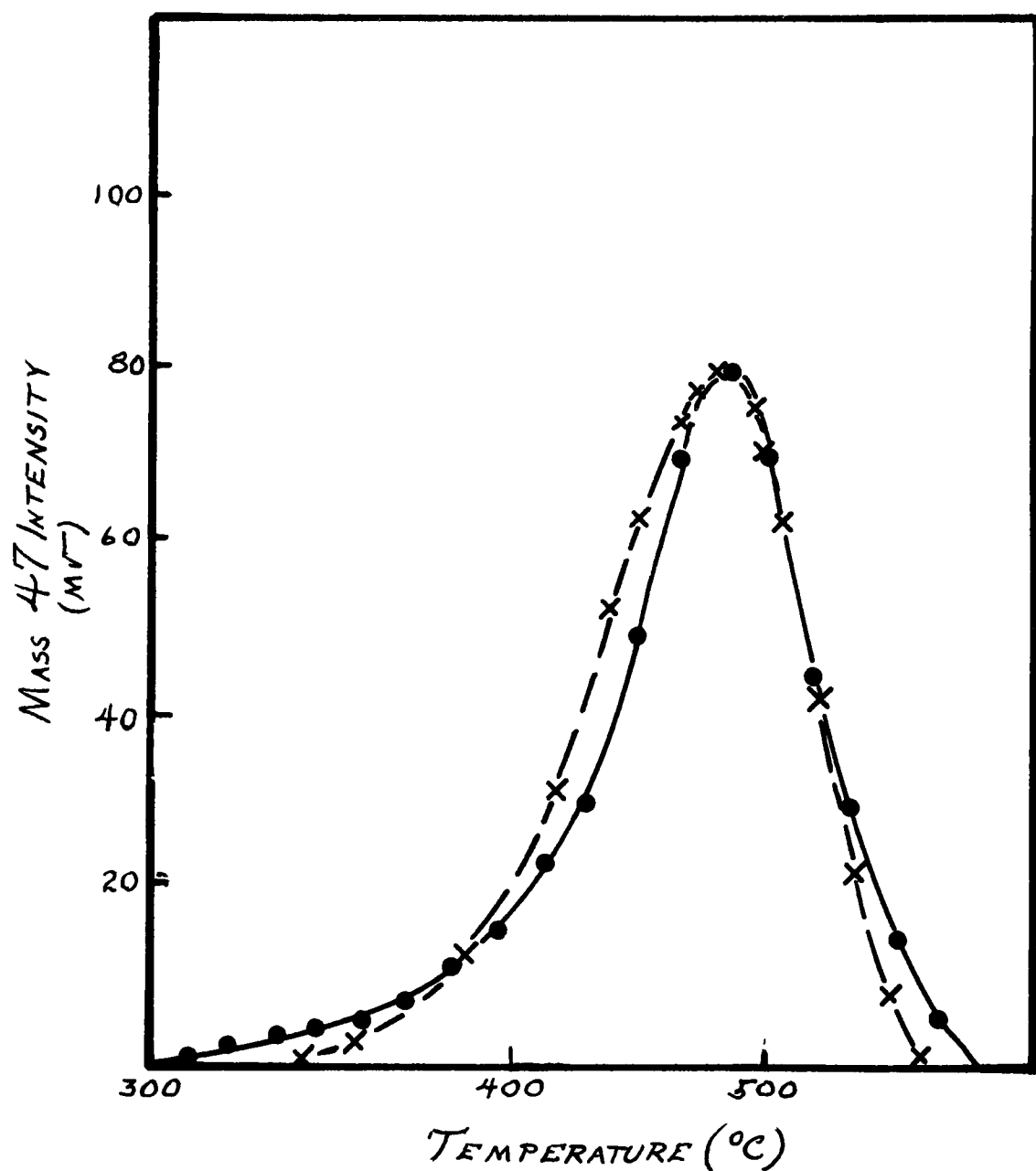
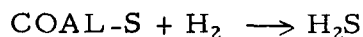


Figure 3. Evolution of CH_3SH in a non-isothermal pyrolysis in hydrogen.
 —●— experimental data
 - - - x - - - calculated from values of E and k_0 by analysis of experimental results.

H₂S EVOLUTION IN REACTIONS CHARACTERISTIC OF COAL DESULFURIZATION

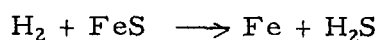
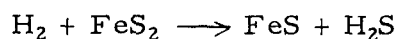
In a hydrogen atmosphere the sulfur in the coal reacts with hydrogen to produce hydrogen sulfide. A typical H₂S evolution curve for a non-isothermal experiment on coal heated in hydrogen is given in Figure 4. These results were obtained using a hydrogen flow rate of 1 litre per minute over a 250 mg sample of Illinois coal No. 4, as identified in our Report No. SRIC 69-10. The heating rate was 4°C per minute. Clearly the H₂S evolution does not occur by a single process such as that producing methyl mercaptan, as shown in Figure 3. Since sulfur exists in coal in many different forms, e.g. pyrite, sulfide, sulfate and several different types of organic sulfur, this result is expected. Each individual reaction of the form



should yield an H₂S evolution curve similar to that shown in Figure 1. The parameters characterizing that curve T_0 , V_0 , and $(dV/dT)_{T_0}$ should reflect the kinetics for the individual process. The overall H₂S evolution curve will be composed of the sum of the set of overlapping curves characterizing each of the individual reactions. In the absence of any knowledge on the individual processes an experimental result such as given in Figure 4 can be resolved into individual processes in infinitely many ways. However, if the kinetics of the individual processes are known a priori, a unique resolution of the experimental results can be achieved.

Iron Pyrite

Since iron pyrite is known to be a major source of sulfur in coal, we conducted non-isothermal experiments on samples of iron pyrite obtained from the U.S. Bureau of Mines. In these experiments the back reaction of H_2S with iron was suppressed by using a very high hydrogen flow rate and a very small sample of iron pyrite. The heating rate employed was 4°C per minute. The experimental data on the non-isothermal evolution of H_2S from pyrite are shown in Figure 5. These results clearly indicate two reactions producing hydrogen sulfide. It is reasonable to suppose that these reactions are the following:



Independent measurements on the reactions of hydrogen with iron sulfide have confirmed that the higher temperature peak corresponds to the sulfide reduction. The experimental data shown in Figure 5 was obtained using a hydrogen pressure of one atmosphere. Isothermal measurements on the kinetics of these reactions as a function of pressure have established the first order dependence on hydrogen pressure.

These experimental results on pyrite may be analyzed in a straight forward manner to yield the kinetic parameters for the two reactions. The procedure used is as follows: First we sketch in two peaks of the type shown in Figure 1 which give a reasonable fit to the experimental points. The values of the parameters characterizing the curves are read off of these curves. These parameters are the temperature corresponding to each of the peaks, T_0 ($^\circ\text{K}$), the area of the peak, V_0 , and the amplitude of the peak at T_0 . From these values a dimensionless

parameter β as given by Equation (9) is computed and using this value the value of the dimensionless parameter α is read off the curve given in Figure 2. The values of the activation energies E and pre-exponential factor k_0 are then computed using Equations (14) and (15). The results are then double checked by recomputing the H_2S evolution peak corresponding to these parameter values using Equation (5). The calculated peaks are then replotted with the experimental data and the accuracy of the fit is checked. By these procedures we find for the pyrite reaction

$$E = 47 \text{ kilocalories per mole}$$

$$k_0 = 2.8 \times 10^{12} (\text{atm } H_2)^{-1} \text{ min}^{-1}$$

and for the sulfide reduction

$$E = 55 \text{ kilocalories per mole}$$

$$k_0 = 2.1 \times 10^{13} (\text{atm } H_2)^{-1} \text{ min}^{-1}$$

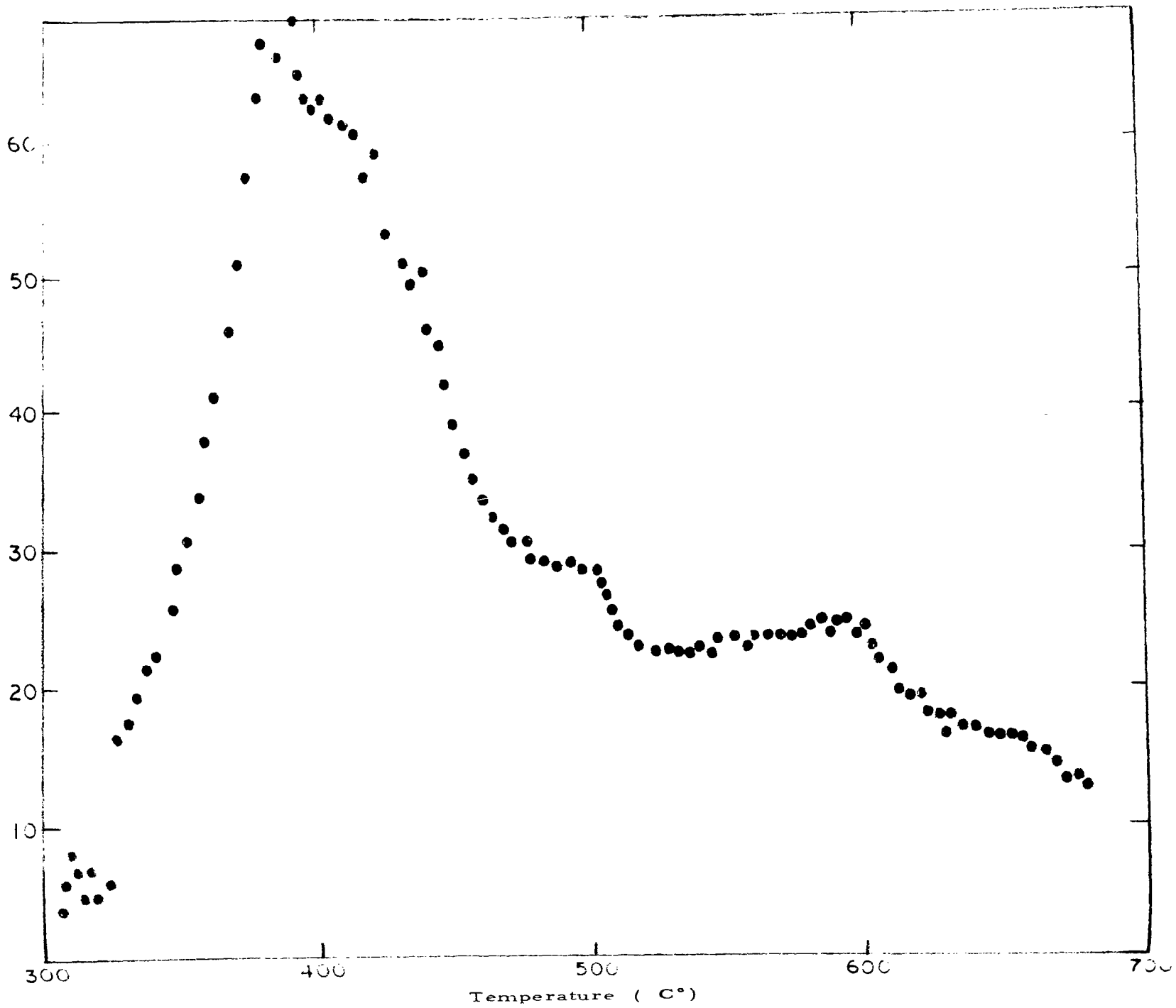
The calculated H_2S evolution curves for these two reactions are compared with the experimental data in Figure 6. The calculated H_2S evolution for the sum of the two processes is shown in the dash line in the figure. The fit between calculation and experimental could obviously be improved by slightly adjusting the amplitudes of the two peaks. However, the amplitudes reflect the stoichiometries of the reaction while the locations and shapes of the peaks reflect the kinetics. These results suggest that the pyrite sample was not pure FeS_2 but rather initially contained a small amount of sulfide.

The details of the analysis of the non-isothermal results for pyrite are illustrated in Table I and Figures 6 and 7. The temperature at the pyrite peak is read from Figure 6 as $510^\circ C$ which, for the calculation, is converted to $^\circ K$ giving $T_0 = 783^\circ K$. The peak drawn in on Figure 6

to approximate the experimental results has an amplitude of 51 units where in this case the concentration unit is taken arbitrarily as millivolts of mass spectrometer response to the mass 34 H_2S^+ peak. The area of the peak V_0 is 3360 °K mv. From this parameter value the calculated value of the dimensionless parameter $\beta = 11.9$ and the quantity required in graphical analysis, $1 + \ln \beta = 3.48$. To define α we located this value of $1 + \ln \beta$ on the ordinate of Figure 7. Then, as illustrated in Figure 7, the corresponding value of the abscissa for the plotted function gives the value of α which, in this case, is 30.6. The activation energy and pre-exponential factor are then calculated from the value of α according to Equations (14) and (15), giving the values shown on Figure 6 and Table I. A simple detailed step by step analysis of the sulfide reduction is also illustrated in Table I and Figures 6 and 7.

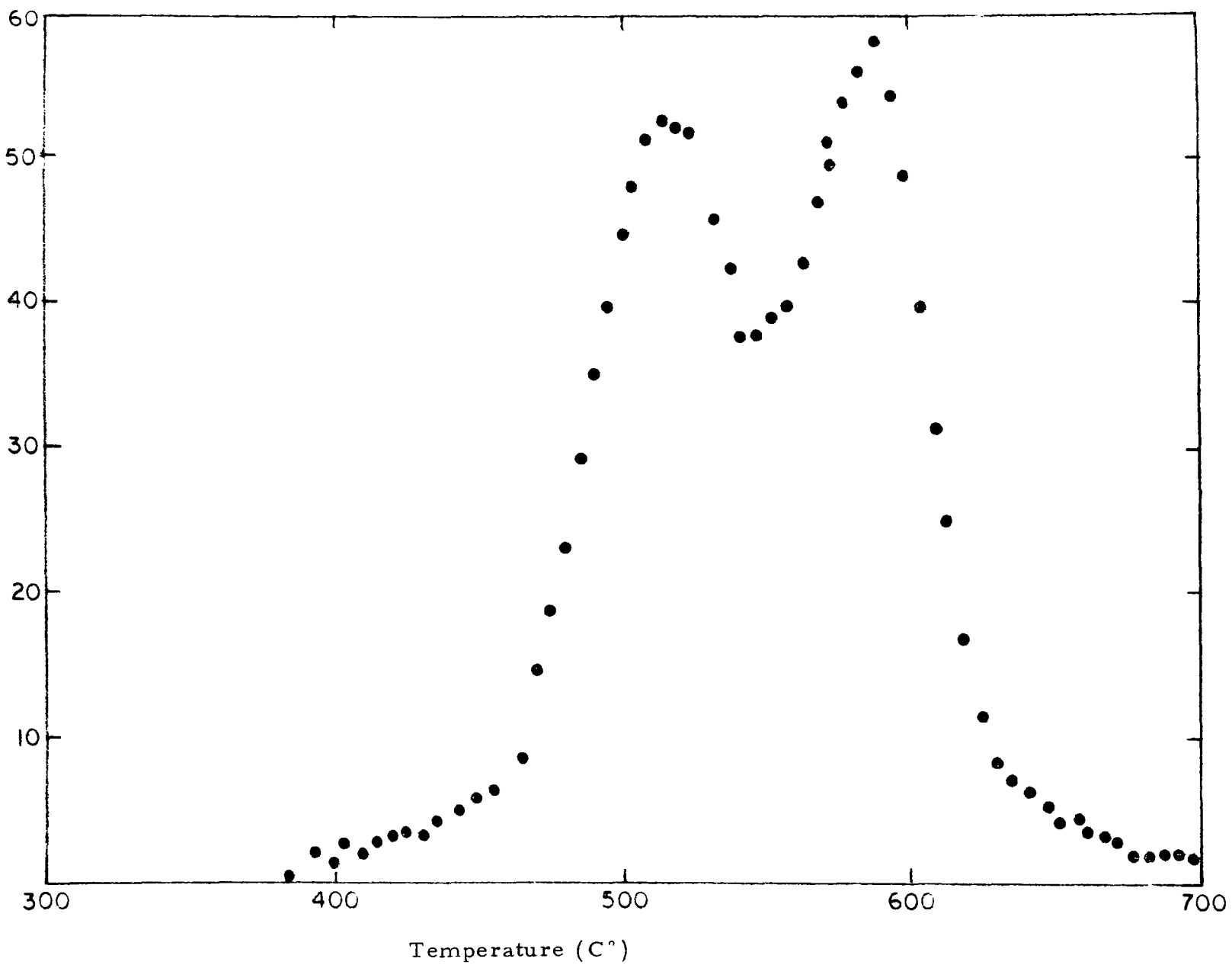
Organic Sulfur

The pyrite sulfur clearly accounts for most of the inorganic sulfur found in coal, but there is also generally substantial amounts of organic sulfur and it is well known that this sulfur may exist in many different kinds of bonding arrangements within the coal. In an attempt to investigate behavior of the organic sulfur on a somewhat simpler, but, related system, we prepared artificially some organic sulfur-containing material. A sample of essentially mineral free charcoal was reacted with hydrogen sulfide in a stream of helium to produce a sulfurated carbon which contained approximately 2.5% sulfur. Non-isothermal measurements on the desulfurization of this material in both hydrogen and helium were carried out. The results of one such experiment are given in Figure 8. In this experiment the sample size and flow rate of hydrogen used were the same as that employed on the major series of non-isothermal experi-



H₂S Concentration (Arbitrary Units)

Figure 4. H₂S evolution in a non-isothermal experiment at one atmosphere of hydrogen on Illinois 5% sulfur coal, SRI No. 4.



H_2S Concentration (Arbitrary Units)

Figure 5. H_2S evolution in a non-isothermal experiment at one atmosphere of hydrogen on pyrite

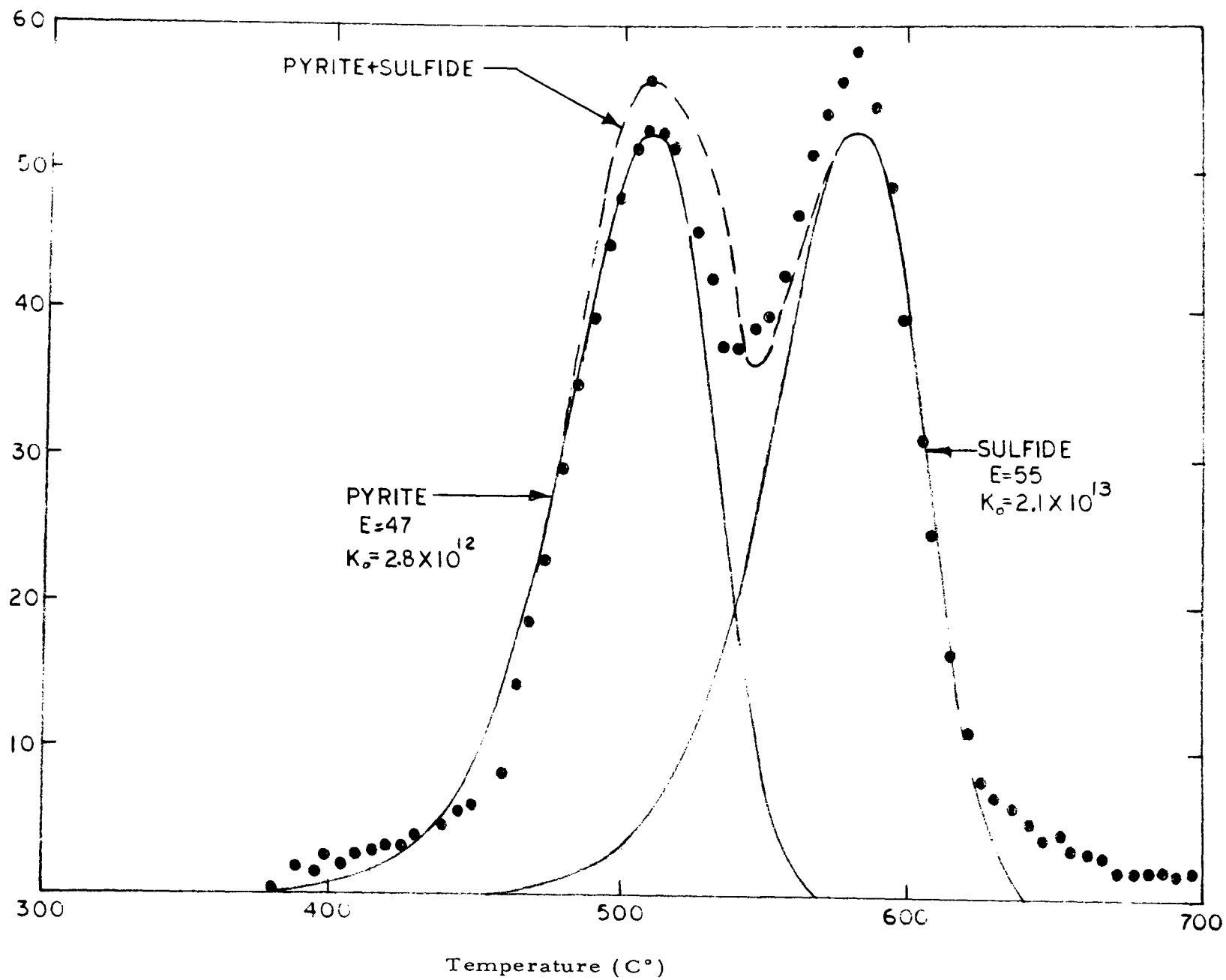


Figure 6. Kinetic analysis of the non-isothermal measurement on pyrite

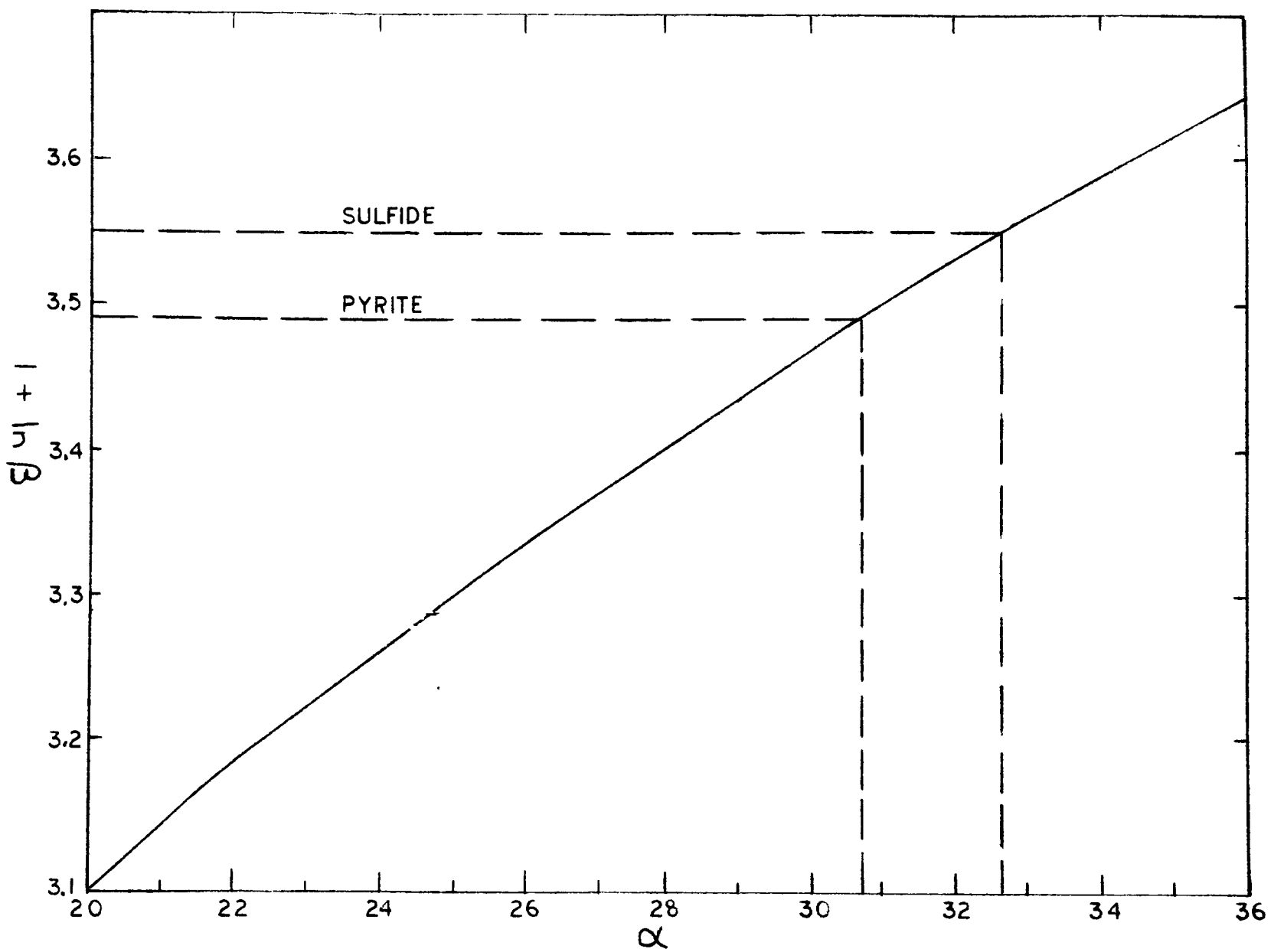
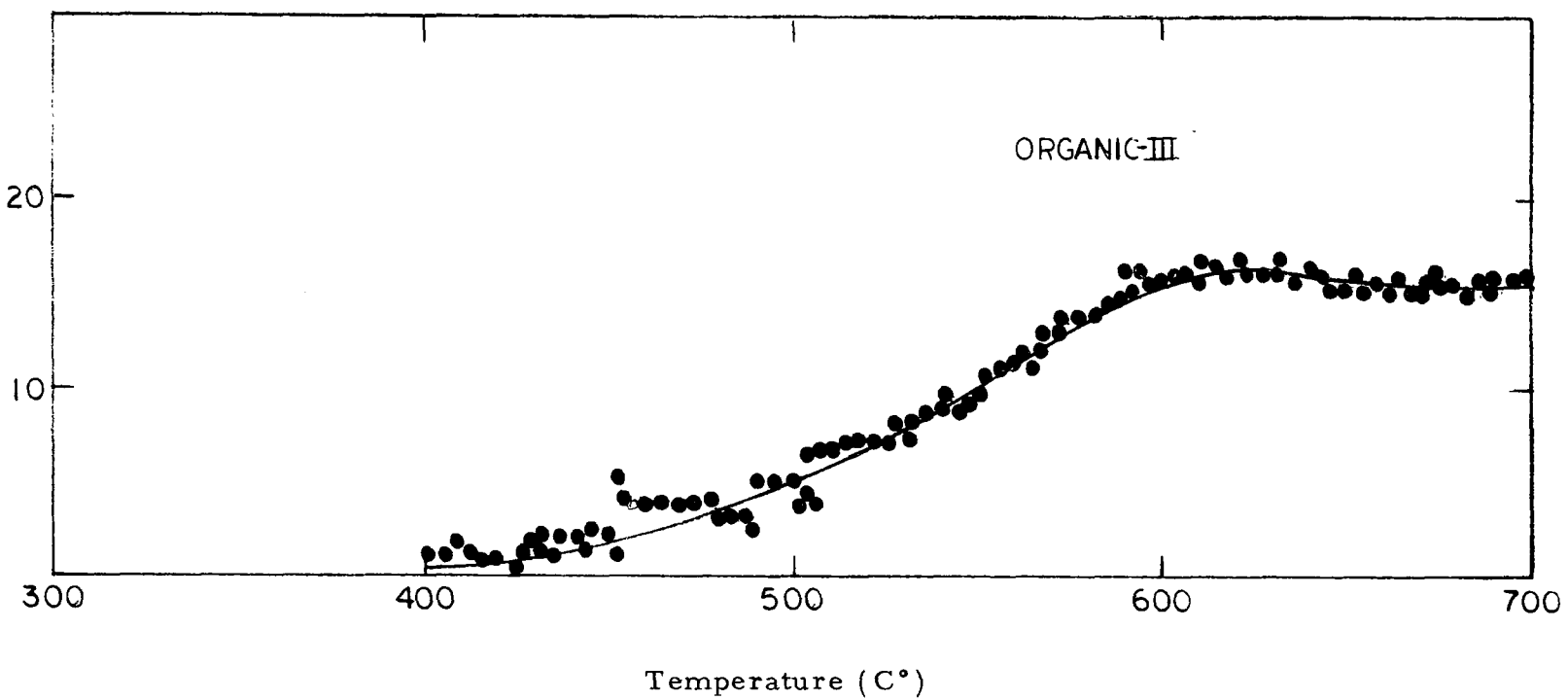


Figure 7. Graph for obtaining the kinetic parameters from non-isothermal experimental data. The dash lines illustrate the calculations involved in the analysis of the experiment on pyrite.

TABLE I DETAILED ANALYSIS OF NON-ISOTHERMAL EXPERIMENT
ON PYRITE

| <u>REACTION</u> | <u>$\text{FeS}_2 + \text{H}_2 \rightarrow \text{FeS} + \text{H}_2\text{S}$</u> | <u>$\text{FeS} + \text{H}_2 \rightarrow \text{Fe} + \text{H}_2\text{S}$</u> |
|---|---|--|
| T_o (°K) | 783 | 853 |
| $(dV/dT)_{T_o}$ (mv) | 51 | 51 |
| V_o (°K. mv) | 3360 | 3360 |
| $\beta = \frac{T_o}{V_o} \frac{dV}{dT}_{T_o}$ | 11.9 | 12.8 |
| $1 + \ln \beta$ | 3.48 | 3.55 |
| α | 30.6 | 32.5 |
| $E = RT_o \alpha$ (kcal/mole) | 47 | 55 |
| $k_o = \frac{M_o}{T_o} e^{\alpha}$ (min ⁻¹) | 2.8×10^{12} | 2.1×10^{13} |



H₂S Concentration (Arbitrary Units)

Figure 8. H₂S evolution in non-isothermal experiment at one atmosphere of hydrogen on sulfurated carbon prepared from charcoal

ments on coals. It is clear from the results of studies to date on the sulfurated carbon that a single simple reaction does not account for the behavior of this material. Pending the completion of the kinetic investigation on the complex sequence of reactions involved in the desulfurization of these relatively stable organic sulfur species the empirical result corresponding to the smooth curve shown in Figure 8 has been used in the analysis on the results on coal. We have designated this form of organic sulfur as Organic III.

As will be discussed in the next section of this report, the kinetic evidence strongly suggests that the low-temperature peak in Figure 4 arises from reactions of two types of organic sulfur. We have designated these types as Organic I and II.

KINETICS OF H₂S EVOLUTION FROM TEN COALS

In the previous section it was shown how the non-isothermal evolution of H₂S from the coal designated as SRI-4 (see Figure 4) could not be attributed to a single reaction, as was the case for CH₃SH (see Figure 3). In point of fact, a minimum of five reactions is necessary to account for the non-isothermal H₂S evolution curve in Figure 4. The H₂S evolution in some characteristic reactions probably involved in coal desulfurization is discussed in the previous section.

To proceed further in our analysis it is useful to consider H₂S evolution studies, similar to that depicted in Figure 4, of ten diverse samples of coal. The results of non-isothermal kinetic experiments for these ten coals are summarized in Figures 9 and 10. Certain points in common and certain differences should be noted in these results. All of the H₂S evolution curves show a peak in the range between 380°C and 430°C. All of the coals high in pyrite show secondary peaks very close to those found experimentally for the sample of pyrite as illustrated in Figure 6. However, in general for these coals these peaks appear to occur at slightly lower temperatures typically from 10 - 20°C. If we assume that results on the pyrite are valid for coal we would expect that the presence of the carbon should have little effect on the activation energies for these reactions. But, because of both the production of hydrogen from within the coal and the possibility of the absorption of hydrogen on the carbon surface, we might expect that the pre-exponential factor, which is expressed in terms of the concentration of hydrogen in the bulk gas stream, might be increased in the case of the coal by these effects, increasing the

surface concentration of hydrogen for a given bulk gas concentration of hydrogen. A downward shift in the temperature corresponding to the peak in the H₂S evolution from pyrite of 20° C corresponds to an increase in the pre-exponential factor of about 40%. Data obtained by us and by Powell in his earlier work on the forms of sulfur in char, as a function of carbonizing temperature, support the hypothesis that the secondary peaks in these non-isothermal results do correspond to the reaction of the pyritic and sulfide sulfurs. Similarly from this work, we suggest that the low temperature peaks in the non-isothermal results correspond to the reaction of relatively more reactive organic sulfur compounds in coal. A single reaction cannot account for the variation in the location and shape of the low temperature peak for all of these ten coals. However, we have found that two processes, one with T₀ corresponding to 380° C and a second with T₀ corresponding to 430° C satisfactorily account for the low temperature peak in all ten coals. The kinetic parameters for these processes which we have designed as Organic I and Organic II are as follows:

ORGANIC I

E=34.5 kcal/mole

k₀=3.1 x 10¹⁰ atm H₂⁻¹ min⁻¹

ORGANIC II

E=41.5 kcal/mole

k₀=2.8 x 10¹¹ atm H₂⁻¹ min⁻¹

It is, of course, possible that more than two processes contribute to this low temperature peak, however, only the two are required to account for the experimental results.

We are now in a position to discuss the resolution of the H₂S evolution curve for SRI No. 4 given in Figure 4, into individual processes. The five processes we have identified in the preceeding discussion are the conversions to H₂S of three forms of organic sulfur, of pyrite, and of sulfide. This resolution into the individual processes was performed graphically by drawing in the peaks corresponding to the individual processes and

adjusting the amplitude of the peak, without changing the peak location, until a best fit to the experimental data is obtained. The fit is determined by comparing the sum of all of the H_2S evolution peaks with the experimental data. The result of this analysis is shown in Figure 11. In the figure the dashed line represents the sum of the individual processes shown in the figure and the agreement with the experimental points is quite satisfactory with one exception. In the region about 530° there appears to be a significant amount of sulfur evolution which is not accounted for by these five processes. This discrepancy occurs in most of the coals studied but is particularly prominent in coal No. 7, the Maryland coal. This discrepancy may indicate that an additional desulfurization process occurs which we have not taken into account; however, our recent experiments, in an attempt to further understand the Organic III set of reactions, have indicated that the results obtained on the artificial sample of sulfurated carbon may not be directly applicable to coal. It now appears that a proper representation of the Organic III sulfur removal may remove this discrepancy.

One additional point that should be mentioned concerning this analysis of the desulfurization of the coal designated as SRI-4 is that the total amount of sulfur evolved from the pyrite and sulfide processes appears rather lower than would be expected from the amount of iron pyrite in the coal from the ASTM analysis. However, this coal contains an unusually high calcium content. Our separate experiments on the reaction of H_2S with calcium oxide and calcium carbonate have shown that the reaction of H_2S with these materials in the temperature range above 500° is extremely fast so that nearly one half of the sulfur, which might otherwise be evolved in the pyrite and sulfur peaks, is converted to calcium sulfide and retained in the char.

In view of the success achieved in resolving the H_2S evolution curve for SRI-4, we have applied the same technique to the resolution of the non-

isothermal H₂S evolution curves for nine other representative coal samples. The overall evolution curves are shown in Figure 9 and 10 while in Figures 12-20 each curve is shown in more detail and is resolved into the contribution from the five characteristic reactions previously discussed.

In each case a sample of coal was heated at 4° per minute in hydrogen at one atmosphere. Flow conditions were maintained with appropriate control of residence time. The exit gases were analyzed continuously for hydrogen sulfide by mass spectrometry. Preliminary calibrations showed that the continuous mass spectrometric measurements were in agreement with analyses by gas liquid chromatography. Details of the experimental methods are given in the Appendix of report SRI 68-13.

The ten coal samples investigated were from Illinois, Ohio, Maryland, Pennsylvania, and Kentucky. With the exception of two coals these are all high in sulfur. The Illinois coals were provided by Mr. Jack Simon of the Illinois State Geological Survey. The coals from other states were provided by the U.S. Bureau of Mines.

Identification and ASTM Analyses of Ten Coals

Tables II-VI summarize the identification and analyses of the ten coal samples. In Table II the source, nominal percent sulfur, and the bed are shown. In addition, permission was obtained to list the mine from which each sample was obtained.

In Table III the forms of sulfur are shown as percent of coal. These analyses and the ones summarized in Table IV through VI were done according to the ASTM procedures. Table IV shows the mineral analysis, Table V

shows the proximate analysis, and the sulfur in ash and in coke are given in Table VI.

As mentioned previously the H_2S evolution curves from the non-isothermal desulfurization of ten diverse coals are shown in Figures 11-20. For each coal the overall evolution curve is resolved into contributions from the five specific desulfurization reactions of Organic I, II, III, pyrite and sulfide and in all cases these five processes account for from 87-99% of the total H_2S evolution. The successful decomposition of any one H_2S evolution curve into five characteristic processes is by itself, not too significant. However, the successful decomposition of the H_2S evolution curves for all ten coals into the same characteristic five processes is highly significant and strengthens our conclusion that to a reasonably good approximation the temperature-programmed desulfurization may be viewed as a sequence of characteristic and independent chemical reactions applicable to coal in general.

The principal discrepancy in this approximation appears to occur in the temperature region around 520° C and above 600°. This may be due to an oversimplified treatment of the poorly-understood series of reactions comprising the desulfurization of Organic III, to additional reactions not yet identified, or both.

Finally, in Table VII we summarize the relative contributions of the five characteristic processes to the total desulfurization process of each coal.

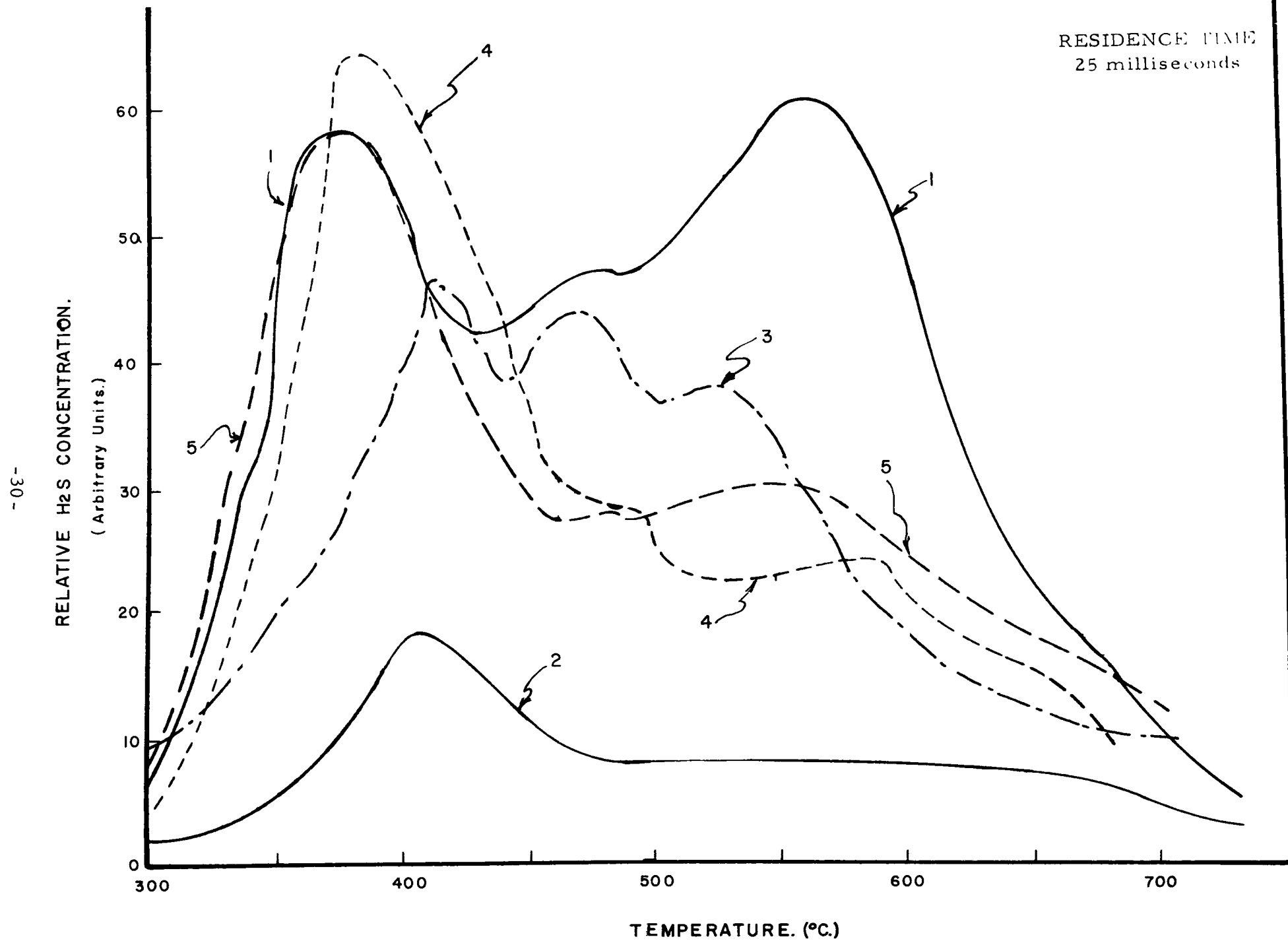


FIGURE 9. NON-ISOTHERMAL H₂S EVOLUTIONS IN H₂ FROM COALS SRI

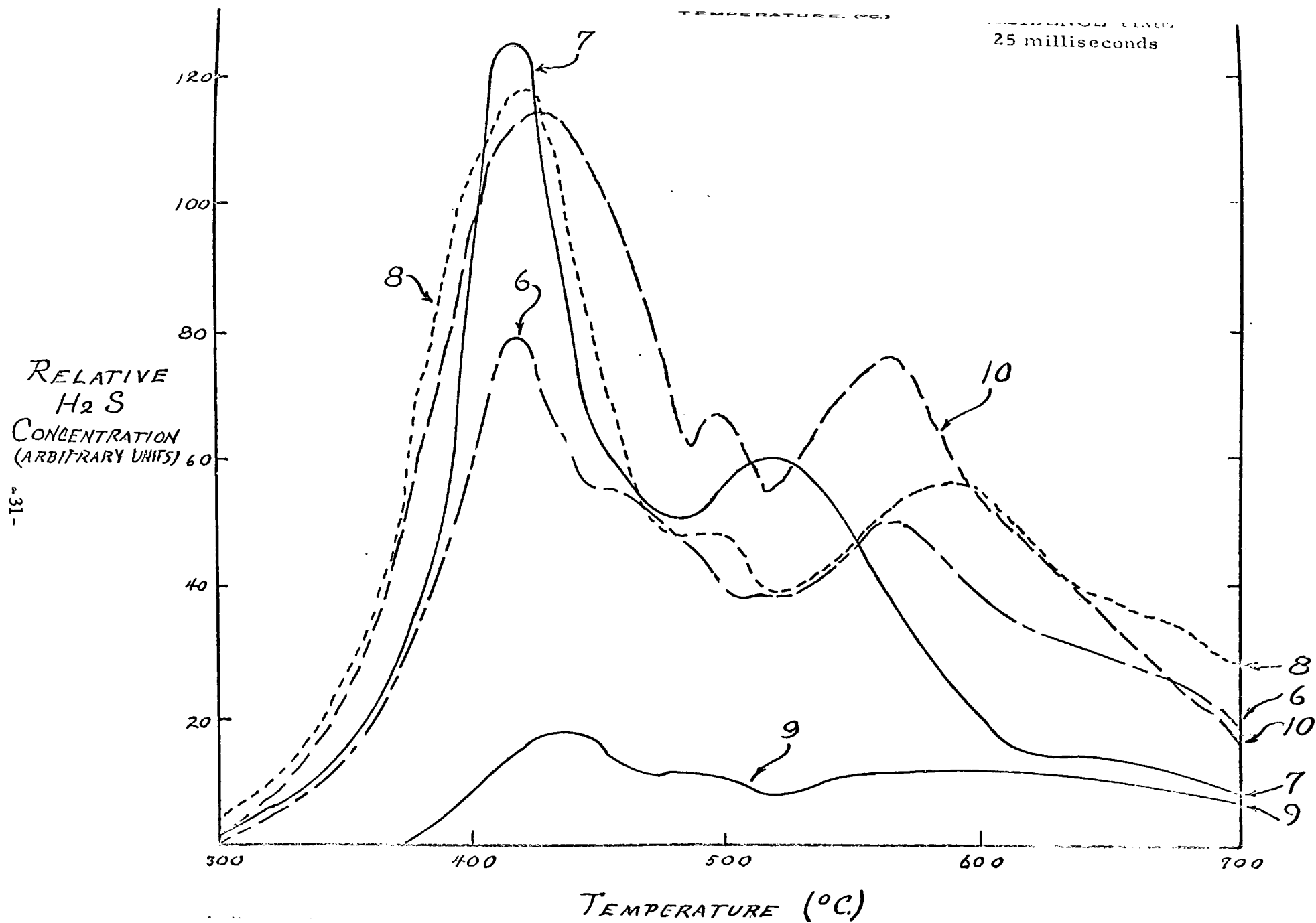


FIGURE 10. NON-ISOTHERMAL H_2S EVOLUTIONS IN H_2 FROM COALS SRI NUMBERS 6 THROUGH 10.

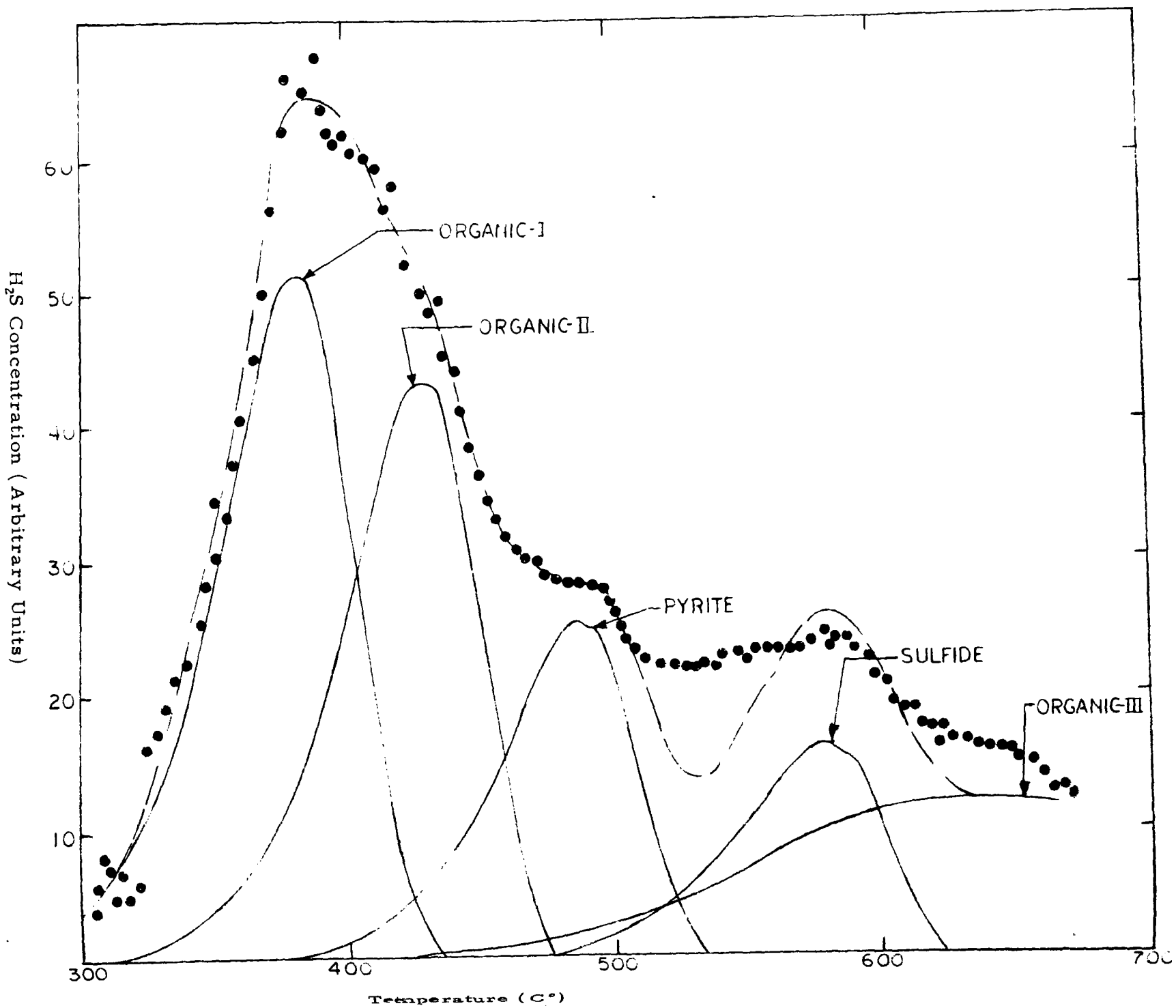


Figure 11. Kinetic analysis and resolution into individual processes of the H₂S evolution in a non-isothermal experiment at one atmosphere of hydrogen on Illinois 5% sulfur coal, SRI No. 1.

TABLE II. SUMMARY OF ANALYSES OF TEN COALS
COAL SAMPLE IDENTIFICATION

| <u>SRI NO.</u> | <u>SOURCE</u> | <u>% SULFUR NOMINAL</u> | <u>MINE CROWN</u> | <u>BED SEAM</u> |
|--------------------|------------------------------|-----------------------------|-----------------------|---------------------------|
| 1 | ILLINOIS ISGS: 1-1 | 5 | | 6 |
| 2 | ILLINOIS ISGS: 5-1 | 1 | NO. 21 | 6 |
| 3 | ILLINOIS ISGS: 25-1 | 2.5 | NORTHERN ILLINOIS | 2 |
| 4 | ILLINOIS ISGS: 28-1 | 5 | WILL SCARLET | DAVIS |
| 5 | ILLINOIS ISGS: 32-1-1.60F | 4.5 | LITTLE DOG | SEAM No. 6 |
| 6 | OHIO USBM: 205 | 3 | STANLEY | PITTSBURGH NO. 8 |
| 7 | MARYLAND USBM: 106 | 3 | ROYAL | FRANKLIN |
| 8 | OHIO USBM: 107 | 3.5 | CRAVAT | PITTSBURGH NO. 8 |
| 9 | PENNSYLVANIA USBM: 109 | 1 | GREENWICH NO. 8 | LOWER KITTAN- NING (B) |
| 10 | KENTUCKY USBM: 110 | 4 | SHAMROCK | NO. 14 |

TABLE III. SUMMARY OF ANALYSES OF TEN COALS
FORMS OF SULFUR (Percent of Coal)

| <u>SRI NO.</u> | <u>SAMPLE</u> | <u>SULFATE</u> | <u>PYRITIC SULFUR</u> | <u>ORGANIC SULFUR</u> | <u>TOTAL</u> |
|--------------------|-----------------|----------------|---------------------------|---------------------------|--------------|
| 1 | ILLINOIS 5% | 0.38 | 0.96 | 2.48 | 3.82 |
| | | 0.79 | 2.71 | 0.91 | 4.41 |
| | | 0.36 | 1.89 | 2.47 | 4.72 |
| 2 | ILLINOIS 1% | 0.02 | 0.25 | 0.62 | 0.89 |
| | | 0.00 | 0.29 | 0.62 | 0.91 |
| 3 | ILLINOIS 2.5% | 0.14 | 1.30 | 1.18 | 2.62 |
| | | 0.35 | 1.28 | 0.84 | 2.47 |
| 4 | ILLINOIS 5% | 0.13 | 3.10 | 2.06 | 5.29 |
| | | 0.13 | 3.22 | 1.27 | 4.62 |
| 5 | ILLINOIS 4.5% | 0.13 | 1.15 | 2.86 | 4.14 |
| | | 0.10 | 1.21 | 2.87 | 4.18 |
| 6 | OHIO 3% | 0.00 | 1.70 | 1.08 | 2.78 |
| | | 0.00 | 1.26 | 1.51 | 2.77 |
| 7 | MARYLAND 3% | 0.00 | 2.13 | 0.83 | 2.96 |
| | | 0.01 | 1.56 | 1.18 | 2.75 |
| 8 | OHIO 3.5% | 0.14 | 1.68 | 1.25 | 3.07 |
| | | 0.00 | 1.33 | 1.91 | 3.25 |
| 9 | PENNSYLVANIA 1% | 0.02 | 0.17 | 0.72 | 0.91 |
| | | 0.00 | 0.23 | 0.86 | 1.09 |
| 10 | KENTUCKY 4% | 0.00 | 3.50 | 1.15 | 4.65 |
| | | 0.00 | 1.81 | 1.35 | 3.16 |

TABLE IV. SUMMARY OF ANALYSES OF TEN COALS
MINERAL ANALYSES (Percent of Coal)

| <u>SRI NO.</u> | <u>SAMPLE</u> | <u>CALCIUM</u> | <u>MAGNESIUM</u> | <u>TOTAL IRON</u> | <u>PYRITIC IRON</u> |
|--------------------|-----------------|----------------|------------------|-----------------------|-------------------------|
| 1 | ILLINOIS 5% | 0.18 | 0.006 | 1.06 | 0.84 |
| 2 | ILLINOIS 1% | 0.007 | 0.02 | 0.34 | 0.22 |
| 3 | ILLINOIS 2.5% | 0.06 | 0.09 | 1.76 | 1.04 |
| 4 | ILLINOIS 5% | 1.39 | 0.07 | 3.54 | 2.70 |
| 5 | ILLINOIS 4.5% | 0.10 | 0.06 | 1.12 | 0.74 |
| 6 | OHIO 3% | 0.14 | 0.03 | 1.29 | 1.08 |
| 7 | MARYLAND 3% | 0.14 | 0.05 | 1.43 | 1.35 |
| 8 | OHIO 3.5% | 0.18 | 0.03 | 1.61 | 1.14 |
| 9 | PENNSYLVANIA 1% | 0.05 | 0.02 | 0.78 | 0.23 |
| 10 | KENTUCKY 4% | 0.29 | 0.05 | 2.41 | 1.55 |

TABLE V. SUMMARY OF ANALYSES OF TEN COALS
PROXIMATE ANALYSIS (Percent of Coal)

| <u>SRI NO.</u> | <u>SAMPLE</u> | <u>MOISTURE</u> | <u>VOLATILES</u> | <u>FIXED CARBON</u> | <u>ASH</u> |
|--------------------|-----------------|-----------------|------------------|-------------------------|------------|
| 1 | ILLINOIS 5% | 8.0 | 36.2 | 44.7 | 11.1 |
| 2 | ILLINOIS 1% | 5.4 | 33.8 | 54.6 | 6.2 |
| 3 | ILLINOIS 2.5% | 7.8 | 33.7 | 42.5 | 16.0 |
| 4 | ILLINOIS 5% | 1.9 | 37.6 | 43.2 | 17.3 |
| 5 | ILLINOIS 4.5% | 5.1 | 40.8 | 44.1 | 10.0 |
| 6 | OHIO 3% | 1.6 | 38.1 | 49.6 | 10.7 |
| 7 | MARYLAND 3% | 0.6 | 20.5 | 62.8 | 16.1 |
| 8 | OHIO 3.5% | 1.7 | 37.2 | 50.4 | 10.7 |
| 9 | PENNSYLVANIA 1% | 0.8 | 27.9 | 64.2 | 7.1 |
| 10 | KENTUCKY 4% | 1.8 | 31.3 | 46.5 | 20.4 |

SULFUR IN ASH AND COKE

| <u>SRI NO.</u> | <u>SAMPLE</u> | <u>SULFUR IN ASH % of ash</u> | <u>SULFUR IN FIXED CARBON</u> |
|--------------------|-----------------|-----------------------------------|-----------------------------------|
| 1 | ILLINOIS 5% | 1.18 | 3.84 |
| 2 | ILLINOIS 1% | 0.51 | 0.60 |
| 3 | ILLINOIS 2.5% | 0.26 | 2.00 |
| 4 | ILLINOIS 5% | 4.80 | 4.96 |
| 5 | ILLINOIS 4.5% | 0.12 | 1.99 |
| 6 | OHIO 3% | 0.03 | 2.47 |
| 7 | MARYLAND 3% | 0.07 | 2.29 |
| 8 | OHIO 3.5% | 0.31 | 2.73 |
| 9 | PENNSYLVANIA 1% | 0.31 | 0.80 |
| 10 | KENTUCKY 4% | 0.00 | 2.70 |

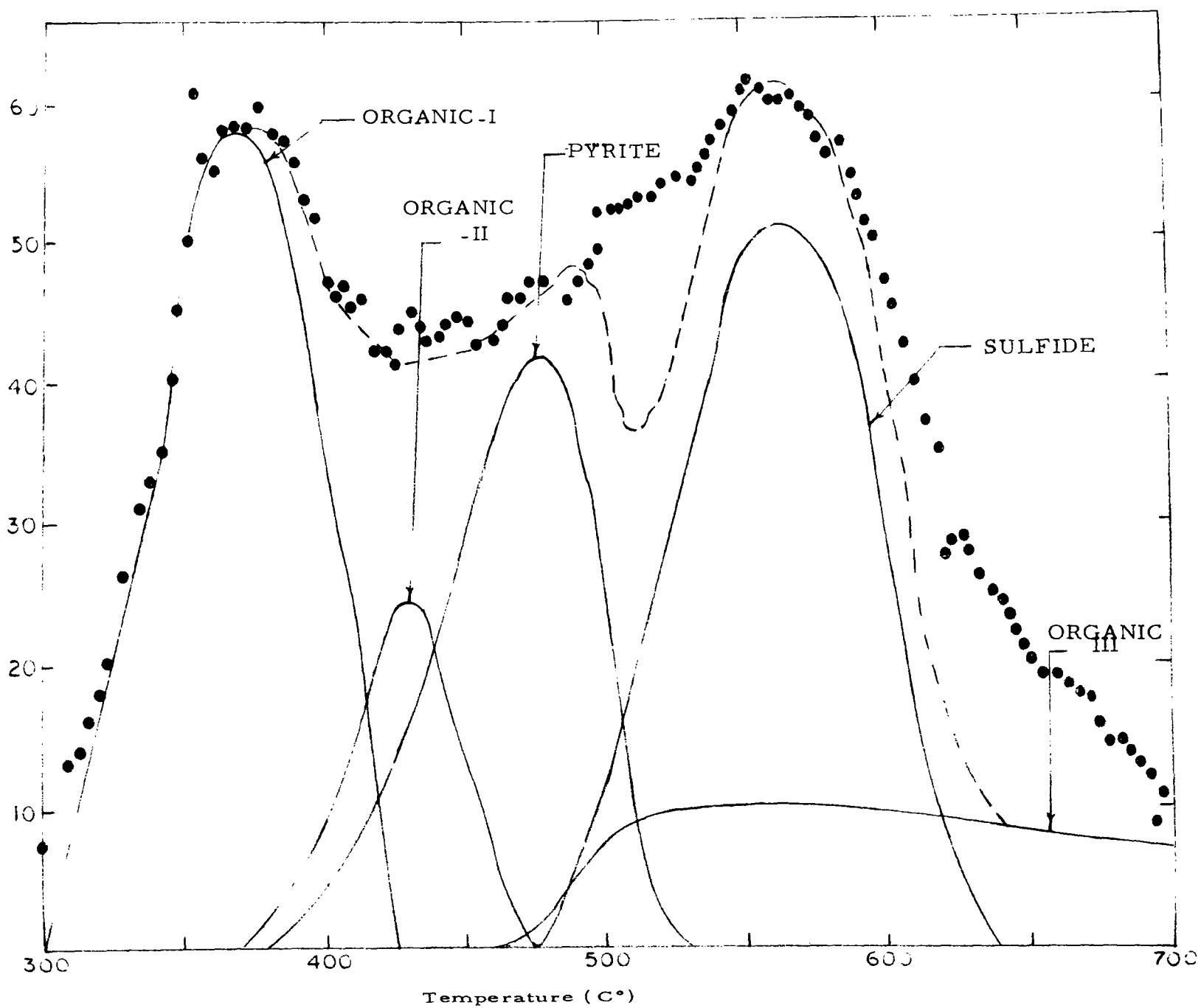


Figure 12. Kinetic analysis and resolution into individual processes of the H_2S evolution in a non-isothermal experiment at one atmosphere of hydrogen on Illinois 5% sulfur coal, SRI No. 1.

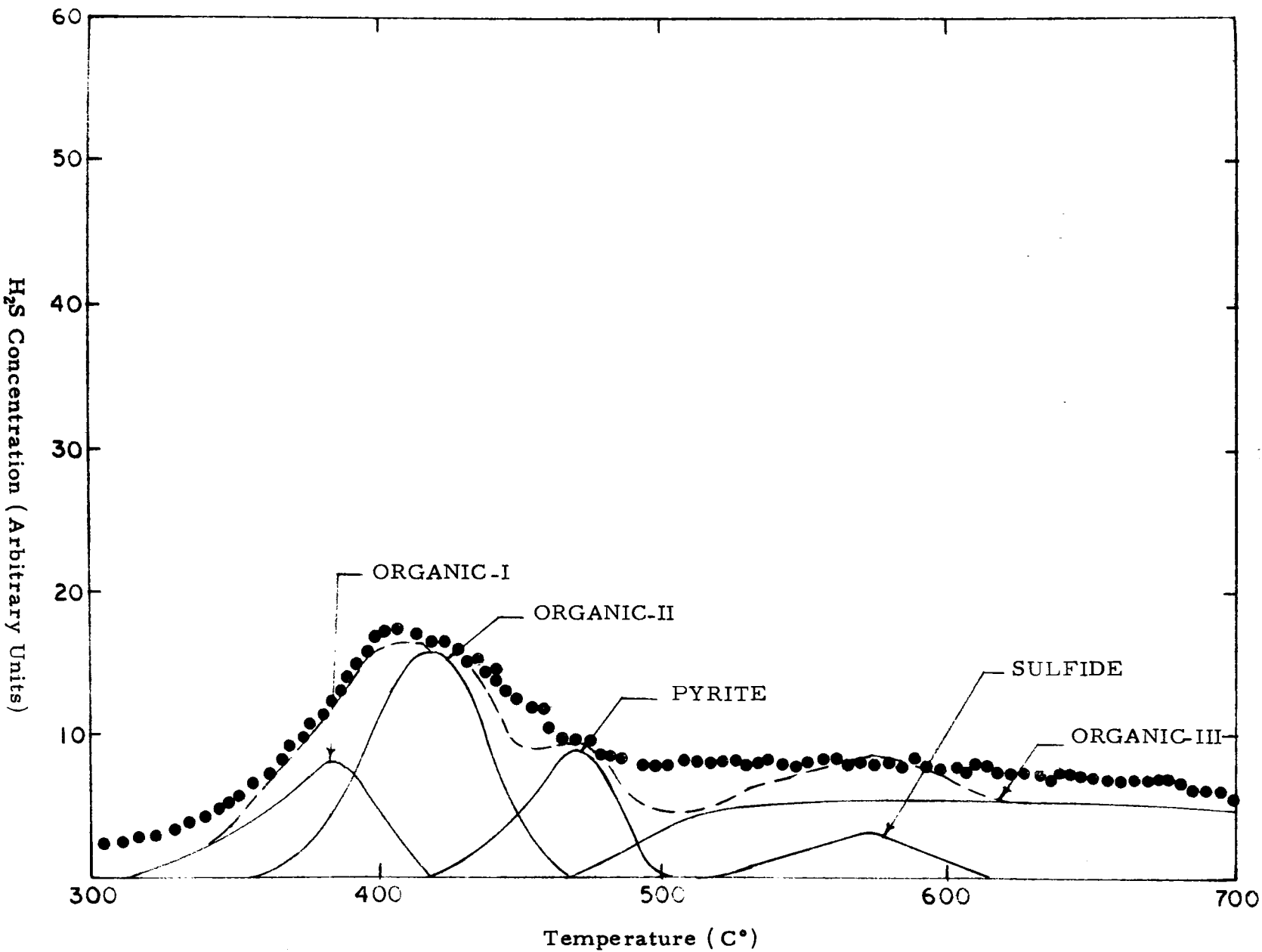
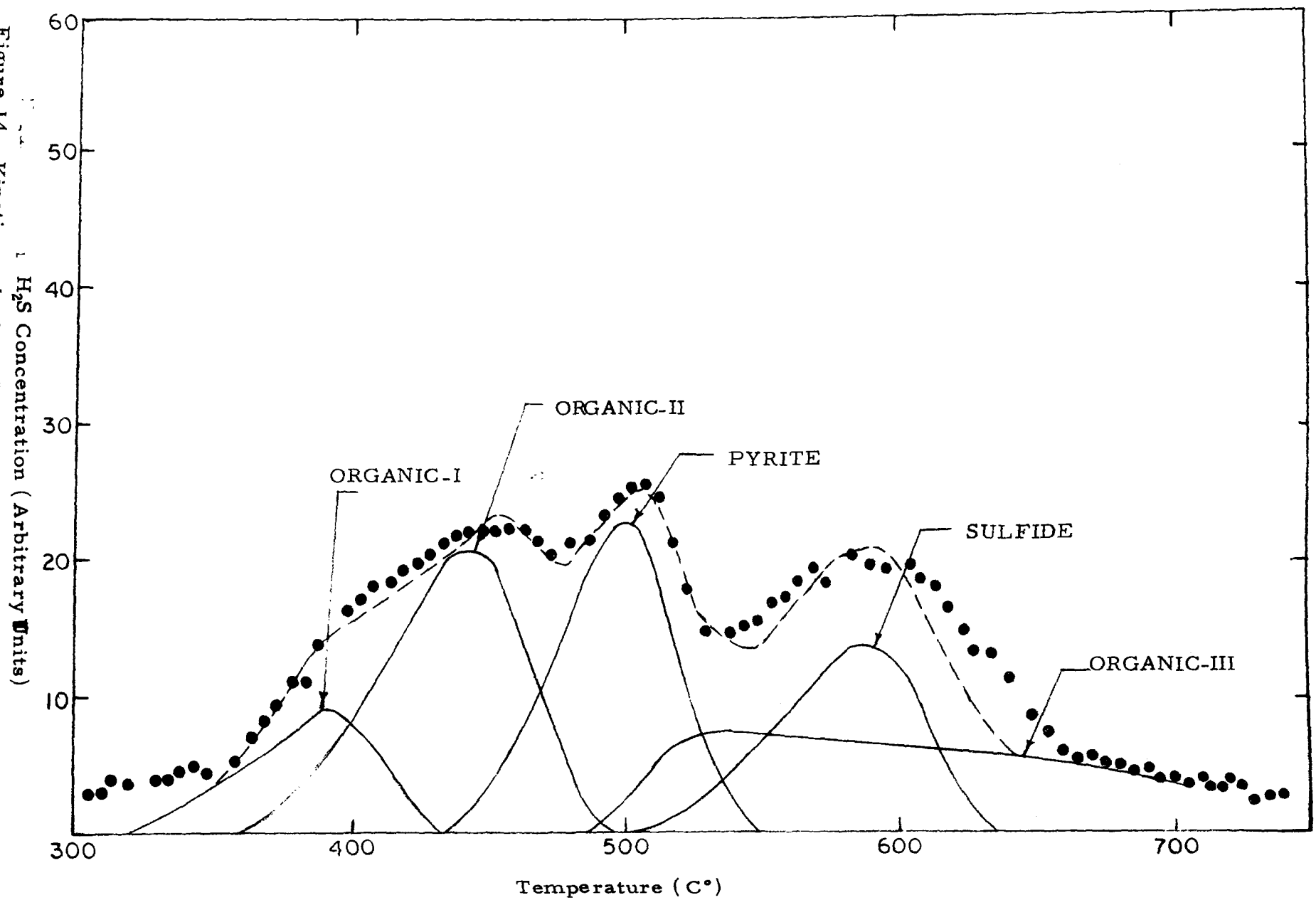


Figure 13. Kinetic analysis and resolution into individual processes of the H_2S evolution in a non-isothermal experiment at one atmosphere of hydrogen on Illinois 1% sulfur coal, SRI No. 2. -39-

Figure 14. Kinetic analysis and resolution into individual processes of the H_2S evolution in a non-isothermal experiment at one atmosphere of hydrogen on Illinois 2.5% sulfur coal, SRI No. 3



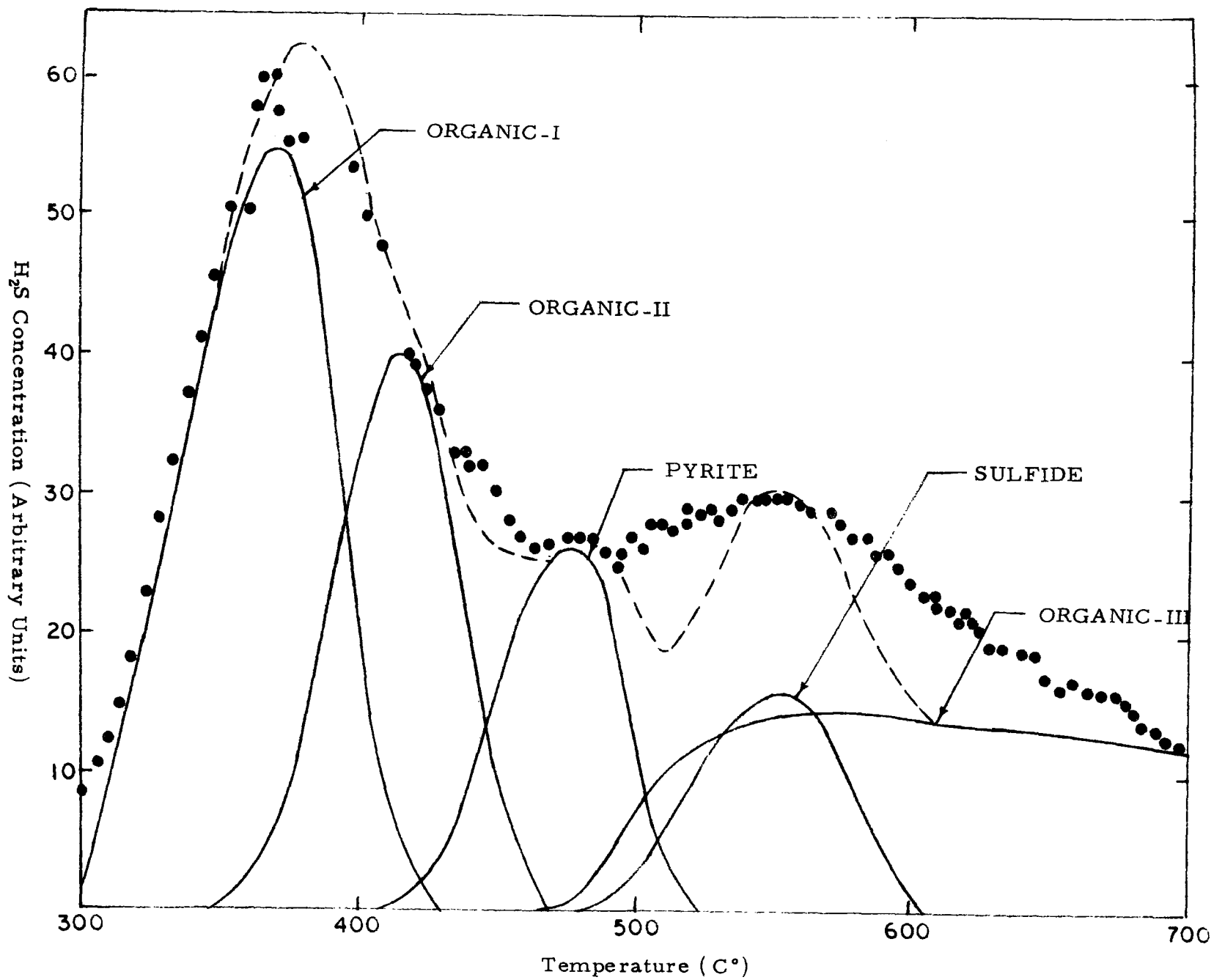


Figure 15. Kinetic analysis and resolution into individual processes of the H_2S evolution in a non-isothermal experiment at one atmosphere of hydrogen on Illinois 4.5% sulfur coal, SRI No. 5

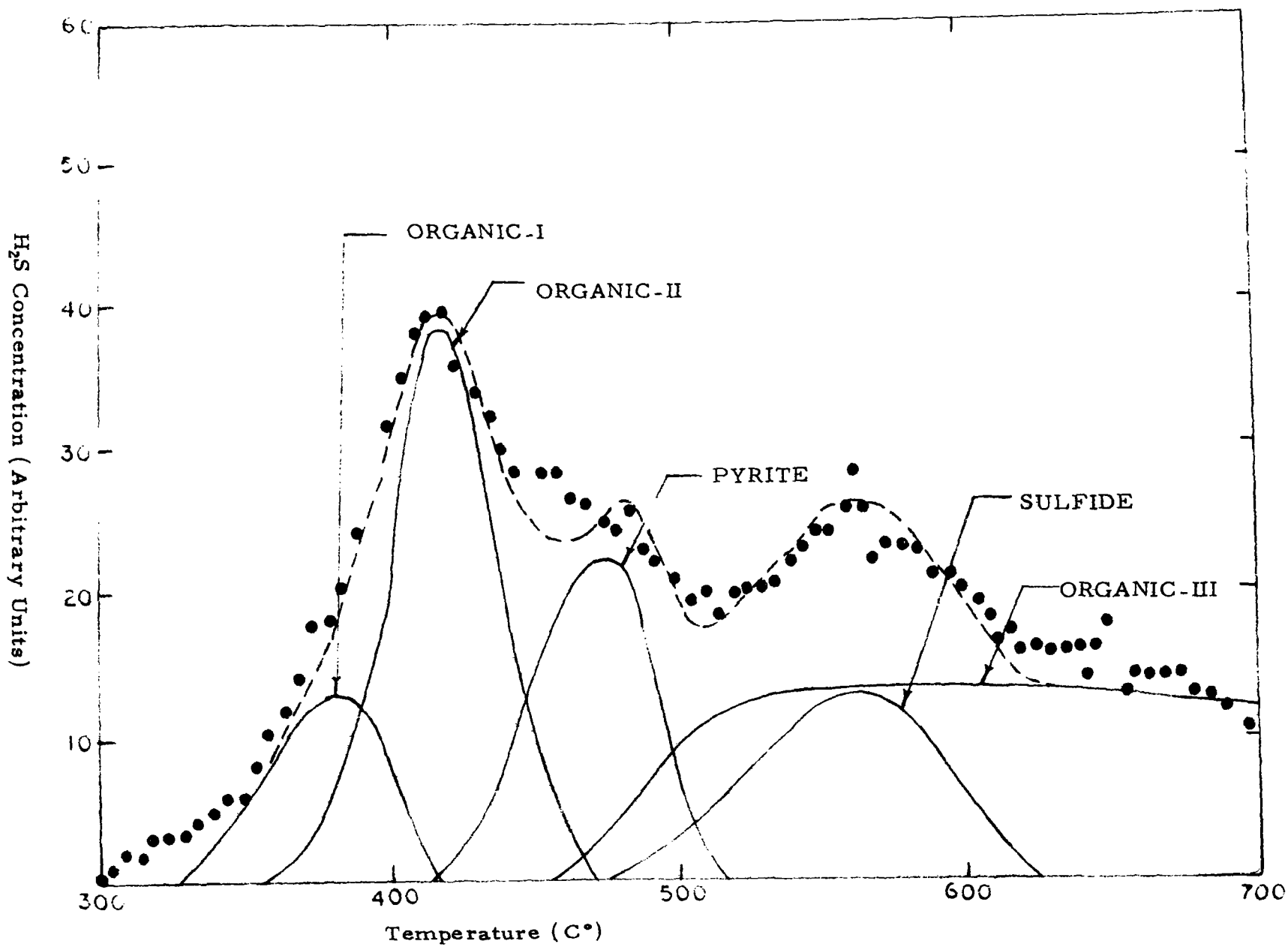
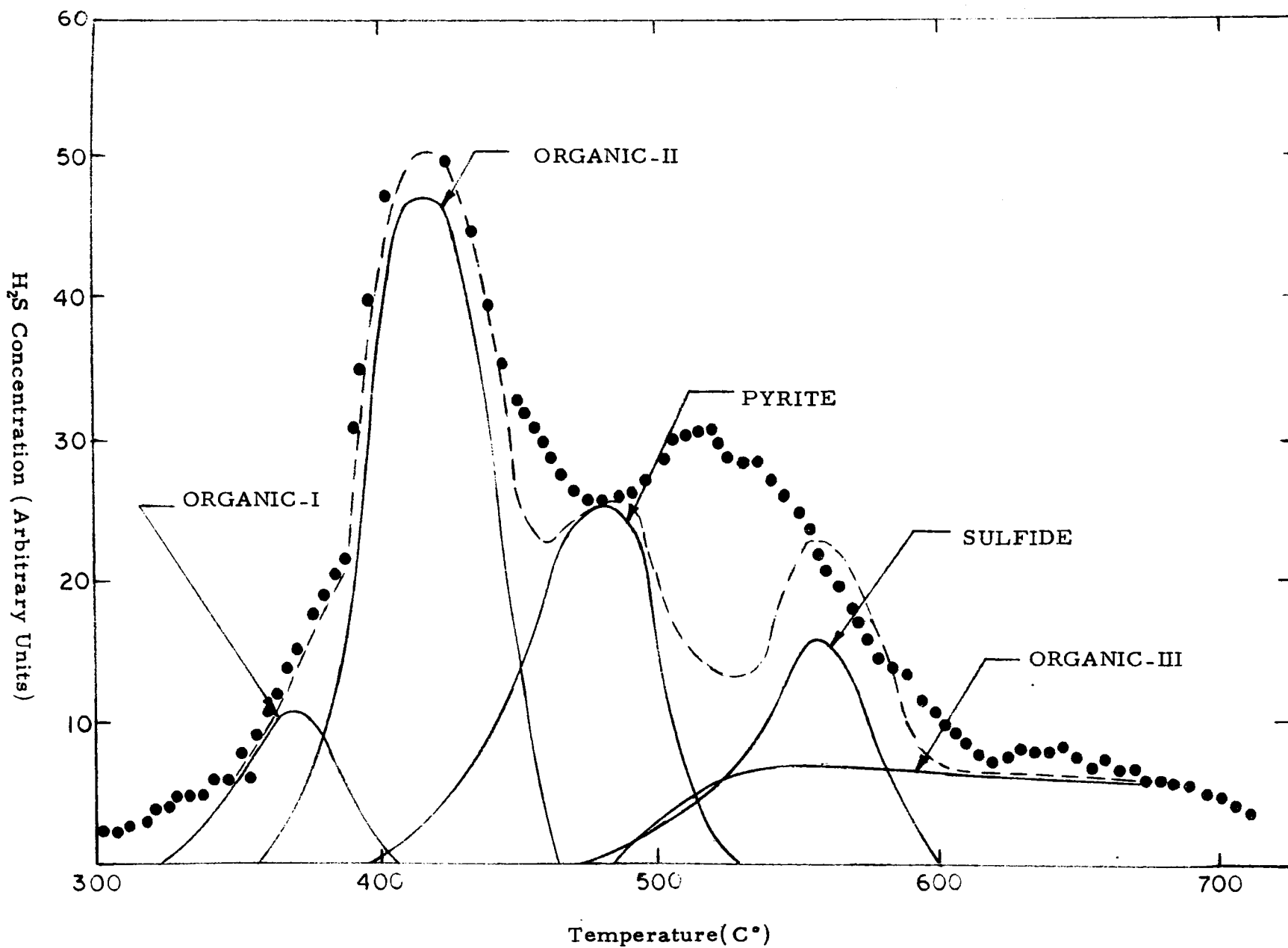


Figure 16. Kinetic analysis and resolution into individual processes of the H_2S evolution in a non-isothermal experiment at one atmosphere of hydrogen on Ohio 3% sulfur coal, SRI No. 6. -42-

Figure 17. Kinetic analysis and resolution into individual processes of the H_2S evolution in a non-isothermal experiment at one atmosphere of hydrogen on Maryland 3% sulfur coal, SRI No. 7



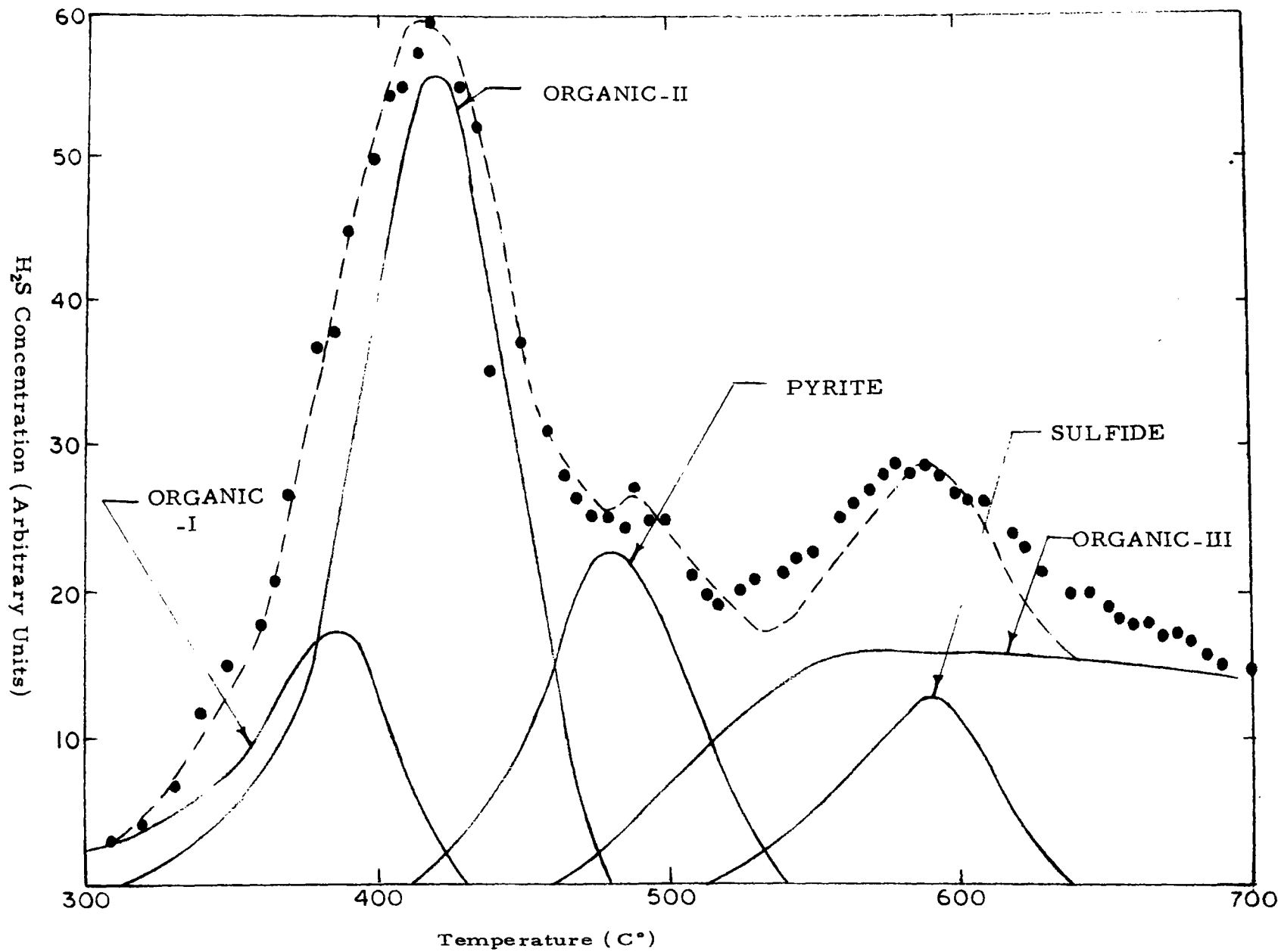


Figure 18. Kinetic analysis and resolution into individual processes of the H_2S evolution in a non-isothermal experiment at one atmosphere of hydrogen on Ohio 3.5% sulfur coal, SRI No. 8.

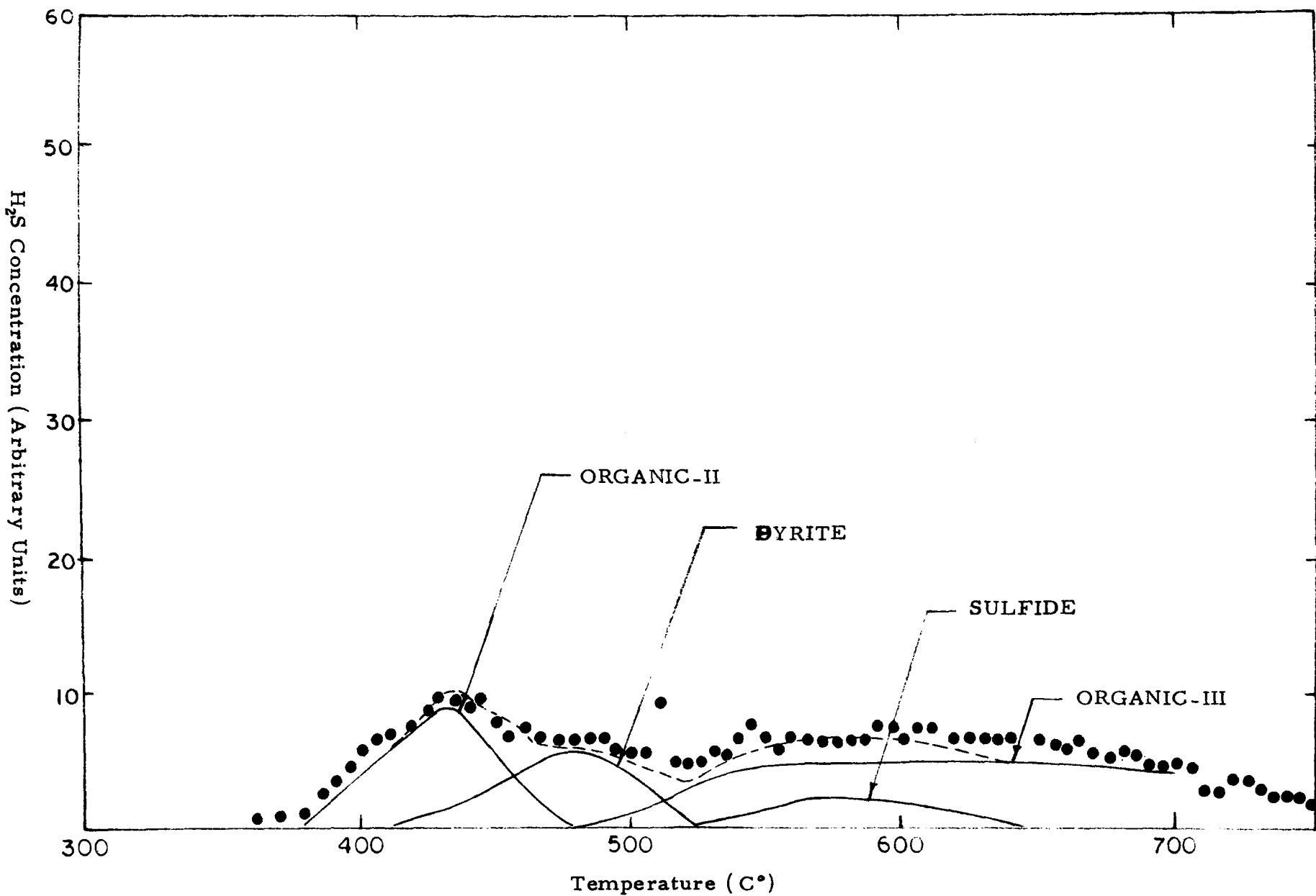


Figure 19. Kinetic analysis and resolution into individual processes of the H_2S evolution in a non-isothermal experiment at one atmosphere of hydrogen on Pennsylvania 1% sulfur coal, SRI No. 9.

Figure 20. Kinetic analysis and resolution into individual processes of the H_2S evolution in a non-isothermal experiment at one atmosphere of hydrogen on Kentucky 4% sulfur coal, SRI No. 10.

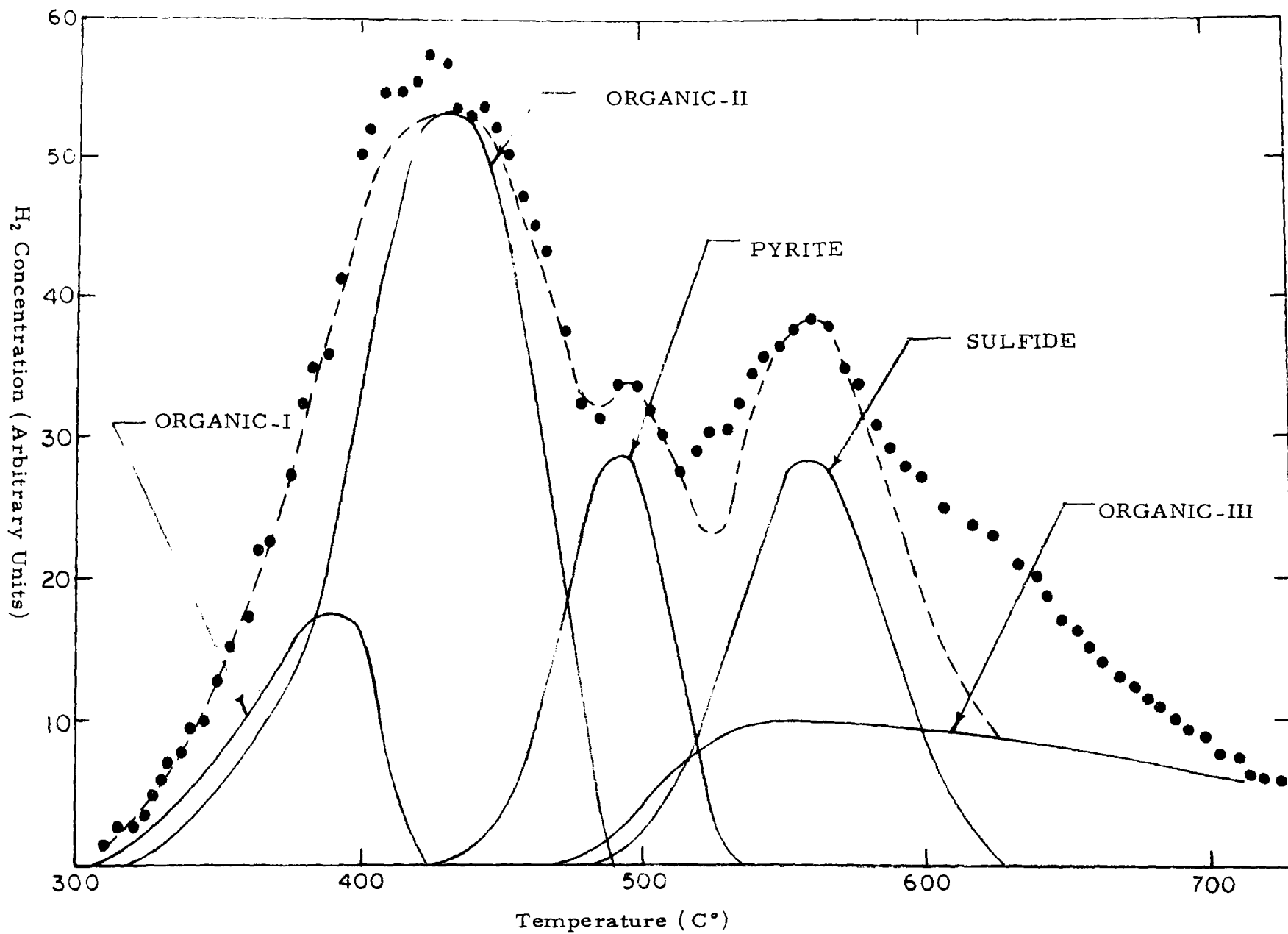


TABLE VII. RESOLUTION OF THE H₂S EVOLUTION CURVES INTO INDIVIDUAL REACTIONS

| COAL SRI NO. | SAMPLE | PERCENT OF TOTAL H ₂ S EVOLVED IN EACH DESULFURIZATION REACTION | | | | | |
|--------------------|-----------------|--|---------------|--------|---------|----------------|---------|
| | | ORGANIC I | ORGANIC II | PYRITE | SULFIDE | ORGANIC III | UNKNOWN |
| 1 | ILLINOIS 5% | 25 | 8 | 20 | 25 | 10 | 9 |
| 2 | ILLINOIS 1% | 17 | 30 | 15 | 6 | 20 | 11 |
| 3 | ILLINOIS 2.5% | 9 | 26 | 24 | 19 | 19 | 2 |
| 4 | ILLINOIS 5% | 33 | 27 | 15 | 6 | 16 | 3 |
| 5 | ILLINOIS 4.5% | 29 | 18 | 12 | 9 | 24 | 7 |
| 6 | OHIO 3% | 9 | 26 | 15 | 13 | 35 | 2 |
| 7 | MARYLAND 3% | 6 | 34 | 23 | 14 | 10 | 13 |
| 8 | OHIO 3.5% | 11 | 36 | 13 | 7 | 29 | 4 |
| 9 | PENNSYLVANIA 1% | - | 25 | 15 | 6 | 50 | 1 |
| 10 | KENTUCKY 4% | 8 | 40 | 11 | 17 | 15 | 8 |

DEPENDENCE OF DESULFURIZATION KINETICS ON HYDROGEN PRESSURE

Several isothermal experiments were conducted to determine the dependence of the desulfurization kinetics on hydrogen pressure. The initial series of experiments each used approximately three grams of the nominally 5% sulfur coal and were conducted at a temperature of 500°C. Substantial agglomeration of the sample occurred in these runs and it was felt that this might affect the validity of the data. Therefore, a second series of experiments was conducted using approximately one gram samples of char prepared by pyrolysis in helium at 500°C for twenty minutes. The char was ground, and resieved to 20-40 mesh size before the hydrogen experiments were conducted. This second series of experiments was conducted at a temperature of 475°C and at hydrogen pressures of one atmosphere, 4.9 atmosphere, and 10 atmospheres. In these experiments the sample was heated to the reaction temperature in helium. The gas stream was then quickly switched to hydrogen at the desired pressure and the H₂S concentration was monitored using the mass spectrometer. In these experiments the flow rate was adjusted so that a residence time of approximately 0.25 seconds was maintained for all three experiments. The logarithm of the height of the H₂S peak in the mass spectrum is plotted as a function of time after hydrogen introduction, in FigureZI. Under the conditions used in these experiments the H₂S evolved corresponds to the reduction of pyrite and the reduction of sulfide and stable organic sulfur. The kinetics for these processes was determined at a hydrogen pressure of one atmosphere using the non-isothermal method.

In the non-isothermal measurements the rate parameters for the reduction of pyrite to sulfide were found to be

$$\begin{aligned} k_0 &= 2.8 \times 10^{12} \text{ min}^{-1} \\ E &= 47 \text{ kcal/mole} \end{aligned} \quad (17)$$

Correspondingly the parameters found for the reduction of the sulfide were

$$\begin{aligned} k_0 &= 2.1 \times 10^{13} \text{ min}^{-1} \\ E &= 55 \text{ kcal/mole} \end{aligned} \quad (18)$$

These values were obtained for a hydrogen pressure of one atmosphere. If these processes are first order in hydrogen, then under isothermal conditions the rate constant for a given reaction is given by

$$k = k_0 P_{H_2} e^{-E/RT} \quad (19)$$

where k_0 and E are given above, P_{H_2} is the hydrogen pressure in atmospheres, T is the absolute temperature in $^{\circ}\text{K}$, and R is the gas constant in $\text{kcal}/^{\circ}\text{K}\text{-mole}$. In the isothermal experiment the concentration of H_2S in the effluent stream is given by

$$C = C^{\circ} e^{-kt} \quad (20)$$

where t is the time after introduction of hydrogen, and C° is the initial concentration. Taking the logarithm and differentiating, gives

$$\begin{aligned} \frac{d}{dt} \left(\ln \frac{C}{C^{\circ}} \right) &= -k \\ \frac{d}{dt} (\ln C - \ln C^{\circ}) &= -k \\ \frac{d \ln C}{dt} &= -k \end{aligned} \quad (21)$$

and changing to log base 10 gives,

$$\frac{d \log C}{dt} = \frac{-k}{2.303} \quad (22)$$

The data of log C versus t are given for three different pressures in Figure 21. If the reactions of H₂ with pyrite and sulfide are first order in hydrogen, then the kinetic parameters from the non-isothermal measurements give the straight lines shown for comparison in Figure 21. The overall agreement between the calculated lines from the non-isothermal data and the experimental data in the present runs is excellent. It is reasonable, therefore, to consider the reactions first order with respect to hydrogen pressure over a range from 1 to 10 atmospheres.

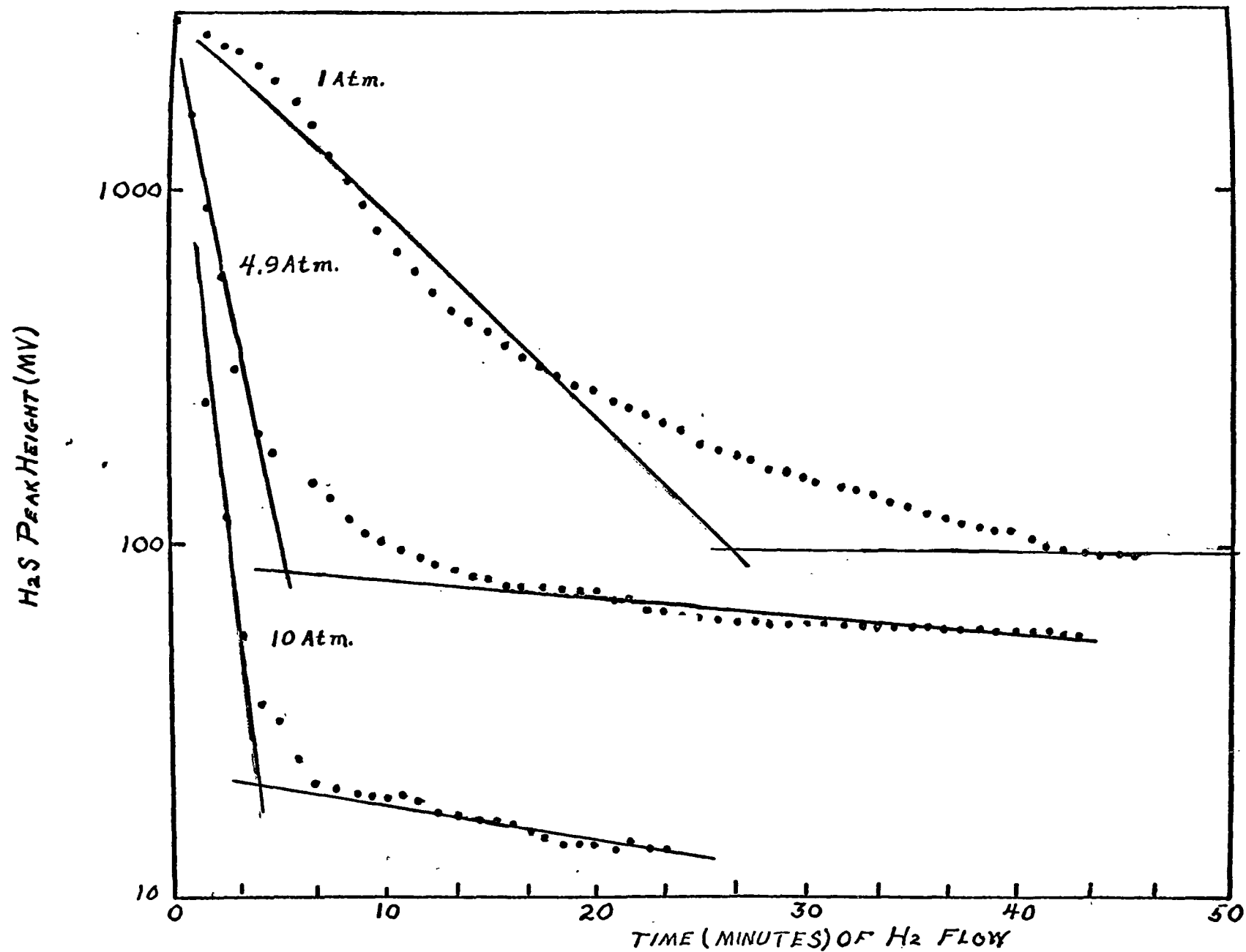


Figure 21. 1st order dependence on H_2 pressure: comparison of non-isothermal rate constants (straight lines) with isothermal data at $475^\circ C$ and pressures of 1, 4.9 and 10 atm. of H_2 .

FORMS OF SULFUR IN CHAR AS FUNCTIONS OF CARBONIZING TEMPERATURE

A series of isothermal experiments were conducted in which coal was carbonized in a hydrogen atmosphere at several different temperatures in the range from 325°C to 700°C. These experiments were conducted each using approximately three gram samples riffled from the nominally 5% sulfur Illinois coal. A flow rate of 1000 ml/min of H₂ at one atmosphere corresponding to a residence time of 0.08 secs was used in each experiment. The samples were heated at a rate of 33° per minute to the desired reaction temperature and held at this temperature for a period of ten minutes. At this time the hydrogen flow was replaced by helium and a helium flow was maintained during the time required to cool the reactor to room temperature. The resulting char samples were then removed from the reactor, weighed, and analyzed for forms of sulfur and total sulfur by conventional techniques. The results of these experiments are summarized in Figure 22.

A second series of ten isothermal experiments were conducted in which coal was carbonized in hydrogen at one atmosphere and at 25°C increments in the range from 300°C to 525°C. The results of these experiments are summarized in Figure 23. The experimental conditions and procedures were similar to those used in the first series of experiments on forms of sulfur as functions of carbonizing temperature, except that in this present series a much lower hydrogen flow rate (100 ml/min) was used to allow efficient cryogenic trapping of the condensible gases evolved. The trapped gases were measured using the gas chromatograph. The results for hydrogen sulfide, which accounts for more than 95% of the gaseous sulfur compounds detected, are included in Figure 23.

The purpose of these experiments was to confirm our conclusion from the non-isothermal studies concerning the origins of the evolved H_2S and the order in which the various H_2S peaks evolve. While there is considerable scatter of the data in Figures 22 and 23, the results are quite consistent with our conclusion that an organic type (or types) of sulfur is first removed, followed by pyritic sulfur and then sulfide. A comparison of Figures 22 and 23 with the non-isothermal data appears to indicate that sulfate sulfur is removed at about the same temperature as the first organic sulfur.

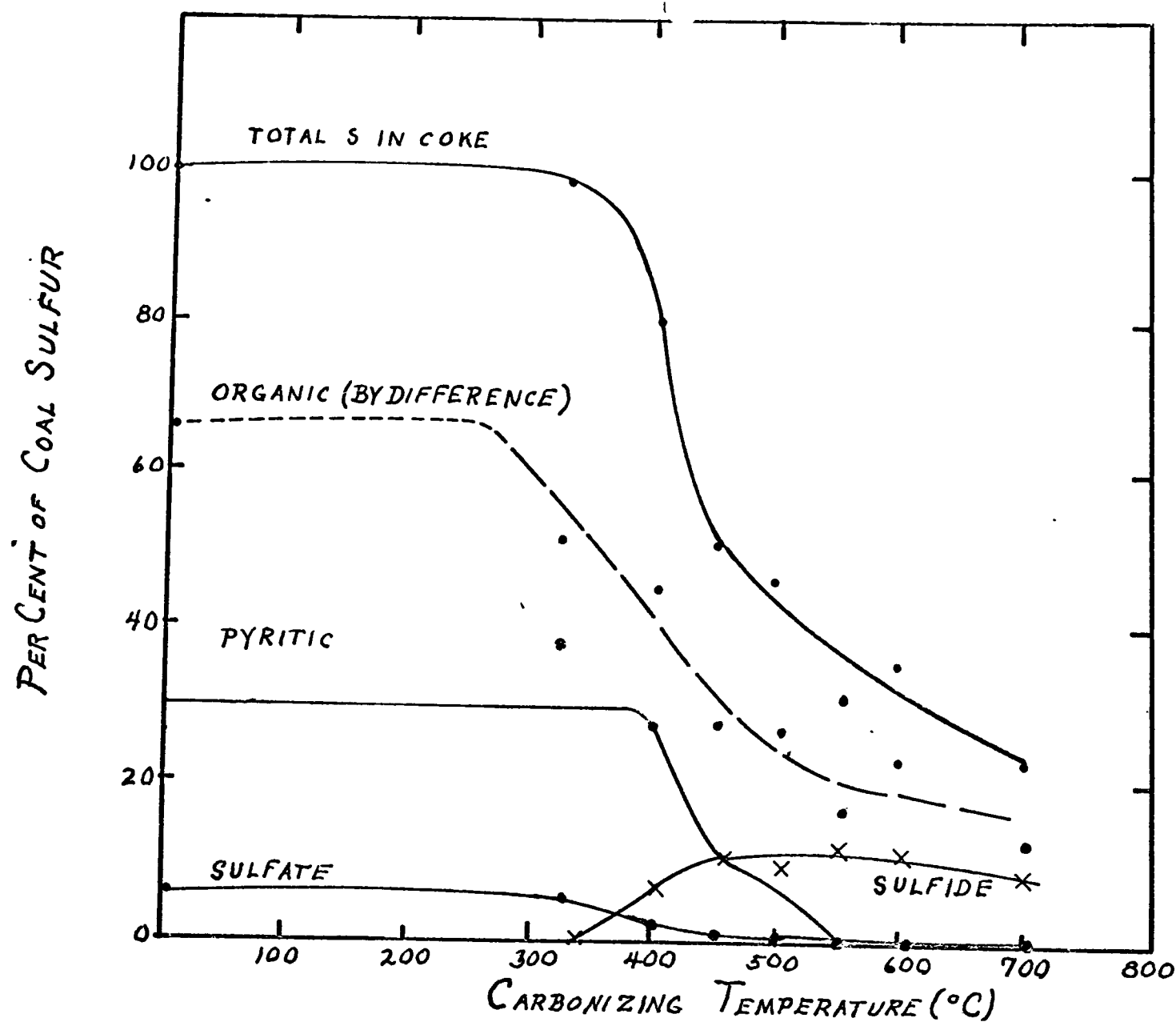


Figure 22. Variations in the amount and forms of sulfur in coke produced from the nominally 5% sulfur Illinois coal carbonized in hydrogen as functions of carbonizing temperature for a H_2 flow rate of 1000 ml/min.

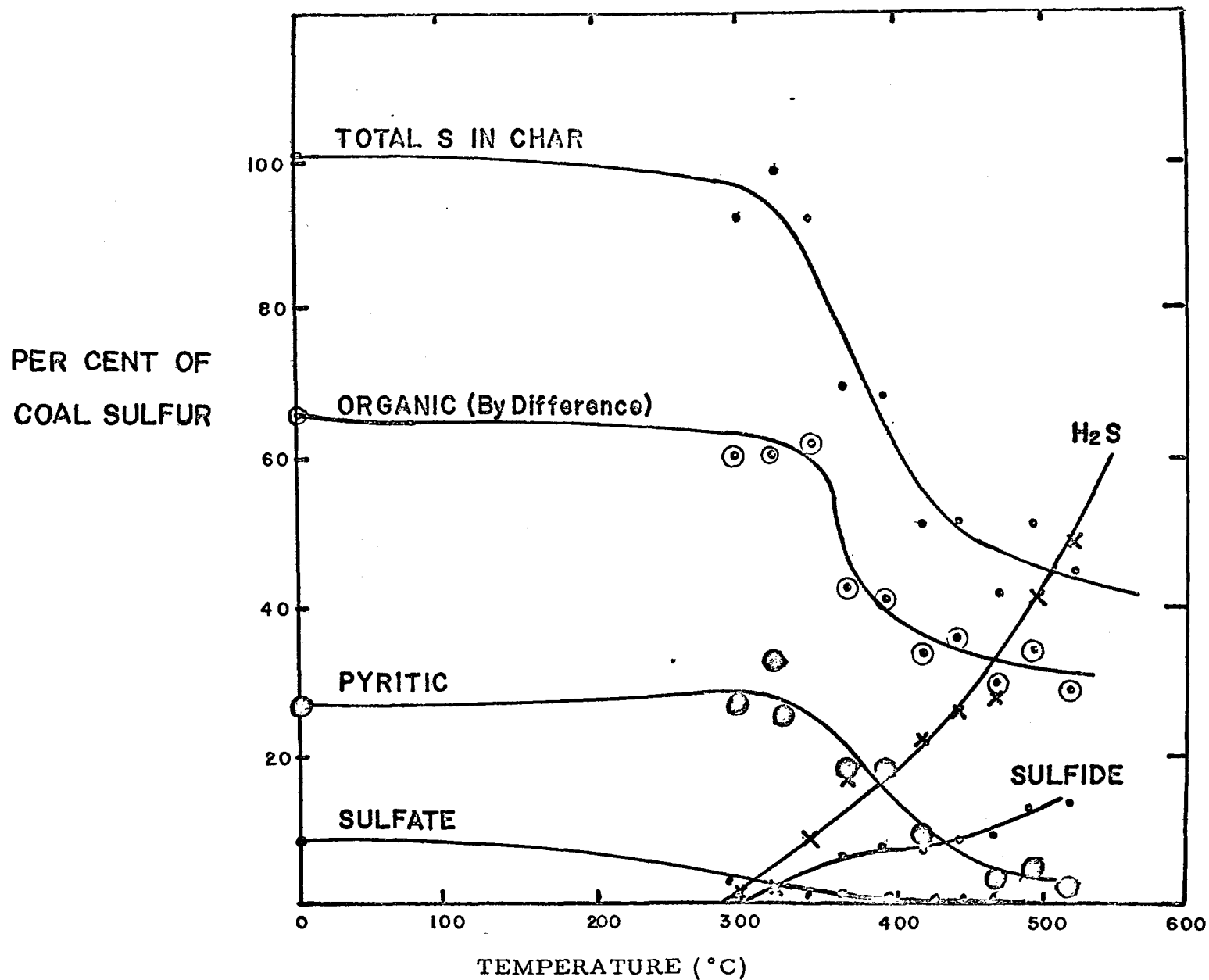


Figure 23. Variations in the amount and forms of sulfur in char and gas produced from the normally 5% sulfur Illinois coal carbonized in hydrogen as a function of carbonizing temperature for a H₂ flow rate of 100 ml/min.

THE KINETICS OF H_2S REACTIONS WITH COAL CHAR

Previous work has demonstrated that reactions of H_2S with coal char inhibit desulfurization; however, little data was available on the kinetics of H_2S reactions with coal char and its components. In this work the non-isothermal method has been applied to a study of the kinetics of these reactions. The experimental and theoretical procedures developed for this purpose are described in our report on Phase I.

A series of non-isothermal measurements on the kinetics of the reactions of hydrogen sulfide with coal char were conducted. Those experiments were carried out using a heating rate of $5^\circ/\text{minute}$ and H_2S concentrations in helium in the range from 500 ppm to 2300 ppm. Data on sulfur content of the original coal and the coke before and after reaction with H_2S are given in Table VIII. The relative H_2S concentrations in the gaseous effluents from the reactant beds are given for several of these experiments in Figure 24. These results indicate that the kinetics of the reactions of H_2S with char are quite dependent on properties of the char sample. Since the char samples used in these measurements were all prepared from the coal in a similar manner, it appears that these differences are due to variations in some component of the original coal. In duplicate analyses of several samples riffled from the same batch of coal, one of the components which is most variable in amount is the pyrite.

The effect of pyrite variability was investigated using the 1% sulfur Illinois coal SRI No. 2 which is initially very low in pyrite and in total iron (see Tables II-VI). The results of runs using char prepared from the 1% sulfur coal (N45) and char prepared from the 1% sulfur coal with 5% by

weight added pyrite (N43) are given in Figure 24 and Table VIII. The addition of the pyrite substantially increases the amount of sulfur absorbed by the coke, both as inorganic S and organic S. It is also interesting to note that in none of the experiments conducted to date is the per cent sulfur in the char after reaction with H_2S higher than the percentage in the original coal, despite the fact that a considerable excess of H_2S was available for reaction in the temperature range in which the reactions would be expected to be rapid. A significant part of the excess sulfur is desorbed as CS_2 in the range from $900^\circ C$ to $1000^\circ C$ in all of these experiments.

In an effort to investigate separately the several reactions apparently involved in the absorption of H_2S by coal char a series of non-isothermal experiments were conducted on the reactions of H_2S with the principal reactive components of coal char including carbon, iron, and calcium oxide. The results are described in the next two sections of the report.

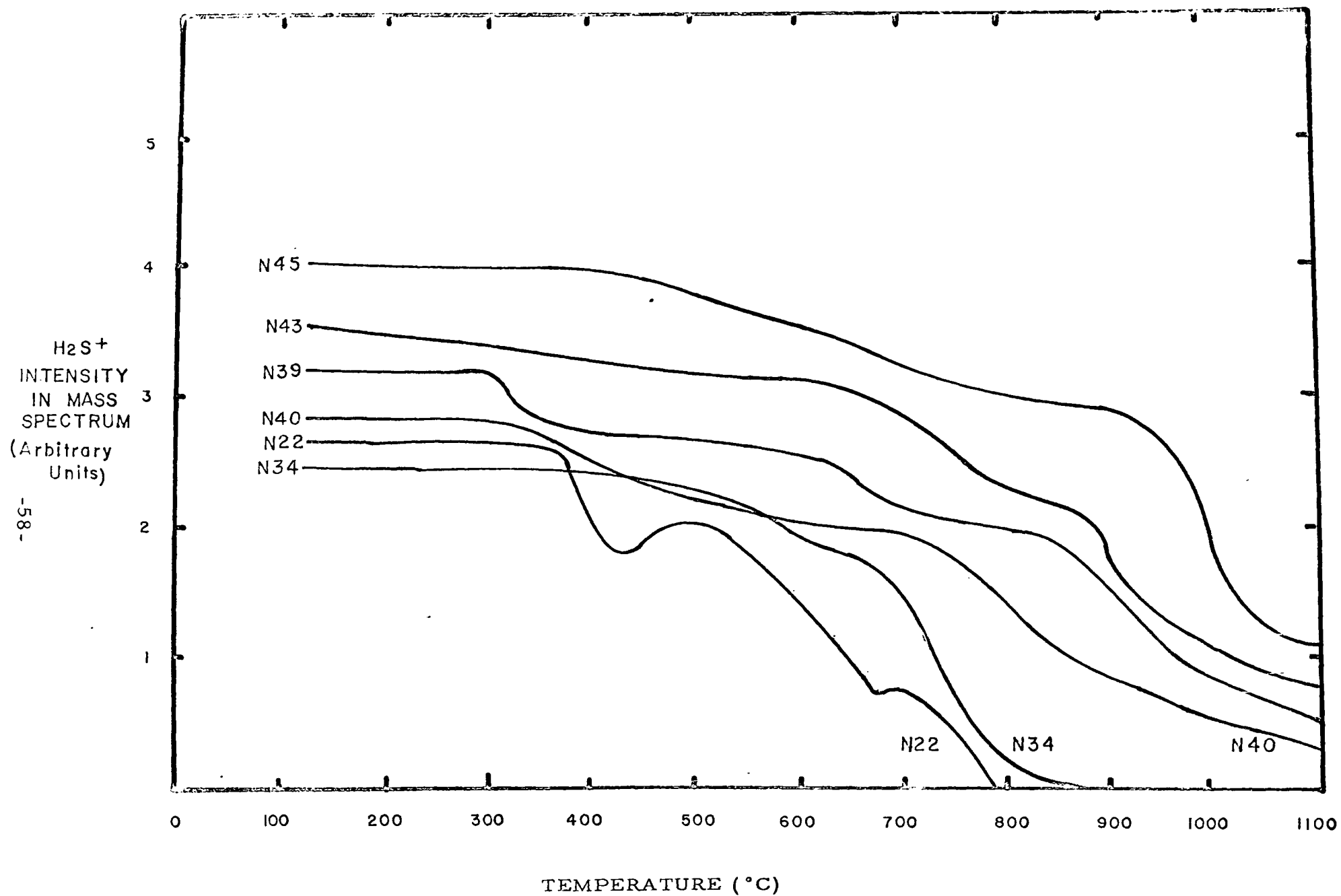


Figure 24. Relative H_2S concentrations in the effluent gases from six non-isothermal measurements on the kinetics of the reactions of H_2S with coke.

TABLE VIII .SUMMARY OF DATA ON REACTIONS OF H₂S WITH COKE

| <u>RUN</u> | <u>PERCENT SULFUR</u> | | | <u>H₂S</u> | <u>RESIDENCE</u> |
|---------------|----------------------------|----------------------------|---|-------------------------------------|----------------------------|
| | <u>COAL</u> ⁽¹⁾ | <u>COKE</u> ⁽²⁾ | <u>COKE + H₂S</u> ⁽³⁾ | <u>CONCENTRATION</u> ⁽⁴⁾ | <u>TIME</u> ⁽⁵⁾ |
| N22 | 4.2 | 1.9 | 4.2 | 0.1 | 0.14 |
| N34 | 4.2 | 0.1 | 3.1 | 0.05 | 0.04 |
| N39 | 3.8 | 1.6 | 3.8 | 0.2 | 0.3 |
| N40 | 3.8 | 1.0 | 2.4 | 0.2 | 0.25 |
| N41 | 3.8 | 1.0 | 2.5 | 0.1 | 0.13 |
| N43 inorganic | 2.75 | < 0.1 | 1.31 | 0.23 | 0.22 |
| organic | 0.62 | | 0.90 | | |
| N45 inorganic | 0.27 | < 0.1 | 0.36 | 0.1 | 0.22 |
| organic | 0.62 | | 0.58 | | |

(1) In coal sample from same riffing as sample used in coke prepared for the H₂S run.

(2) In coke sample before reaction with H₂S.

(3) In coke sample after reaction with H₂S.

(4) Concentration of H₂S in helium sweep gas.

(5) Average time in seconds required for a volume element of gas to sweep through the reactant bed.

KINETICS OF H_2S REACTIONS WITH CARBON

In Figure 25 the results of several non-isothermal measurements of H_2S absorption by chars from three different coals are compared to similar results for iron and charcoal. These results show that the absorption of H_2S on coal char at temperatures below 500°C is principally due to reaction with iron to form iron sulfide while at higher temperature the reactions with carbon also become important.

Non-isothermal kinetic measurements were carried out on the reactions of H_2S with carbon in the form of activated charcoal. One gram of the powdered charcoal was placed in the reactor and heated to 800°C in a flow of helium and held at that temperature until gas evolution from the charcoal had ceased as determined by monitoring the effluent with the mass spectrometer. The reactor was then cooled to room temperature with the helium flow maintained. The non-isothermal kinetic measurements were accomplished by flowing a mixture of 1000 ppm of H_2S in helium through the reactor at a rate of 220 ml/min. The heating rate was $4^\circ/\text{min}$. The relative H_2S concentration in the effluent for one such experiment is given as a function of temperature in Figure 25. Detectable absorption of H_2S begins at about 450°C and becomes substantial in the region between 600 and 700°C . Above 750°C the H_2S concentration in the effluent remains constant with temperature at about 10% of the inlet concentration. In the range between 900 and 950°C , CS_2 evolution occurs. Beginning at about 600°C deposition of sulfur on the walls of the reactor outside the hot zone of the furnace is observed. This deposition of free sulfur indicates that not all of the H_2S loss involves reaction with the carbon, but rather indicates some loss due to the reaction

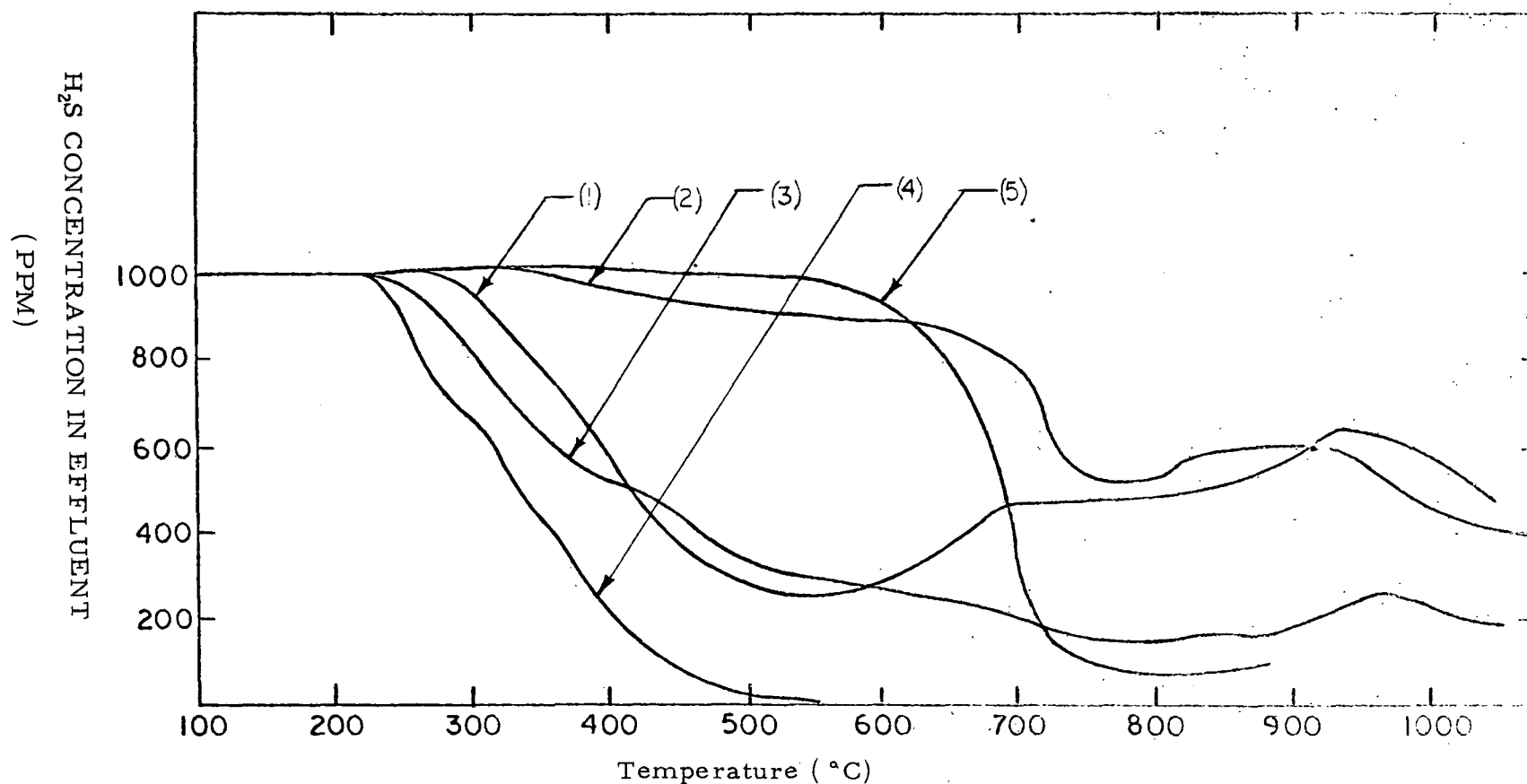


Figure 25. H₂S absorption in non-isothermal experiments on char, charcoal and iron. 1,000 ppm of H₂S in helium was passed over approximately 1 gram of the solid at a total flow rate of 220 ml/min; the heating rate was 4°C/min, (1) Char from coal SRI No. 1, a nominally 5% sulfur Illinois coal, (2) Char from coal SRI No. 2, a nominally 1% Illinois coal, (3) Char from coal SRI No. 4, a nominally 5% sulfur Illinois coal with a high calcium content, (4) Iron filings, (5) Charcoal.



which may occur on the carbon surface. The solid residue from the H_2S absorption on carbon contained 2.3% sulfur, while the original charcoal sample contained no detectable sulfur.

The results of some additional non-isothermal kinetic measurements on the reaction of H_2S with carbon are given in Figure 26. The experiment on the activated charcoal was carried out as described above and a similar experiment was performed using graphite. In all of these experiments the sample has been held in place in the reaction chamber by a plug of quartz wool placed above and below the sample. The third run in this series was done as a blank using only the quartz wool plug, otherwise the procedures were the same as those used in the experiments on activated charcoal and graphite. The blank experiment shows that the H_2S in the effluent from the reactor begins to drop below the input H_2S concentration at about 740°C , even when no reactant is present. This loss in H_2S coupled by the observation of sulfur formations shows that under the conditions employed a homogenous decomposition of H_2S occurs. Since (23) is the most favored decomposition on thermodynamic grounds, the blank experiment describe suggests strongly that above 700°C (23) occurs homogenously.

Analysis of the data from this experiment indicates that this reaction occurs with an activation energy of 38 kcal/mole. Since similar effects are observed in the H_2S reaction on char and carbon presumably the drop in effluent H_2S concentration in the region of 700°C is due primarily to the homogenous reaction (23) rather than to a heterogenous decomposition on the carbon surface at this temperature. However, since the steep drop in H_2S concentration occurs at a lower temperature in the case of the carbon

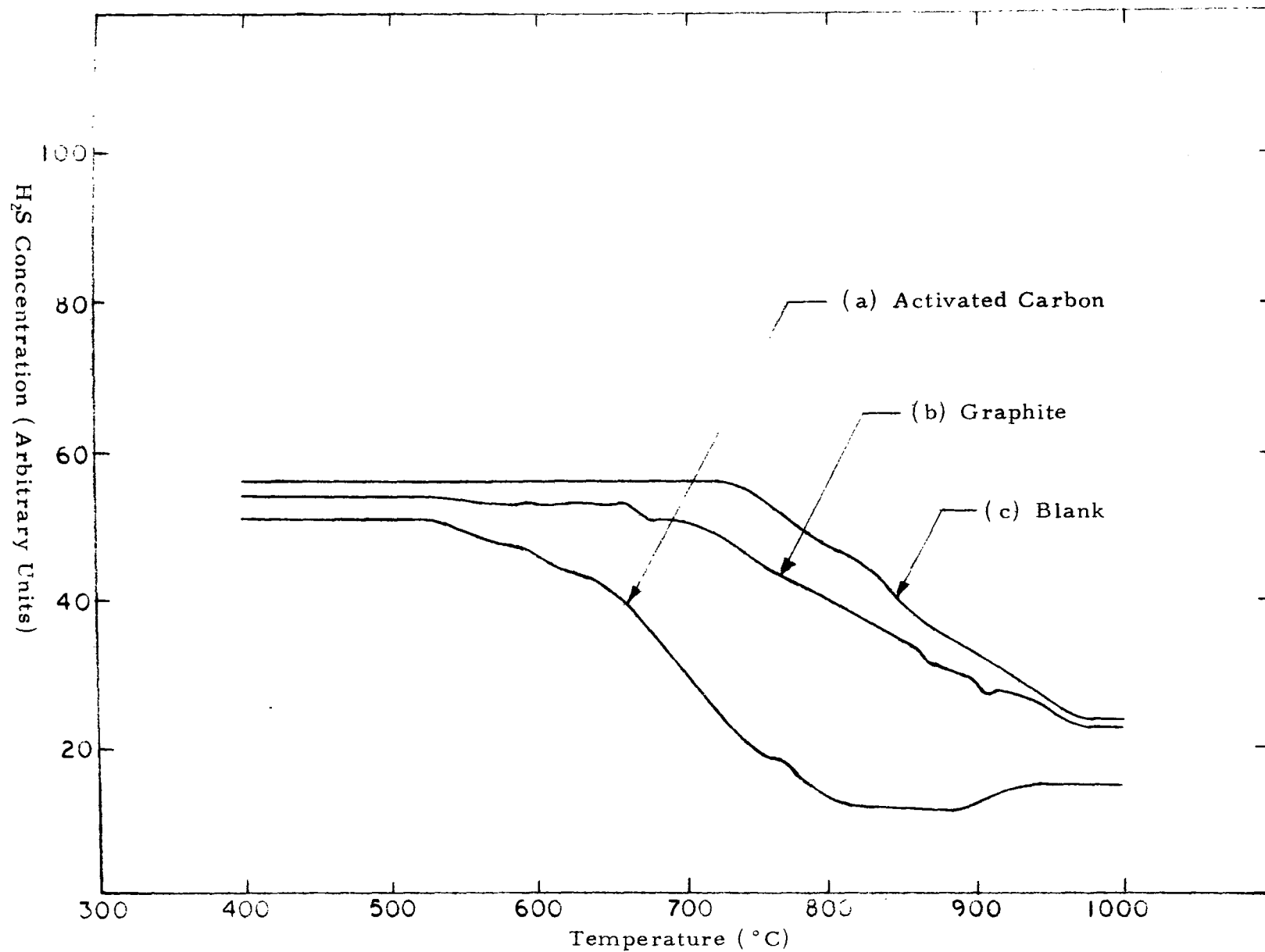
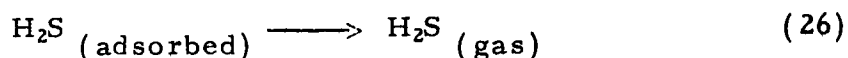
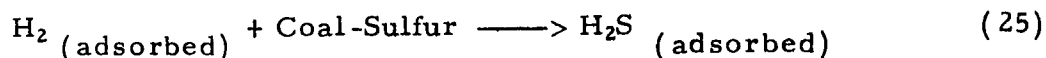
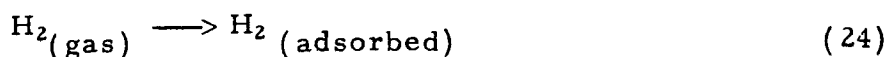


Figure 26. Non-isothermal absorption of hydrogen sulfide on (a) 1 gram activated charcoal (b) 1 gram graphite and (c) a blank in which the quartz wool plug normally used to hold the sample in place was used but with no sample. These experiments used 0.1% H₂S in He at a flow of 220 ml/min.

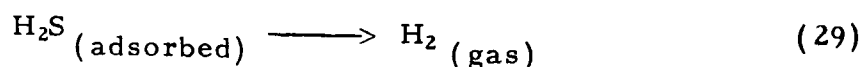
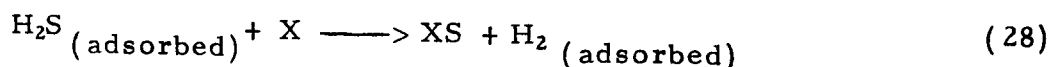
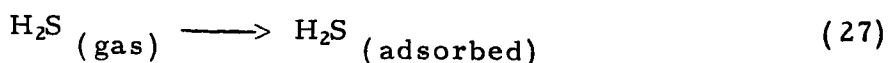
as compared to the blank it appears likely that the dissociation reaction may also be catalyzed by the carbon surface.

An understanding of the details of the interactions of H_2S with coal char is of great importance both to the interpretation of the non-isothermal kinetic data and to the applications of these data to the design of practical processes. The sequence of reactions involved in the desulfurization of coal with hydrogen may be written as follows:



where reaction (25) represents several reactions corresponding to reaction of the several different kinds of sulfur in the coal, and reaction (26) may represent more than one desorption process, if (as is often the case in heterogenous reactions) more than one type of H_2S adsorption site is present. It certainly is reasonable to suppose that adsorption sites in the neighborhood of an iron pyrite particle are different than those in the neighborhood of an organic sulfur compound.

For the capture of H_2S by coal char the sequence of reactions may be written as follows:



where X is a reactive component of the coal, for example, iron, calcium oxide, or carbon. Non-isothermal kinetic measurements have been conducted on the reactions of H_2S with iron and calcium oxide; the results of these investigations are presented in the next section. For this section we are concerned with the reaction of H_2S with carbon.

The reaction model proposed here is a reasonable working hypothesis within which to examine kinetically the desulfurization inhibition that is known to arise because of the reaction of H_2S with various constituents of coal char. For (27) - (28) to be important, it is only necessary for the desulfurization (24) - (26) to have proceeded to a measurable extent because (27) - (29) are merely the back reactions (24) - (26), the desulfurization processes.

In connection with the measurement on the kinetics of desulfurization of the ten coals studied in this work, it was found that the behavior of the most stable form of organic sulfur in coal (designated as Organic III in the previous discussion) could be approximated by a ~~sulfurated~~ carbon prepared by reacting H_2S with activated charcoal.

Non-isothermal kinetic data on the reaction of H_2 with the sulfurated carbon and with a high sulfur coal char are compared in Figure 27. The coal char was prepared from the 5% sulfur Illinois coal, SRI No. 1, by pyrolysis in helium at 800°C for one hour. The char contained 3.4% sulfur by standard ASTM analysis. A non-isothermal measurement on this char using helium sweep gas showed that no significant desorption of H_2S occurred in the absence of an external source of hydrogen. The sulfurated carbon was prepared as described above. The difference between the non-isothermal H_2S evolution curves for these

two experiments may be ascribed to the FeS present in the coal char. The resolution of the result into two processes corresponding to reaction of H_2 with FeS and with organic-S III is illustrated in Figure 27.

In addition to the strongly-bound organic-S III, H_2S may be adsorbed on the carbon surface apparently without losing its chemical identity. The organic-S III is stable in an inert atmosphere to at least $1000^\circ C$ while the adsorbed H_2S may be desorbed at high temperatures in an inert atmosphere. The results of three non-isothermal experiments on the desorption of H_2S from char are summarized in Figure 28. These results are on the desorption of H_2S from sulfurated charcoal, sulfurated coal char from 5% sulfur Illinois coal SRI No. 1, and sulfurated graphite. The sulfur contents of the chars were 2.3% for the charcoal; 3.4% for the coal char; and 0.2% for the graphite. The sulfur contents were not increased by further reaction with 1000 ppm of H_2S in helium at temperatures up to $800^\circ C$, indicating that the chemically stable forms of sulfur were fully saturated. Each of these chars was then treated at $500^\circ C$ by passing 1000 ppm of H_2S in helium over 5 g of the sample at a flow rate of 200 ml/min for one hour. The temperature was then lowered to $300^\circ C$ while maintaining the flow of the H_2S -helium mixture. The flow was then switched to pure helium and the linear temperature programmer started to give a heating rate of $4^\circ C$ per minute. The results given in Figure 28 indicate that the high temperature desorption of H_2S from coal char may be quite slow and may be somewhat variable from coal to coal depending on the structure of the carbon matrix.

To summarize the results of this set of experiments:

(1) Figure 27 compared to Figure 8 shows clearly that the difference in desulfurization behavior between a sulfurated carbon and a high sulfur coal char is the presence of FeS in the latter. Further, it is shown in Figure 27 that in the desulfurization of a high sulfur coal char, the

desulfurization process can be represented quite by desulfurization from FeS sites and from organic-S III type sites.

(2) Figure 28 shows that H_2S may also be physically adsorbed on a carbon surface such as charcoal (curve a) without losing its identity. This figure also indicates that the situation is not always as simple as might be thought from Figure 27 because as curve (b) shows the desulfurization from coal char can require considerably higher temperatures than those for Organic I and II. Also as a comparison of curves (a) and (b) indicates, the desulfurization from coal to coal might be very dependent upon the structure of the carbon matrix.

The non-isothermal evolution of H_2S from sulfurated carbon by reaction with H_2S is given for different H_2 flow rates in Figure 29. The desorption of H_2S from charcoal in helium is included in Figure 29 for comparison. The kinetics corresponding to this H_2S evolution represents the maximum rate at which H_2S may be evolved from coal in this temperature range, even if the chemical reaction were infinitely fast and if there were no back chemical reaction. This relatively slow desorption of H_2S may account for some of the small discrepancies observed in the resolution of the desulfurization kinetics for the ten coals into individual processes.

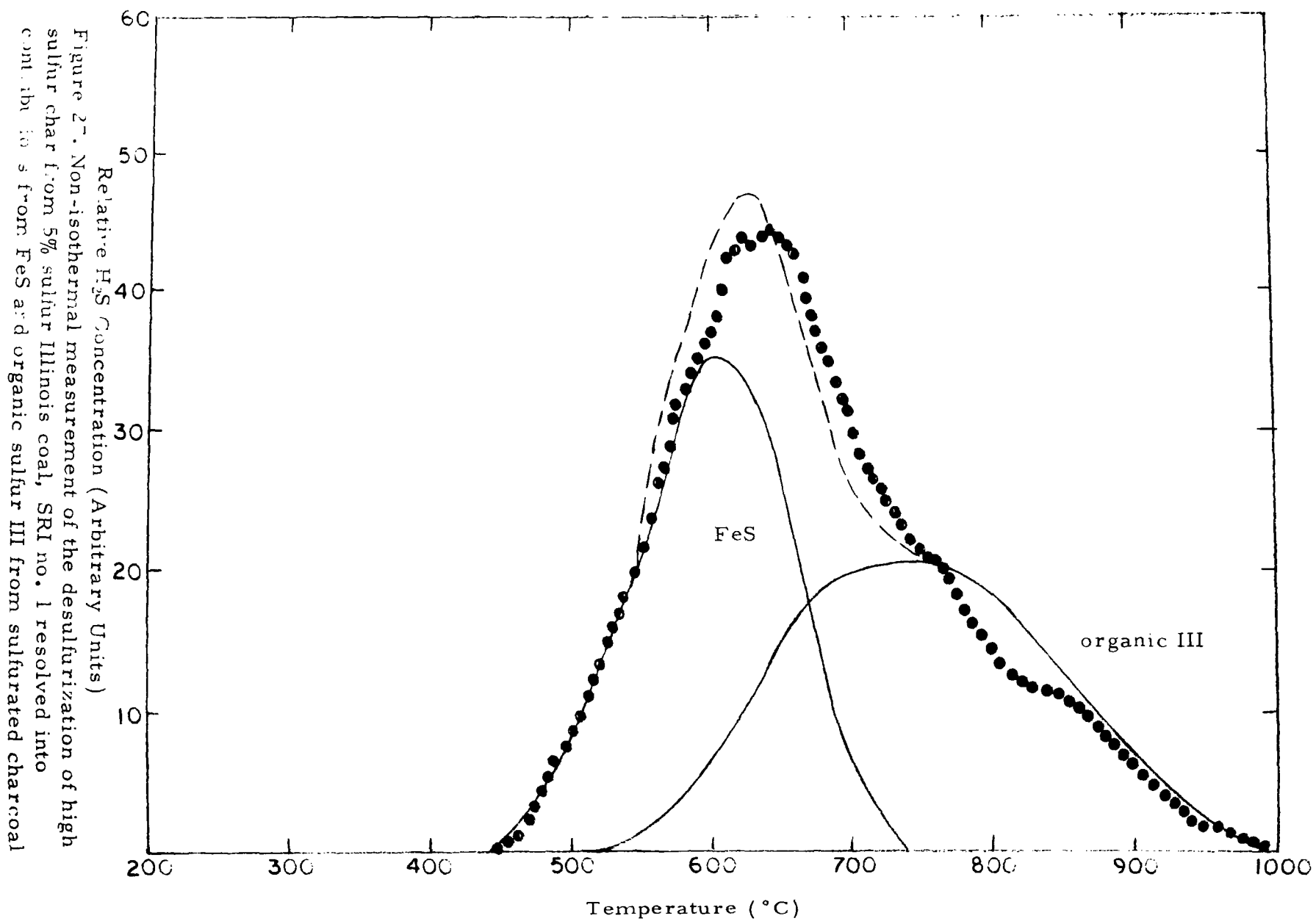


Figure 27. Non-isothermal measurement of the desulfurization of high sulfur char from 5% sulfur Illinois coal, SRI no. 1 resolved into contributions from FeS and organic sulfur III from sulfured charcoal

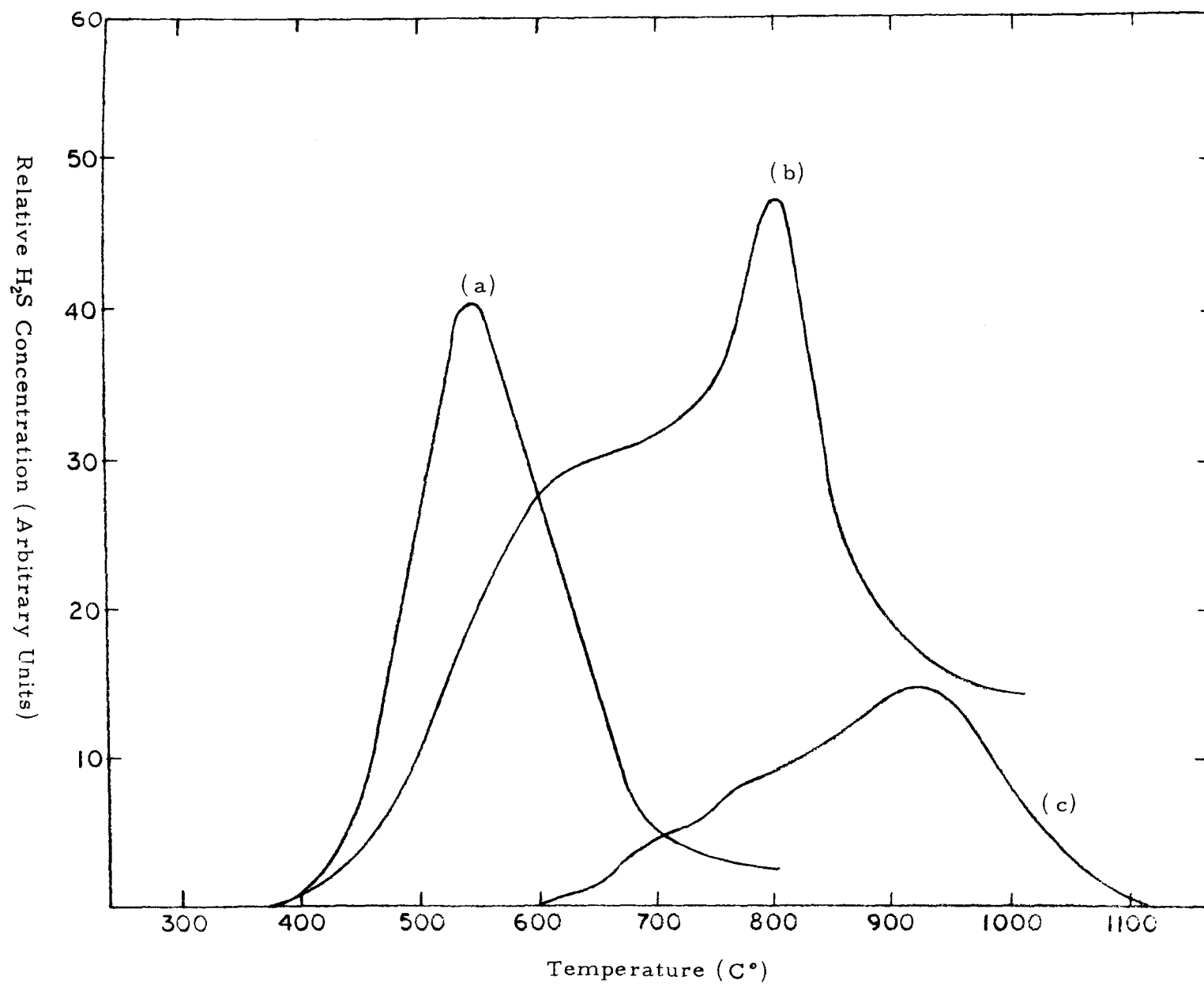


Figure 28. Desorption in He of H₂S adsorbed on (a) charcoal (b) char from SRI coal No. 1, (c) graphite.

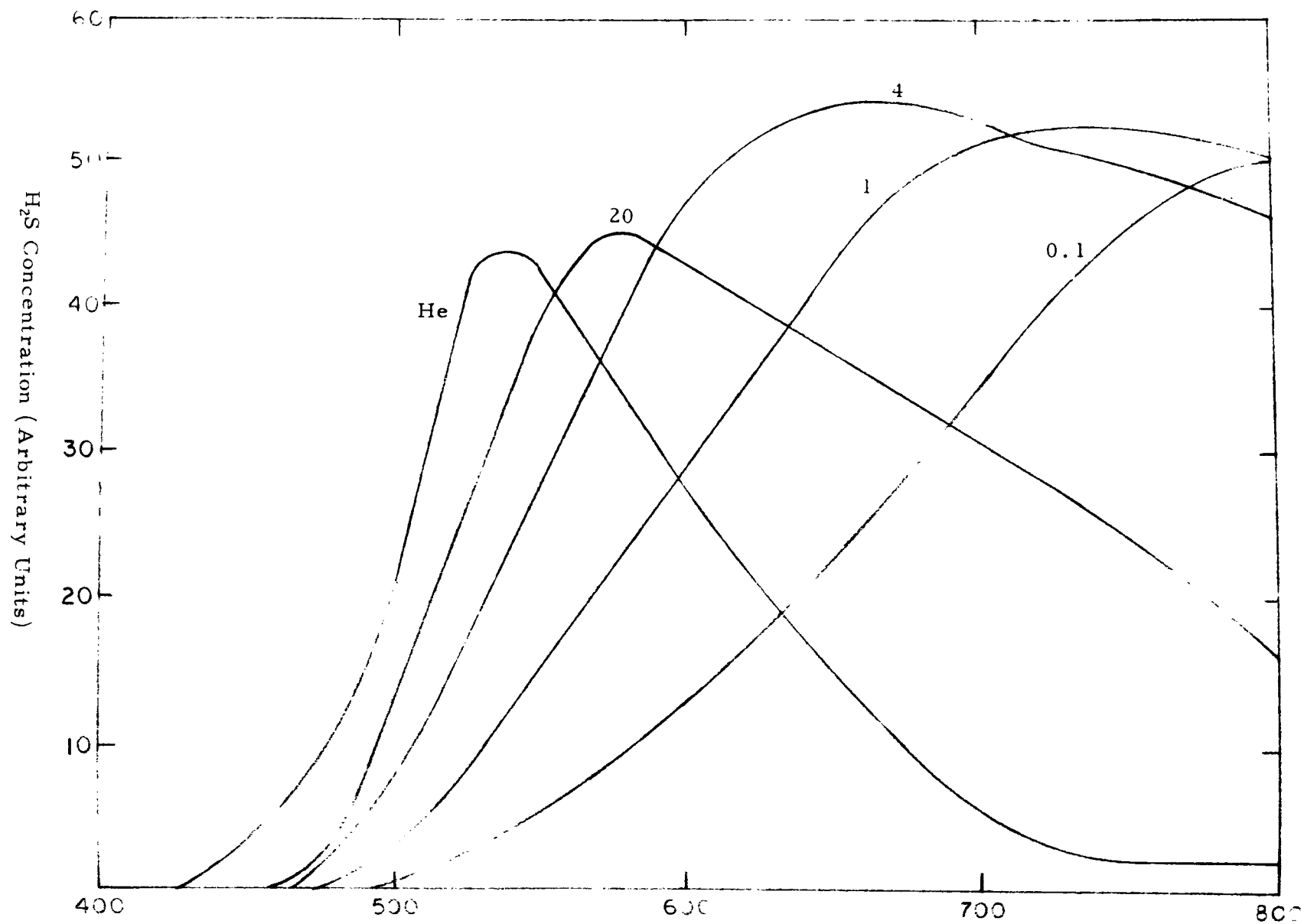


Figure 29. Non-isothermal measurements of the desulfurization of sulfurated charcoal. The numbers identifying the curves give the H₂ flow in litres/min/g of sample. Desorption in He

KINETICS OF H₂S CAPTURE BY Fe AND BY CaO

The reactions of H₂S with Fe and CaO are important, not only because of the role of these reactions in inhibiting desulfurization but also because of the potential use of these materials as sulfur acceptors. We have performed several non-isothermal kinetic experiments using iron prepared by hydrosulfurization of pyrite in hydrogen at 800°C. One such experiment was performed by passing a stream of helium over the iron with 1,000 ppm of H₂S in the helium. These data are plotted in an Arrhenius type plot in Figure 30. The region of reaction limitation is shown, at approximately one half this rate the region of diffusion limitation takes over at higher temperatures.

This reaction of iron with H₂S to form FeS and H₂ is extremely fast. The kinetic parameters are

$$E = 18 \text{ kcal/mole}$$

$$k_0 = 6.5 \times 10^6 (\text{atm} \cdot \text{H}_2\text{S})^{-1} \text{ min}^{-1}$$

where $k = k_0 e^{-E/RT}$ and the rate equation for the reaction is written in terms of the solid reactant;

$$\frac{d[S]}{dt} = K [S] P_{\text{H}_2\text{S}} \quad (30)$$

where $[S]$ is the concentration of sulfur in the solid product.

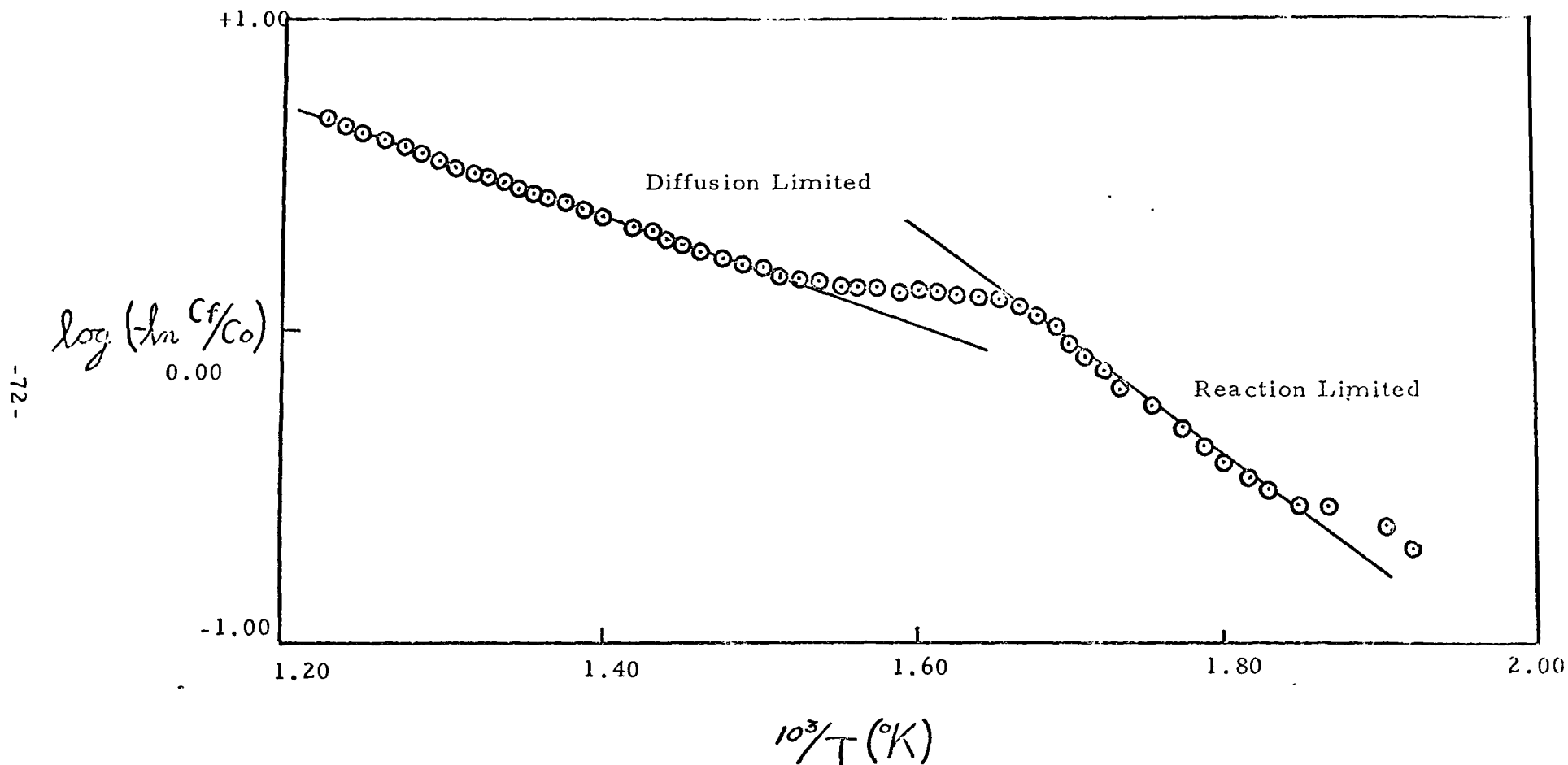


Figure 30. Arrhenius type plot of the H_2S absorption by iron in a non-isothermal kinetic experiment. The iron was prepared by the hydrodesulfurization of pyrite with a 4 litre flow of H_2 at $800^{\circ}C$. The absorption experiment was performed by passing a 1,000 ppm of H_2S in helium over 1 gram of

The reactions of H_2S with calcium oxide are also of considerable significance, both because of the importance of CaO as a potential sulfur absorbent, as well as the contribution to the back reaction for coals containing calcium in the ash. The results of three non-isothermal kinetic measurements on the reactions of H_2S with CaO from different precursors are shown in Figure 31. Similar measurements using MgO formed by calcining precipitated MgCO_3 indicate that the MgO component of the calcined dolomites is essentially unreactive to H_2S .

The Arrhenius plot of the data for the dolomite is shown in Figure 32. The kinetic parameters for the reaction limited regions are

$$E = 38 \text{ kcal/mole}$$

$$k_0 = 1.7 \times 10^{13} (\text{atm. H}_2\text{S})^{-1} \text{ min}^{-1}$$

where the form of the rate equation is the same as given above for the iron reactions.

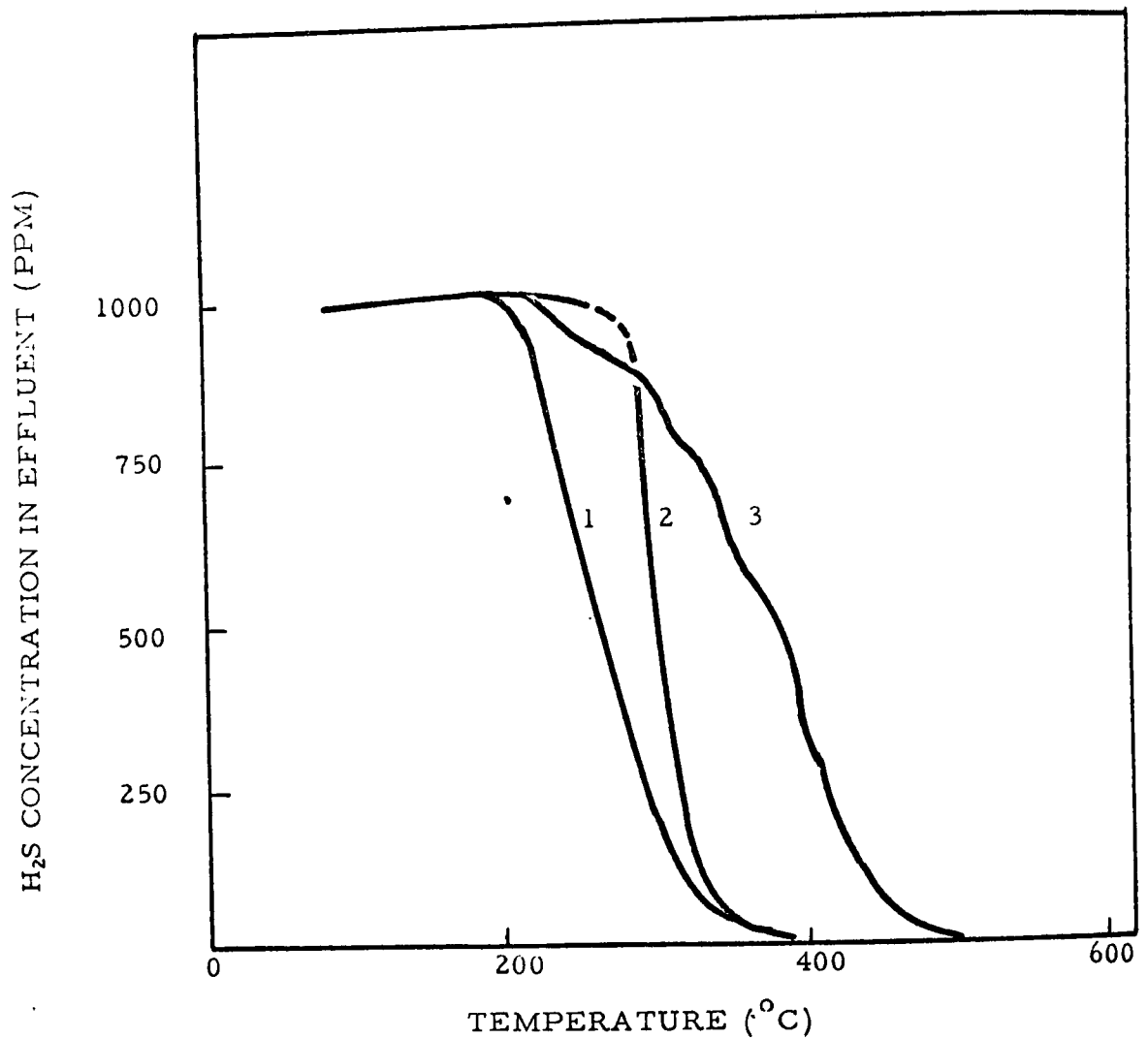


Figure 31. H₂S absorption in non-isothermal kinetic experiments on calcium oxide. 1,000 ppm of H₂S in helium was passed over 1.5 grams of solid at a total flow rate of 150 ml/min, the heating rate was 4°C/min. (1) Calcium oxide from calcination of -200 mesh precipitated calcium carbonate, (2) Calcium oxide from calcination of -140 mesh No. 1930 dolomite, (3) Calcium oxide from calcination of -140 mesh No. 1683 dolomite.

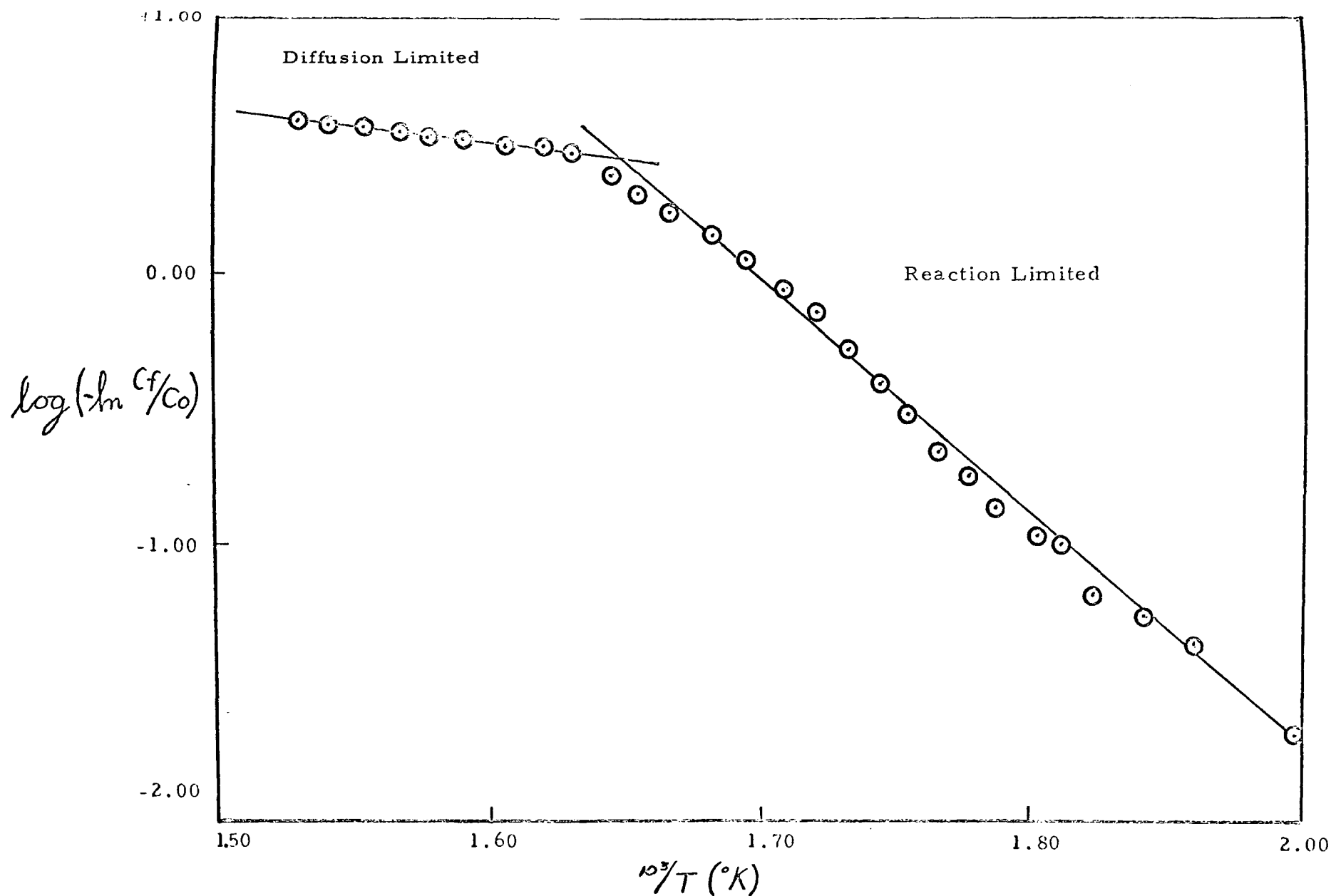


Figure 32. Arrhenius type plot of the H_2S absorption by calcined No. 1930 dolomite in a non-isothermal kinetic experiment. The absorption experiment was performed by passing a 1,000 ppm of H_2S in helium over 1 gram of the solid at 150 ml/min; heating rate was $4^{\circ}C/min$.

KINETICS OF CALCINATION OF DOLOMITES AND LIMESTONES

A series of kinetic experiments were conducted on the calcination of precipitated calcium carbonate. The results of three such experiments are summarized in Figure 33. Run N-46 is the non-isothermal (heating rate $5^{\circ}\text{C}/\text{min}$) calcination of 3.4 g of CaCO_3 with He flowing over the sample at flow rate of 500 ml/min. These parameters correspond to a mean gas residence time in the sample of 0.47 sec. Run N-47 is a similar experiment with the sample reduced to 0.35 g and the helium flow increased to 1000 ml/min. This approximately 20 fold decrease in residence time (to 0.024 sec) causes a shift in the peak CO_2 evolution from 775°C to 650°C . As discussed in connection with the H_2S reactions, this shift may be ascribed to the back reaction of CO_2 with CaO . This is confirmed in non-isothermal run N-51, in which a 50:50 mixture by volume of CO_2 and He at flow rate of 100 ml and a total pressure of 1 atmosphere was passed over 5.7 g of CaO prepared from precipitated CaCO_3 in an earlier calcination run. Detectable absorption of CO_2 begins below 400°C . At 725°C the highly exothermic absorption reaction becomes sufficiently rapid to cause local thermal runaway within the bed. At this point the CaO bed is quickly converted to CaCO_3 and no further absorption occurs.

A series of experiments were conducted on the calcination of limestones and dolomites in helium. In these experiments 250 milligrams of the solid was used with a helium flow rate of 1 litre per minute and a heating rate of 4°C per minute. The results of four such experiments are given in Figure 34 where the carbon dioxide evolutions are given as

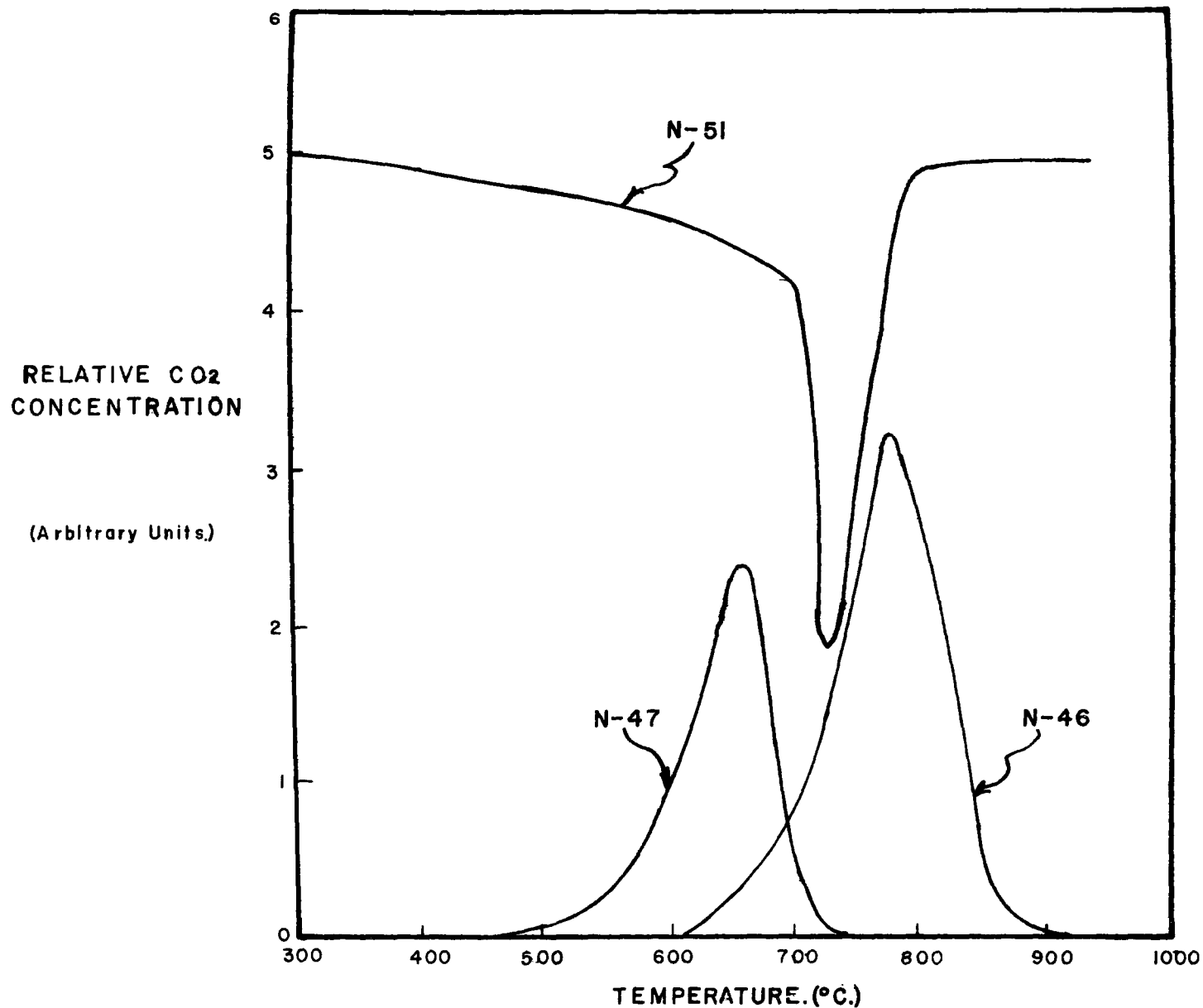


Figure 33. Runs N-46 and N-47 are calcination runs on calcium carbonate in helium with residence times of 0.47 seconds and 0.024 seconds, respectively. The twenty-fold decrease in residence time shifts the peak carbon dioxide evolution from 755°C to 650°C. Experiments on recarbonization on calcium oxide, run N-51, confirm that this shift is due to the back reaction of carbon dioxide with calcium oxide.

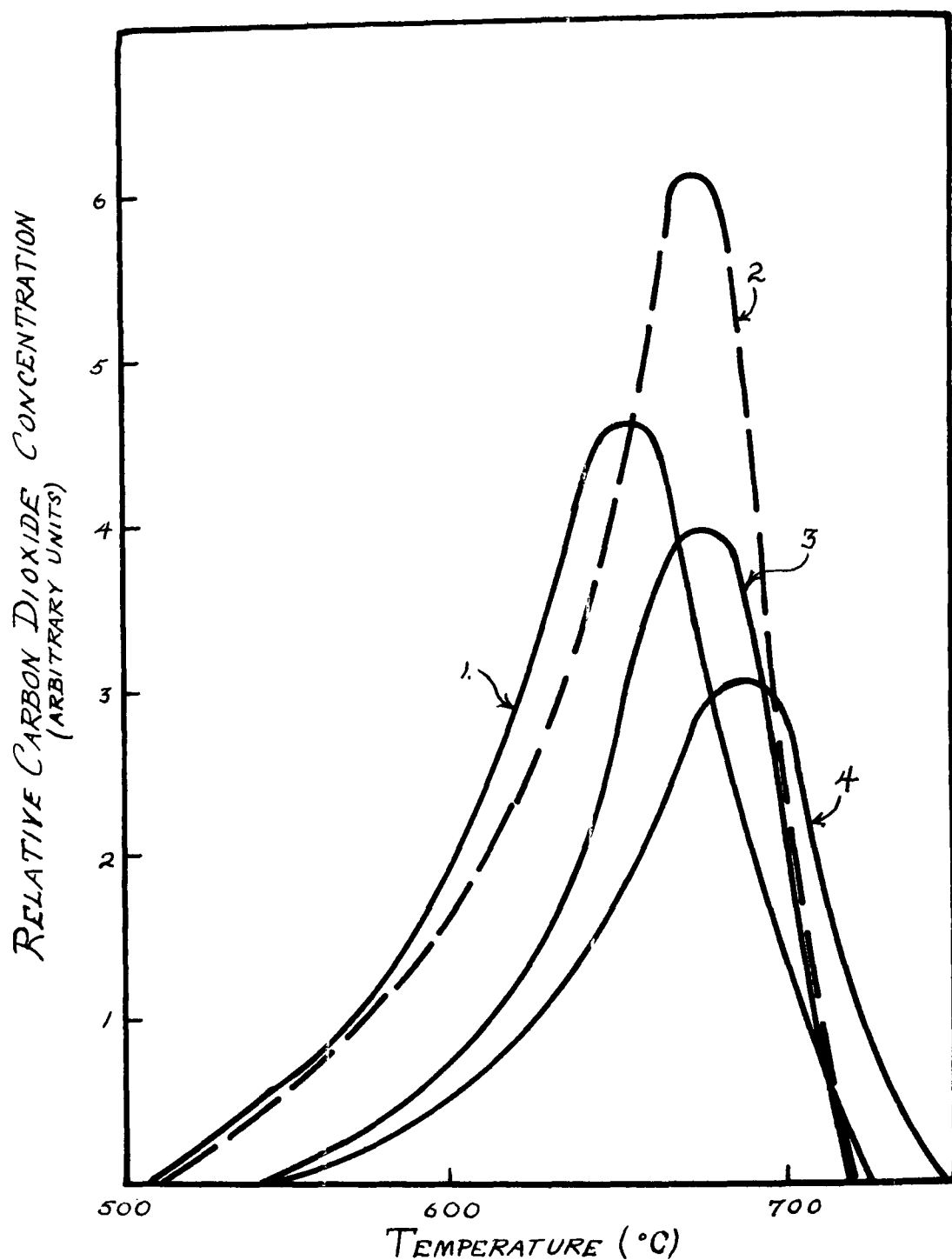


Figure 34. Carbon dioxide evolution from the non-isothermal calcination in helium of precipitated calcium carbonate (1), Limestone sample 1683B (2), Dolomite sample 1930 (3), and Dolomite sample 1380 (4). The heating rate was 4°C/min. and the helium flow rate one l/min.

functions of temperature. Results given in Figure 34 include precipitated calcium carbonate, a limestone and two dolomites. These results indicate that under the conditions employed the calcination kinetics for limestones and dolomites are substantially the same as the kinetics for pure calcium carbonate. Kinetic parameters determined from these results fall within the range

$$E = 58 \pm 5 \text{ kcal/mole}$$

$$\log k_0 = 12.5 \pm 1$$

This similarity of the calcination kinetics probably holds only for low local concentrations of carbon dioxide. At higher CO_2 concentrations it is apparent from the literature that the back reaction inhibits the decomposition of the calcium carbonate with little effect on the decomposition of the magnesium carbonate.

KINETICS OF DECOMPOSITION OF IRON SULFATES

It is well known (see Figure 22-23) that a significant part of the sulfur in coal is in the form of sulfate. Therefore in any kinetic study of the overall coal desulfurization process we must consider the removal of sulfur from this type of compound. With this in mind an orientation series of non-isothermal experiments were conducted on the decomposition and removal of sulfur from ferrous and ferric sulfate in hydrogen and in helium.

The results for the reactions of ferric sulfate in a hydrogen atmosphere are given in Figure 35. Substantial shifts in the shapes and locations of the SO_2 and H_2S evolution peaks occur as the ratio of H_2 flow rate to sample size is varied. Similar results for ferrous sulfate are given in Figure 36. The results for the two iron sulfates are qualitatively similar; the principal difference being the low temperature evolution of SO_2 from the ferric sulfate.

As can be seen in Figures 35-37, we should expect an H_2S evolution peak from sulfate sulfur having an onset of about 410° , a maximum of about 500°C and then a slow decline, vanishing at $650-700^\circ$. Whether such a peak will be visible in a coal desulfurization process depends of course on the relative amounts of sulfate, organic I, organic II, and pyrite. These figures also show that even in a H_2 -atmosphere sulfur will be removed from the sulfates as SO_2 concurrently with the H_2S . In a helium atmosphere only SO_2 is evolved.

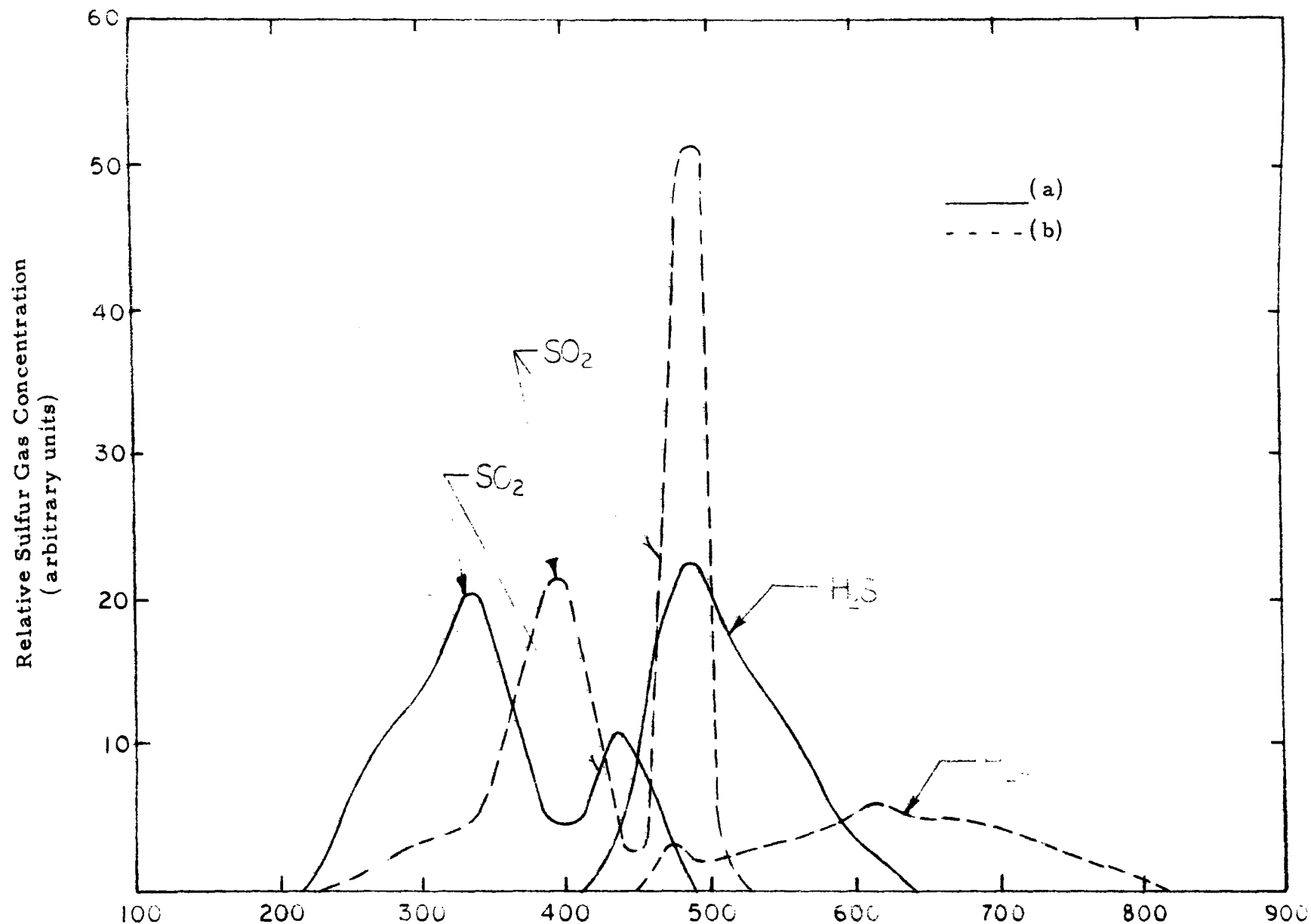


Figure 35. Sulfur gas evolution from pyrolysis in 4 litres/minute of H_2 for (a) 1 gram and (b) 0.036 grams of ferric sulfate.

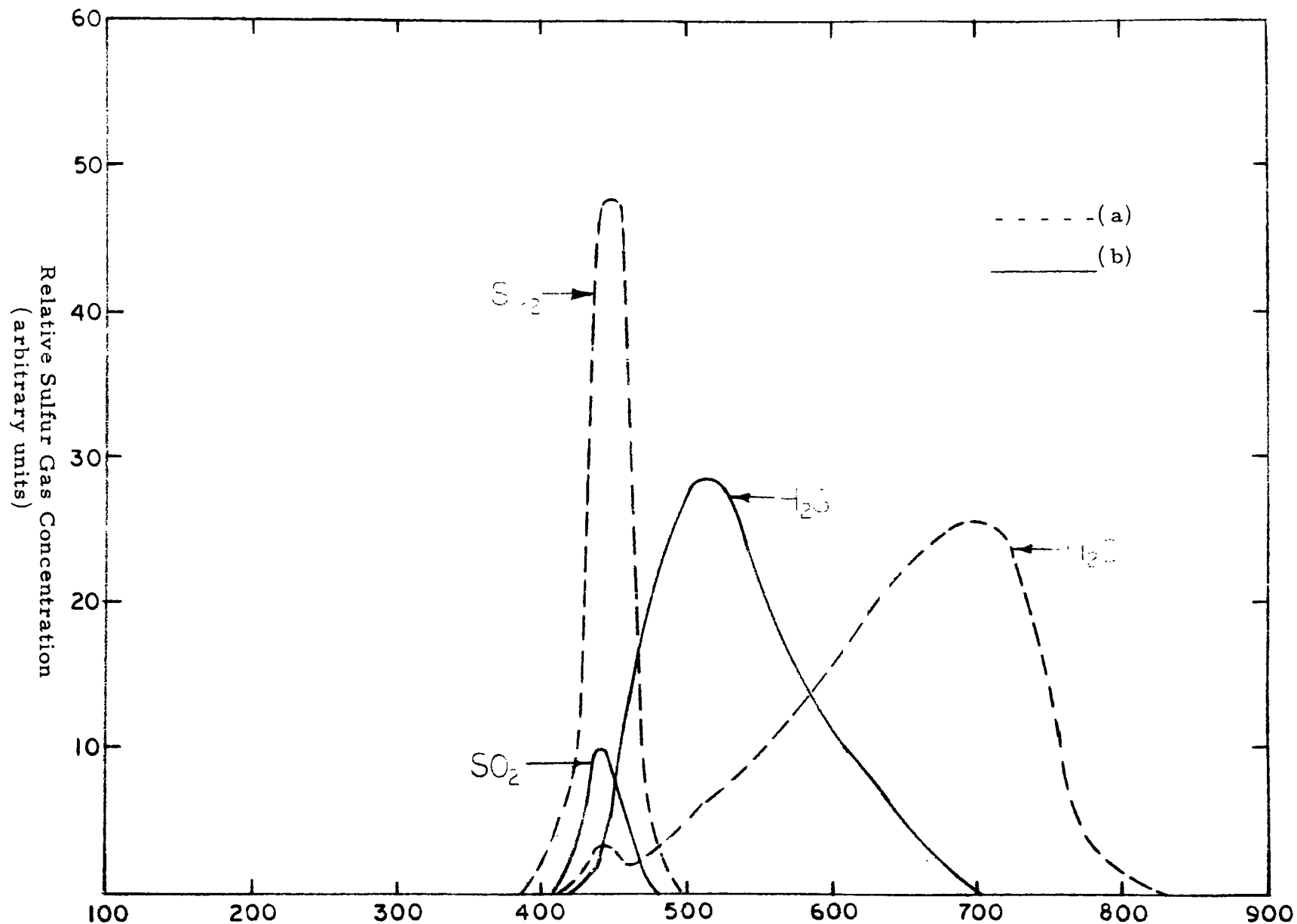


Figure 36. Sulfur gas evolution from pyrolysis in 4 litres/minute of H_2 for (a) 1 gram and (b) 0.028 grams of ferrous sulfate.

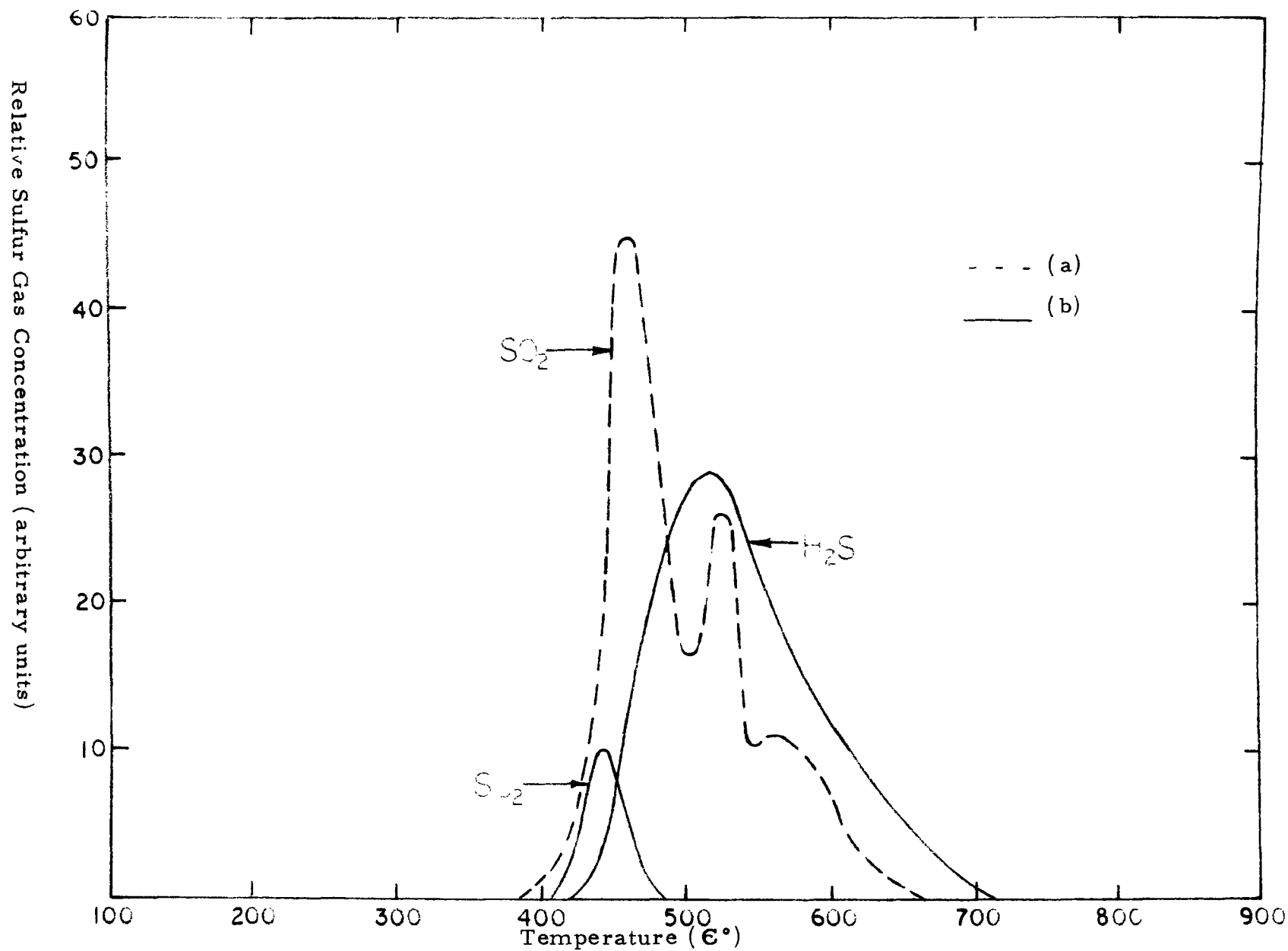


Figure 36. Sulfur gas evolution from pyrolysis of ferrous sulfate in (a) 4 litres/minute of Helium and (b) 4 litres/minute of Hydrogen.

PYROLYSIS AND GASIFICATION OF COAL MIXED WITH CALCIUM OXIDE

Isothermal experiments were performed on mixtures of the nominally 5% sulfur coal mixed with calcium oxide obtained by calcining marble chips. In two of these experiments approximately 7 grams of coal was thoroughly mixed with approximately 7 grams of calcium oxide. An additional gram of calcium oxide was added to the bed on the exit side. In one of these experiments a very low flow (20 millilitres per minute) of helium was used as the sweep gas and in another a somewhat higher flow rate of hydrogen (100 millilitres per minute) was used.

These experiments were conducted isothermally at a temperature of 750°C and the reaction time was fifteen minutes. The bed was heated to reaction temperature at a rate of 33° per minute. In both experiments the gaseous effluent was monitored using the mass spectrometer and the condensable effluents were trapped at liquid nitrogen temperature and analyzed in the gas chromatograph. No H₂S was detected by either method in either experiment giving an upper limit to the total amount of H₂S evolved of less than 0.1 milligram. Sulfur comparison data for these experiments is given in Table IX. Sulfur in the gas consisted entirely of trace amounts of sulfur dioxide and methyl mercaptan.

The char formed in these experiments was separated manually from the calcium oxide. It proved to be quite difficult to achieve a reliable complete separation so that the coke samples analyzed probably contained small amounts of calcium oxide and calcium sulfide. The lower values for sulfur in the coke were obtained by combustion of the coke in oxygen with measurement of the sulfur dioxide evolved using the gas chromato-

graph. The higher values were obtained by the conventional Eschka method. In previous investigations on coal we have found that these two methods normally agree within 10%. However, in separate experiments on oxidation of calcium sulfide, less than one third of the sulfur present was removed as sulfur dioxide. The balance remained as sulfide and sulfate in the solid. Therefore, the difference between these two methods of analysis may be due to the calcium oxide and calcium sulfide present in the sample.

Experiments were conducted on the gasification of coal with steam both with and without added calcium oxide. These experiments were conducted at a temperature of 1000°C and one atmosphere of steam. The reaction time was approximately 100 minutes and the heating rate to reaction temperature was 33°C per minute. Helium flowed over the sample during heat up. In the experiment conducted with coal alone the char yield was 23% of the initial coal weight and this char contained 7% of the sulfur initially present in coal. The tar yield was approximately 8% of the initial coal weight and contained 5% of the entire coal sulfur. More than 99% of the gaseous sulfur evolved was as H_2S . In experiments involving coal mixed with calcium oxide a very small amount of gaseous sulfur was evolved as H_2S during gasification. Analysis of the solid product for carbon at the conclusion of the experiment indicated that at least 99% of the carbon in the coal had been gasified.

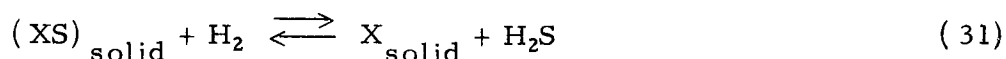
TABLE IX SULFUR COMPARISON DATA FOR ISOTHERMAL REACTIONS
OF NOMINALLY 5% SULFUR COAL MIXED WITH CALCIUM
OXIDE, IN HELIUM AND IN HYDROGEN

(all data are shown in mg of S per gram of coal)

| <u>SULFUR SPECIES</u> | <u>SWEEP GAS</u> | |
|-----------------------|------------------|----------------------|
| | <u>He</u> | <u>H₂</u> |
| S in coal | 42 | 42 |
| S in gas | 0.2 | 0.3 |
| S in tar | 0.7 | -- |
| S in char | | |
| by combustion | 3 | 3 |
| by Eschka | 10 | 6 |

KINETICS OF REVERSIBLE DESULFURIZATION REACTIONS

The reactions involved in the desulfurization of certain constituents of coal can be treated as consisting of two opposing elementary reactions, viz:



where X is a component of the solid coal particle to which sulfur may be bound. Hence, X may represent iron, carbon, or more complex chemical groupings in which the sulfur in coal may exist. An example of such a reaction is the reduction of the iron sulfide in coal.

Since the two reactions are elementary, the law of mass action applies and we may write for the rate of desulfurization

$$\frac{dN_{XS}}{dt} = k_f P_{H_2} N_{XS} - k_b P_{H_2S} N_X = \frac{dN_X}{dt} \quad (32)$$

where N_{XS} is the number of sulfur atoms in the coal bonded to X at time t, N_X is the number of XS linkages destroyed at time t, viz.

$$N_{XS}^0 = N_{XS} + N_X \quad (33)$$

and $P_{H_2} + P_{H_2S}$ are the partial pressures of $H_2 + H_2S$ respectively in the bed volume.

The material balance applied to H_2S , which, in addition to being formed and destroyed in the forward and reverse chemical reactions, is swept out by the flush gas, is

$$N_X = N_{XS}^0 - N_{XS} = N_{H_2S} + \frac{Q}{V_b} \int_0^t N_{H_2S}(t) dt \quad (34)$$

where N_{H_2S} is the number of H_2S molecules in the volume of the bed, Q is the flow rate of the flush gas. Differentiating we obtain

$$\frac{dN_X}{dt} = -\frac{dN_{XS}}{dt} = \frac{dN_{H_2S}}{dt} + \frac{Q}{V_b} N_{H_2S} \quad (35)$$

So that for the time dependence of N_{H_2S} we have

$$\frac{dN_{H_2S}}{dt} = k_f P_{H_2} N_{XS} - k_b P_{H_2S} N_X - \frac{Q}{V_b} N_{H_2S} \quad (36)$$

The units of k_f and k_b are $\text{atm}^{-1} \text{min}^{-1}$.

We now have the two differential equations

$$-\frac{dN_{XS}}{dt} = k_f P_{H_2} N_{XS} - k_b P_{H_2S} N_X \quad (32)$$

$$\frac{dN_{H_2S}}{dt} = k_f P_{H_2} N_{XS} - k_b P_{H_2S} N_X - \frac{Q}{V_b} N_{H_2S} \quad (36)$$

where the relationship between N_{H_2S} and P_{H_2S} is

$$N_{H_2S} = \frac{L V_b}{RT} P_{H_2S} \quad L = \text{Avogadro's number.}$$

Since we have the stoichiometric relationship

$$N_X = N_{XS}^0 - N_{XS}$$

(where N_{XS}^0 is the initial concentration of XS in the solid and the assumption is made that $N_X^0 = 0$). equations (32) and (36) are two simultaneous differential equations in the unknowns N_{XS} and N_{H_2S} (or P_{H_2S}).

Note that if, as an approximation, we take $\frac{dN_{H_2S}}{dt} = 0$ (a steady-state in gas-phase on H_2S), then from (32) and (36) we see that

$$\frac{Q}{V_b} N_{H_2S} = - \frac{dN_{XS}}{dt} \quad (37)$$

or
$$N_{H_2S} = - \frac{V_b}{Q} \frac{dN_{XS}}{dt} \quad (38)$$

or
$$P_{H_2S} = - \frac{RT}{LQ} \frac{dN_{XS}}{dt} \quad (39)$$

Substituting (39) into (32) yields

$$- \frac{dN_{XS}}{dt} = k_f P_{H_2} N_{XS} + k_b (N_{XS}^0 - N_{XS}) \frac{RT}{LQ} \left(\frac{dN_{XS}}{dt} \right) \quad (40)$$

or
$$\left\{ 1 + \frac{RT}{LQ} (N_{XS}^0 - N_{XS}) k_b \right\} \frac{dN_{XS}}{dt} = k_f P_{H_2} N_{XS} \quad (41)$$

$$\text{let } B = \frac{k_b RT N_{XS}^0}{LQ}$$

$$C = k_f P_{H_2} \quad (42)$$

$$y = \frac{N_{XS}}{N_{XS}^0}$$

With these definitions we get

$$\int \frac{1 + B(1-y)}{Cy} dy = \int dt \quad (43)$$

or

$$\int \frac{dy}{y} + B \int \frac{1-y}{y} dy = -Ct + \text{Constant} \quad (44)$$

$$\int \frac{dy}{y} + B \int \frac{dy}{y} - By = -Ct + \text{Constant}$$

$$(1 + B) \ln y - By = -Ct + \text{Constant} \quad (45)$$

$$\left. \begin{array}{l} \text{At } t=0 \\ y=1 \end{array} \right\} \text{ so Constant} = -B \quad (46)$$

$$\text{Then } (1 + B) \ln y - By = -Ct - B \quad (47)$$

$$-Ct = B - By + (1 + B) \ln y \quad (48)$$

$$= B(1-y) + (1 + B) \ln y = B \left[(1-y) + \left(1 + \frac{1}{13}\right) \ln y \right] \quad (49)$$

From the definitions we have

$$-k_f P_{H_2} t = \frac{k_b RT N_{XS}^0}{LQ} \left[\left(1 - \frac{N_{XS}}{N_{XS}^0}\right) + \left(1 + \frac{LQ}{k_b RT N_{XS}^0}\right) \ln \frac{N_{XS}}{N_{XS}^0} \right] \quad (50)$$

Letting $Y = P_{H_2} t$ we get

$$\gamma = -\left(\frac{k_b}{k_f}\right) \frac{N_{XS}^0 RT}{LQ} \left[\left(1 - \frac{N_{XS}}{N_{XS}^0}\right) \left(1 + \frac{LQ}{k_b R T N_{XS}^0}\right) \ln \frac{N_{XS}}{N_{XS}^0} \right] \quad (51)$$

SUMMARY

Three principal factors control the design and performance of a gas-solid reactor; the reaction kinetics for single particles, the particle size distribution for the reactant solid, and the flow patterns for both solids and gases in the reactor. In many practical cases the kinetics are complex and not well known, and, as a result, detailed analysis of the reactor design is not possible. In such cases designs are based largely on the experience gained by many years of operation, innovation, and small changes made on existing reactors. The blast furnace for producing iron is perhaps a most important industrial example of such a system.

The non-isothermal kinetic method provides an extremely powerful tool for obtaining the kinetic data needed for analysis of practical desulfurization systems. Coupled with modern high speed computer techniques for performing the necessary integrations, the kinetic data allow detailed analyses of idealized systems approximating the real processes.

An approach to the analysis of practical systems may be summarized as follows: First the chemical kinetic and reaction mechanisms are determined using the non-isothermal method. Secondly, a model of the gas-solid reaction system is developed for individual particles, and the validity of this model is determined by comparisons of calculations with the results of closely controlled laboratory experiments. Finally, the results for individual particles are averaged over the appropriate particle size, temperature, and composition distribution best approximating the real reactor system.

The major problems involved in such a procedure are in determining the necessary detailed kinetics of the reactions, since, in general, many competing and opposing reactions are involved. The complete analysis of the rate equations requires the use of the computer. The general approach to such analyses for some simple cases which can be handled manually are summarized in the present report.

Chemical Kinetics

The desulfurization of coal during pyrolysis in a hydrogen atmosphere may be considered as a superposition of the parallel and opposing chemical reactions shown in Table X. In addition to identifying the occurrence of these reactions during pyrolysis, we have measured the kinetic parameters given in Table X. The rate constant for one of these processes at an absolute temperature T is expressed by the Arrhenius equation as

$$k = k_0 e^{-E/RT} \quad (52)$$

where E is the activation energy and k_0 is the frequency factor.

The dependence of the rate constants on temperature is shown in Figure 38. The rate constant for all of the desulfurization reactions (reactions 1 through 5) fall within the indicated band. These results were obtained using heating rates of approximately 4°C per minute and as a result the rate constants are measured in the temperature range over which the rate constant varies from approximately 0.01 to $1 \text{ atm}^{-1} \text{ min}^{-1}$. In this range the results should accurately reflect the kinetics of the chemical reaction.

TABLE X. SUMMARY OF KINETIC DATA

| <u>Reaction</u> | <u>E(kcal/mole)</u> | <u>k_o</u> |
|---|---------------------|----------------------------|
| (1) (Org-S) _I + H ₂ → H ₂ S | 34.5 | 3.1 × 10 ¹⁰ (1) |
| (2) (Org-S) _{II} + H ₂ → H ₂ S | 41.5 | 2.8 × 10 ¹¹ (1) |
| (3) FeS ₂ + H ₂ → H ₂ S + FeS | 47 | 2.8 × 10 ¹² (1) |
| (4) FeS + H ₂ → H ₂ S + Fe | 55 | 2.1 × 10 ¹³ (1) |
| (5) (C-S) _{III} + H ₂ → H ₂ S _{ads} | 52 | 2.3 × 10 ⁸ (1) |
| (6) H ₂ S _{ads} ^(I) → H ₂ S _{gas} | 10 | 50 (3) |
| (7) H ₂ S _{ads} ^(II) → H ₂ S _{gas} | 43 | 2.4 × 10 ⁸ (3) |
| (8) Fe + H ₂ S → H ₂ + FeS | 18 | 6.5 × 10 ⁶ (2) |
| (9) (C) + H ₂ S → H ₂ S _{ads} | 32 | 2.3 × 10 ⁸ (2) |
| (10) CaO + H ₂ S → H ₂ O + CaS | 38 | 4.7 × 10 ¹³ (2) |
| (11) CaCO ₃ → CO ₂ + CaO | 58 | 3.8 × 10 ¹² (3) |

(1) Units of (atm. H₂)⁻¹ min⁻¹

(2) Units of (atm. H₂S)⁻¹ min⁻¹

(3) Units of min⁻¹

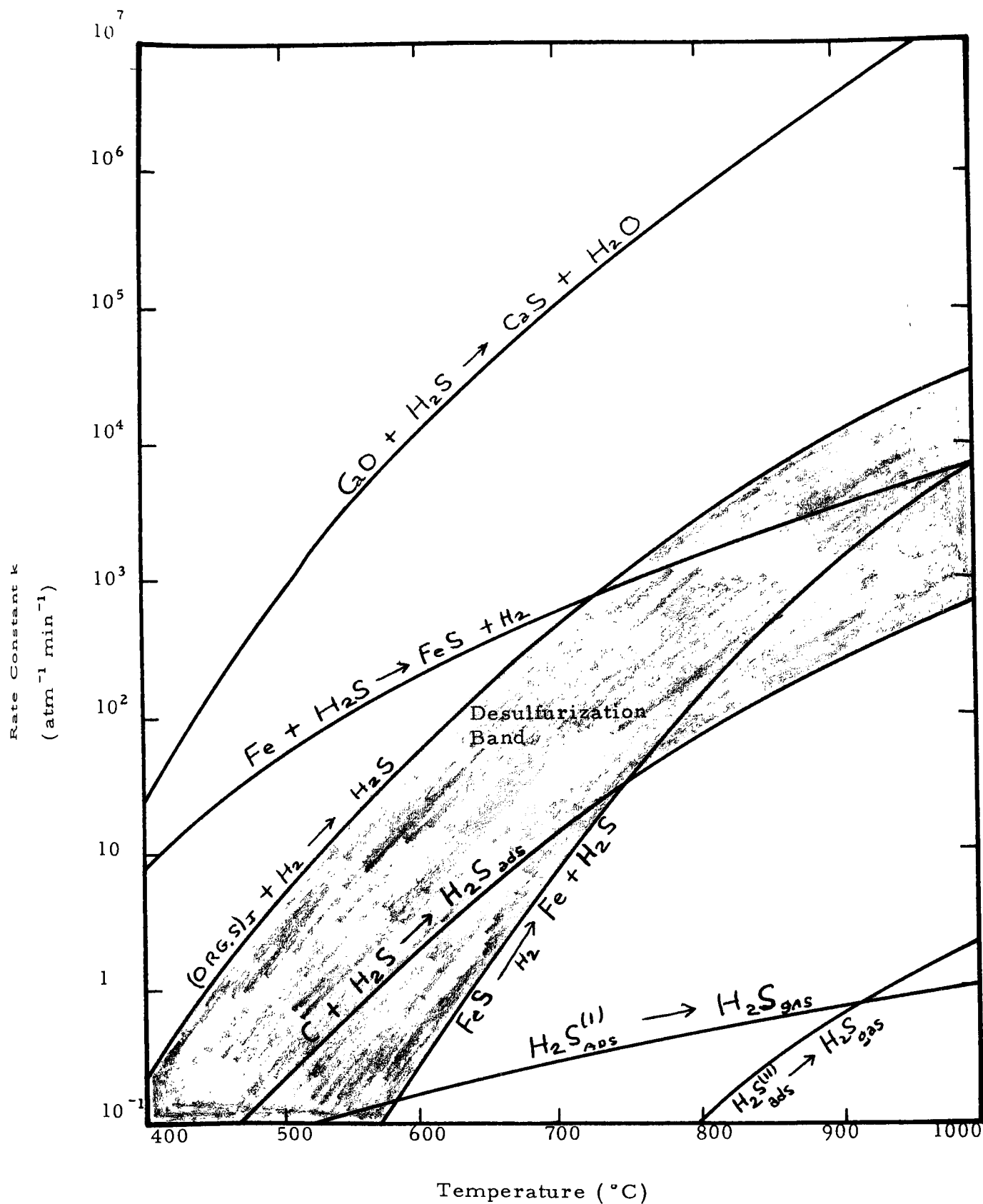


Figure 38. Rate constants for coal desulfurization reactions and for important back reactions as functions of temperature.

Applications of Kinetic Data

The kinetics of diffusion are relatively well understood, but in combination with chemical kinetics the mathematics become somewhat complex. To avoid this added complexity, we first consider the application of the kinetic data in the absence of diffusional effects with the understanding that for larger particle sizes and larger chemical kinetic rate constants the diffusional effects must be taken into consideration.

Reactions 1, 2, and 3 in Table X are simple irreversible chemical reactions. The rate of desulfurization due to one of them, for example, the pyrite, can be expressed by,

$$-\frac{dN_{\text{FeS}_2}}{dt} = k_3 P_{\text{H}_2} N_{\text{FeS}_2} \quad (53)$$

where N_{FeS_2} is the instantaneous number of molecules of pyrite in the reactor, P_{H_2} is the hydrogen partial pressure, and k_3 is the rate constant (units of $\text{atm}^{-1} \text{min}^{-1}$). Integration of equation (53) gives,

$$N_{\text{FeS}_2} = N_{\text{FeS}_2}^0 \exp(-k_3 P_{\text{H}_2} t) \quad (54)$$

where $N_{\text{FeS}_2}^0$ is the initial number of pyrite molecules in the reactor. If we define the extent of desulfurization by the ratio

$$Y_{\text{FeS}_2} = N_{\text{FeS}_2} / N_{\text{FeS}_2}^0 \quad (55)$$

then the time required for a given desulfurization of the pyrite is given by

$$-k_3 P_{\text{H}_2} t = \ln Y_{\text{FeS}_2} \quad (56)$$

The temperature dependence of the rate constant k , is given by the Arrhenius form, Equation (52) with k_0 and E as given in Table X. Thus Equation (56), or the equivalent Equation (54) give the relationship between reaction time, temperature, hydrogen pressure, and extent of desulfurization for the pyritic sulfur. Analogous equations can be written for the other simple, irreversible reactions, namely reactions (1) and (2).

For the reversible reactions the rate equations consist of a set of coupled simultaneous differential equations which are difficult to solve for the general case. An analysis of the reversible reaction rate equations is given in an earlier section. This analysis shows that for a reaction such as



the process variables in the steady state approximation are linked by the equation

$$-kP_{\text{H}_2}t = \frac{k_1RTN_{\text{FeS}}^0}{LQ} \left[(1 - Y_{\text{FeS}}) + \left(1 + \frac{LQ}{k_1RTN_{\text{FeS}}^0} \right) \ln Y_{\text{FeS}} \right] \quad (58)$$

where Y is the extent of desulfurization, N_{FeS}^0 is the initial number of molecules of iron sulfide, L is Avogadro's number, T the absolute temperature, R the gas constant, t the reaction time, P_{H_2} the hydrogen partial pressure, Q the sweep gas flow rate, and k and k_1 the rate constant for the forward and reverse reactions.

Equation (58) can be rewritten in a somewhat simpler form by noting that the total amount of H_2S evolved by the complete reduction of the iron sulfide is given by

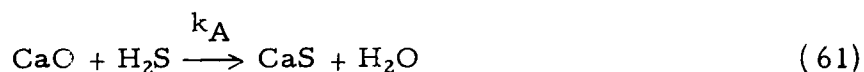
$$(PV)_{\text{H}_2\text{S}}^0 = RT \frac{N_{\text{FeS}}^0}{L} \quad (59)$$

which when substituted into equation (58) gives

$$-kP_{H_2}t = \frac{k^1(PV)^\circ_{H_2S}}{Q} \left[(1 - Y_{FeS}) + \left(1 + \frac{Q}{k^1(PV)^\circ_{H_2S}} \right) \ln Y_{FeS} \right] \quad (60)$$

Note that when the flow rate of the sweep gas Q (cm^3/min) is large compared to the overall rate of H_2S production by reduction of FeS (cm^3 of H_2S/min), equation (60) reduces to the form of Equation (58) for no back reaction. Thus for $Q \gg k^1(PV)^\circ_{H_2S}$ the effect of the back reaction is small.

An alternate method to inhibit the back reactions consists of adding a suitable sulfur adsorbent to the reactor, for example



The rate constant for this reaction has been determined by non-isothermal measurements. Since the CaS is stable in H_2 , the reverse reaction need not be considered so long as the H_2O concentration is small. For the case of absorbent added in an amount greatly in excess of the stoichiometry requirement the desulfurization equation becomes

$$-kP_{H_2}t = \frac{k^1}{k_A f_A} \left[(1 - Y_{FeS}) + \left(1 + \frac{k_A f_A}{k^1} \right) \ln Y_{FeS} \right] \quad (62)$$

where f_A is the ratio of the total capacity of the absorbent for H_2S to the total amount of H_2S evolved by complete reduction of the sulfide, k_A is the ratio constant ($\text{atm}^{-1} \text{min}^{-1}$) for H_2S reaction with the adsorbent, and the other quantities are the same as in Equation (60).

Diffusion And Mass Transport

In the desulfurization of coal we are dealing with heterogenous reactions between gases and solids. Heterogenous reactions occur by a series of diffusional and chemical steps which may be described as follows:

1. Diffusion of reactants from a fluid stream through a relatively stagnant film to the solid surface and to available capillary areas of pore structure.
2. Physical and/or chemical adsorption of reactants on the solid.
3. Surface chemical reaction.
4. Desorption of surface reaction products.
5. Diffusion of products to the bulk gas stream.

Thus the heterogenous reaction mechanism comprises a diffusional part and a chemical kinetic part. A study of gas-solid reaction kinetics must necessarily consider both diffusional and chemical kinetic effects. If the reaction resistance attributed to diffusion comprises nearly the total resistance, the reaction is considered "diffusion controlled". Similarly, the reaction is "kinetically controlled" at negligible diffusion resistance. In the present work most of the kinetic data was obtained by working in the kinetically controlled regime. Therefore, the data obtained should reflect the true chemical kinetics of the processes studied. In the application of these data to process design, the possibility of transition into the

diffusion controlled regime must be considered. These transitions may be expected to occur with an increase in particle size or in chemical kinetic rate constants. Transition from one type of rate control to another is usually indicated when a significant change in apparent activation energy with temperature occurs. Transitions of this type have been observed in our measurements on the reactions of H_2S with various solids.

Future Work

Our studies on desulfurization of coal during gasification have emphasized the theoretical and experimental application and extension of the new method of non-isothermal kinetic measurements developed originally by Juntgen and co-workers. A substantial amount of basic kinetic data relative to the desulfurization of coal during pyrolysis and gasification has been obtained. These data have enabled us to construct a rational mechanistic picture of the process in terms of a set of competing and opposing chemical reactions, the individual rates of which are known under a variety of process conditions.

It is anticipated that the major emphasis in future work will be placed on the applications of the kinetic data to the development and/or improvement of processes for coal desulfurization. Additional kinetic measurements will be needed to apply the basic kinetic data to particular proposed processes. In particular, non-isothermal kinetic measurements will be made on specific feed coals for specific processes; on a series of model organic sulfur compound and limiting cases, such as lignite and anthracite; on the reactions of coal sulfur in an oxidizing atmosphere; and on the absorption of sulfur dioxide by calcined dolomites and limestones. Some non-isothermal measurements will study the transition from reaction controlled kinetics to diffusion controlled kinetics, and for those reactions in which diffusion control is of practical significance, to measure the diffusion controlled kinetics.

R E F E R E N C E S

1. (a) M.L. Vestal et al , "Kinetic Studies on the Pyrolysis, De-sulfurization, and Gasification of Coals with Emphasis on the Non-Isothermal Kinetic Method," Scientific Research Instruments Corporation Rept. SRIC 68-13 (1969).
(b) M.L. Vestal and W.H. Johnston, "Desulfurization Kinetics of Ten Bituminous Coals," Scientific Research Instruments Corporation Rept. SRIC 69-10 (1969).
2. Juntgen, Erdol and Kohle 17, 180 (1964).
3. Van Heek, Juntgen, and Peters, Brennstoff-Chem. 48, No.6, 35 (1967). Translation by Scientific Research Instruments, Inc., Baltimore, 1968.
4. Peters and Juntgen, Brennstoff-Chemie 46, 175 (1965).
5. Van Heek, Juntgen, and Peters, Ber.Bunsen. Phys. 71, 113 (1967).
6. Van Heek, Juntgen, and Peters, "Theoretische und experimentelle Vorstudien zur Kinetik der Kohlenwissenschaftliche Tagung, Munster 1. bis 3, June 1965.
7. Juntgen and Traenckner, Brennstoff-Chem. 45, 105 (1964).
8. Juntgen and van Heek, Fuel 47, 103 (1968).
9. Hanbaba, Juntgen, and Peters, Ber. Bunsenges. phys. Chem. 72, 554 (1968).
10. Button, Greg, and Winsor, Trans. Faraday Soc. 48 63 (1952).
11. Pechkovski and Zvedin, C.A. 56, 5460 (1962).
12. Pagurova, Tables of the Exponential Integral, Pergamon Press, New York, 1961.
13. Mason, Ind. Eng. Chem. 51, 1027 (1959).
14. Zielke, Curran, Gorin, and Goring, Ind. Eng. Chem. 46, 53 (1954).
15. Batchelor, Gorin and Zielke, Ind. Eng. Chem. 52, 161 (1960).

16. Squires, A.M., "Fuel Gasification," Advances in Chemistry Series 69, Robert F. Gould, editor (American Chemical Society, Washington, D.C., 1967, Chapter 14.)
17. Squires, A.M., Trans. Inst. Chem. Engrs. (London) 39, 3 (1961).
18. Squires, A.M., ASME paper 67-WA /PWR-3 (1967).
19. Winkler, F., German patent 437, 970 (1922); U.S. patents 1,687,118 (1928), 1,776,876 (1930).
20. Pyzel, R., U.S. Patents 2,776,132 (1957), 2,874,950 (1959), 2,977,105 (1961), 2,981,531 (1961), 3,013,786 (1961), 3,022,989 (1962).
21. Stephens, Jr., F.M. and W.M. Goldberger, U.S. patent 3,171,369 (1965); W.M. Goldberger, ASME paper 67-WA/FU-3 (1967).
22. Bishop, J.W., L.F. Deming, R. Ederer and F.W. Reinhardt, ASME paper 66-WA/FU-2 (1966); J.W. Bishop, S. Ehrlich, A.K. Jain, E.B. Robison, and P.M. Chen, ASME paper 68-WA/FU-4 (1968).
23. Godel, A.A., Revue Generale de Thermique 5, 349 (1966); U.S. Patents 3,302,597 (1967), 3,302,598 (1967).
24. Parry, V.F., W.S. Landers, E.O. Wagner, J.B. Goodman and G.C. Lammers, U.S. Bur. Mines Rept. Invest. 4954 (1953).
25. Gomez, M., W.S. Landers and E.O. Wagner, U.S. Bur. Mines Rept. Invest. 7141 (1968).